DEVELOPING A CHLOROPHYLL-BASED PREDICTION MODEL FOR EICOSAPENTAENOIC ACID (EPA) PRODUCTION IN PHYTOPLANKTON

by

Michael Cheng

Submitted in partial fulfilment of the requirements
for the degree of Master of Science

at

Dalhousie University
Halifax, Nova Scotia
August, 2020

TABLE OF CONTENTS

LIST OF TABLES

LIST OF FIGURES

ABSTRACT

Phytoplankton are ideal candidates for sustainable high-scale production of polyunsaturated fatty acids such as eicosapentaenoic acid (EPA). However, a rapid and reliable technique to model EPA production has yet to be validated. Chlorophyll-a (Chl-a) and EPA are both constituents of chloroplast membranes and are thought to vary similarly with temperature and irradiance. In contrast to EPA, estimation of Chl-a is rapid, inexpensive, and precise. We predicted that Chl-a would be a reliable proxy for EPA production in microalgae. To test this hypothesis, three EPA-producers, *Nannochloropsis oculata, Pavlova lutheri,* and *Thalassiosira pseudonana*, were grown at three temperatures (15, 20, and 25 ºC) and three irradiances (22, 105, and 260 µmol photons m^{-2} s^{-1}). Overall FA profiles of the three species were different and general patterns in the responses to light and temperature were shared among species. The % EPA (relative to total mass FA) rose as irradiance decreased at a given temperature. As expected, the same trend was observed for the ratio of EPA to cell carbon in *P. lutheri* and *T. pseudonana* but there was no change in *N. oculata*. The highest production rates were found at moderate and high irradiances where specific growth rates were highest, despite decreased biomass fraction. There was little influence of temperature in the range tested. EPA/Chl-a did not show a consistent behavior among the three species, with the maximum value ranging from 1-4 g g^{-1}. However, in *P. lutheri*, the ratio was remarkably predictable, varying consistently with irradiance at all three temperatures. The proposed EPA/Chl-a model can aid in screening out inferior EPA producers using a threshold of 1 g g^{-1}, and provides a database for future EPA/Chl-a analysis in phytoplankton.

LIST OF ABBREVIATIONS USED

AFDW	Ash-free Dry Weight
ALA	α-linolenic Acid
ANOVA	Analysis of Variance
ARA	Arachidonic Acid
CERC	Canada Excellence Research Chair
Chl	Chlorophyll
Chl-a	Chlorophyll-a
CO_2	Carbon Dioxide
DD	Diadinoxanthin
df	Degrees of Freedom
DGCC	Diacylglyceryl-carboxy-hydroxymethyl-choline
DGDG	Digalactosyldiacylglycerol
DGTA	Diacylglyceryl-hydroxymethyl-trimethyl-β-alanine
DGTS	Diacylglyceryl-trimethyl-homoserine
DHA	Docosahexaenoic Acid
DIC	Dissolved Inorganic Carbon
DMSO	Dimethyl Sulfoxide
DPG	Diphosphatidylglycerol
DT	Diatoxanthin
EPA	Eicosapentaenoic Acid
F	Fluorescence
FA	Fatty Acid
FAME	Fatty Acid Methyl Ester or Fatty Acid Methyl Esterification
F_{cum}	Cumulative Fluorescence
FIRe	Fluorescence induction and relaxation system
FL	Fluorescent laser
F_m	Maximum Fluorescence
F_v	Variable Fluorescence
GC-FID	Gas Chromatography - Flame Ionization Detection
GC-MS	Gas Chromatography - Mass Spectrometry
HL	High Light
HPLC	High-pressure Liquid Chromatography
HSD	Honest Significant Difference
HT	High Temperature
KW	Kruskal-Wallis
LC	Long-chain
LL	Low Light
LT	Low Temperature
MDS	Multidimensional Scaling
MGDG	Monogalactosyldiacylglycerol
ML	Medium Light
MT	Medium Temperature
NCMA	National Centre of Marine Algae and Microbiota

PA	Phosphatidic Acid
PAR	Photosynthetically-available radiation
PC	Phosphatidylcholine
PE	Phosphatidylethanolamine
PermANOVA	Permutational Analysis of Variance
PG	Phosphatidylglycerol
PI	Phosphatidylinositol
PL	Phospholipids
PUFA	Polyunsaturated Fatty Acid
RO	Reverse-osmosis
SQDG	Sulfoquinovosyldiacylglycerol
TAG	Triacylglycerol
TOC	Total Organic Carbon
WRST	Wilcoxon Rank Sum Test
μ	Growth Rate

ACKNOWLEDGEMENTS

I would like to acknowledge my supervisor Dr. Suzanne M Budge (Marine Oils Laboratory – Department of Process Engineering and Applied Sciences) and committee members Dr. Hugh MacIntyre (Department of Oceanography) and Dr. Jenna Ritter (Department of Process Engineering and Applied Sciences, Nature's Way Canada Ltd.) on their expertise on related subjects. Carrie Greene (Marine Oils Laboratory) for instruction on fatty acid analysis and Claire Normandeau (Canada Excellence Research Chair; CERC) laboratory manager for carbon analysis of samples.

CHAPTER 1 - INTRODUCTION

Algae are ubiquitous organisms found in all ranges of aquatic and marine habitats. They contribute a huge proportion of primary biomass production and carbon fixation globally. In particular, microalgae are estimated to produce upwards of 45% of global net primary biomass through photosynthetic activity (Field et al., 1998). Diatoms alone contribute up to 20% of global carbon fixation (Sayanova et al., 2017). Microalgae are also able to accumulate and store large amounts of lipids, notably the oleaginous species (Collet et al., 2014). This ability combined with their prevalence and proliferation capabilities has great potential for various industries in the form of biofuels, nutraceuticals, and nutrition (Guschina and Harwood, 2009). Particularly of interest are the omega-3 fatty acids (FA), which include eicosapentaenoic acid (EPA) and docosahexaenoic acid (DHA). These long-chain (LC) polyunsaturated fatty acids (PUFA) can be produced in great quantities relative to total fatty acid composition (Guschina and Harwood, 2009). EPA and other PUFA have a number of beneficial health effects in humans (Asgharpour et al., 2015; Dyall, 2015). As of yet, a rapid method to isolate microalgal strains of superior EPA-production and approximate their yield has not been developed.

EPA is an omega-3 LC-PUFA (20:5n-3) that has been attributed to numerous positive health impacts in humans including cardiovascular benefits, improved phospholipid membrane integrity, immune function, tumour growth inhibition, neuropsychiatric disorder prevention (Narayan et al., 2006); and positive effects on brain disorders (Asgharpour et al., 2015; Dyall, 2015), and reductions in diabetes risk, ateriosclerosis, coronary heart disease, inflammation, and carcinomas (Asgharpour et al., 2015). Humans must directly obtain EPA as mammalian cells cannot effectively perform the necessary elongation and desaturation steps of α-linolenic acid (ALA; 18-3n-3) to form EPA, due to competition for the desaturase enzyme which prevents Δ6 desaturation, the first step of conversion of ALA to EPA (Narayan et al., 2006). In phytoplankton, EPA and other PUFA are speculated to ensure thylakoid membrane fluidity, increasing velocity of electron flow and making photosynthesis under low-light and/or low-temperature more

efficient (Guschina and Harwood, 2009; Narayan et al., 2006). This was supported by increased rate constants between stable electron receptors of photosystem I and II under low light conditions (Guschina and Harwood, 2009).

In EPA-producing microalgae, such as ochrophytes, haptophytes, and diatoms, EPA and other LC-PUFA are found across all lipid species but are predominantly concentrated within plastidial glycolipids such as monogalactosyldiacylglycerols (Fig. 1A; MGDG) and digalactosyldiacylglycerols (Fig. 1B; DGDG), which collect within thylakoid membranes. In phytoplankton, MGDG and DGDG has been found comprising up to 40-55% and 15-35% of thylakoid lipids, respectively (Guschina and Harwood, 2009). These polar lipids appear to have integral roles within photosystems I and II and the light-harvesting complex II (Kelly et al., 2016). Sulfoquinovosyldiacylglycerol (Fig. 1C; SQDG) is another plastidial glycolipid, which provides structural and functional integrity in photosystem II (Sugimoto et al., 2010). SQDG is especially dominant in diatom species and may explain the additional high content of LC-PUFA in some diatoms (Sayanova et al., 2017).

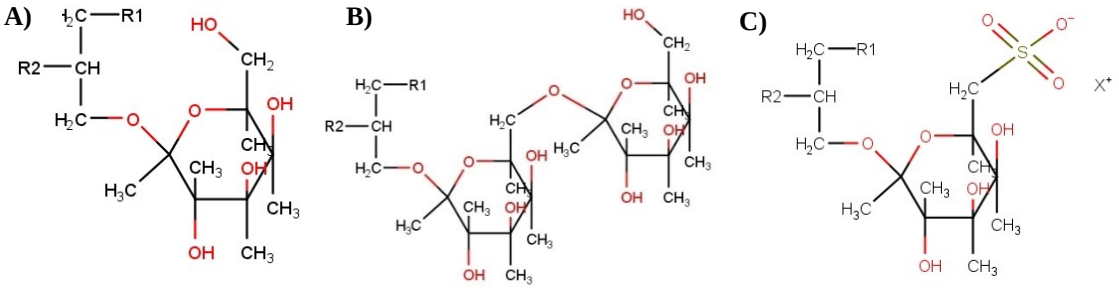

Figure 1. A) Monogalactosyldiacylglycerol (MGDG), B) digalactosyldiacylglycerol (DGDG), and C) sulfoquinovosyldiacylglycerol (SQDG) with general fatty acyl location (R1 and R2). X^+ represents a charge-stabilizing ion.

Among glycolipids, TAG and glycerophospholipids (PL; phospholipids) are also prevalent in microalgae. TAG is the dominant lipid form, found in the cell cytoplasm and presumably serves as a site for fatty acyl storage (Harwood and Jones, 1989; Zienkiewicz et al., 2016). Common microalgal phospholipids include phosphatidylglycerol (Fig. 2B;

PG), phosphatidylcholine (Fig. 2C; PC), phosphatidylethanolamine (Fig. 2D; PE), and phosphatidylinositol (Fig. 2E; PI) (Harwood and Jones, 1989; Guschina and Harwood, 2009). Phosphatidic acid (Fig. 2F; PA) is also found in microalgae but usually in trace amounts presumably due to an intermediary role in lipid biosynthesis (Harwood and Jones, 1989). Phospholipids are found in extra-plastidial membranes, with the exception of PG, which is thylakoid membrane-bound (Guschina and Harwood, 2009). Studies on chlorophytes *Chlamydomonas* and *Chlorella* sp., and the ochrophyte *Nannochloropsis* sp. have indicated that PG plays a similar role to SQDG in chloroplast function and structural integrity of chloroplast membranes (Martin et al., 2014). PC acts as an acyl donor in the synthesis of TAG (Kim et al., 2013), and is a major component of plant membranes (Christie, 2006). The role PE plays in algae is much less obvious but it is usually the second most abundant phospholipid in plants; whether this includes phytoplankton is not known (Christie, 2006). PI appears to be related to cell signalling and is likely important under osmotic, drought, and salt stresses in the chlorophyte *Dunaliella tertiolecta*, given elevated production levels under these conditions (Kim et al. 2013). PA is a precursor to other glycerolipids (Fig. 1; Christie, 2006; Sayanova et al., 2017).

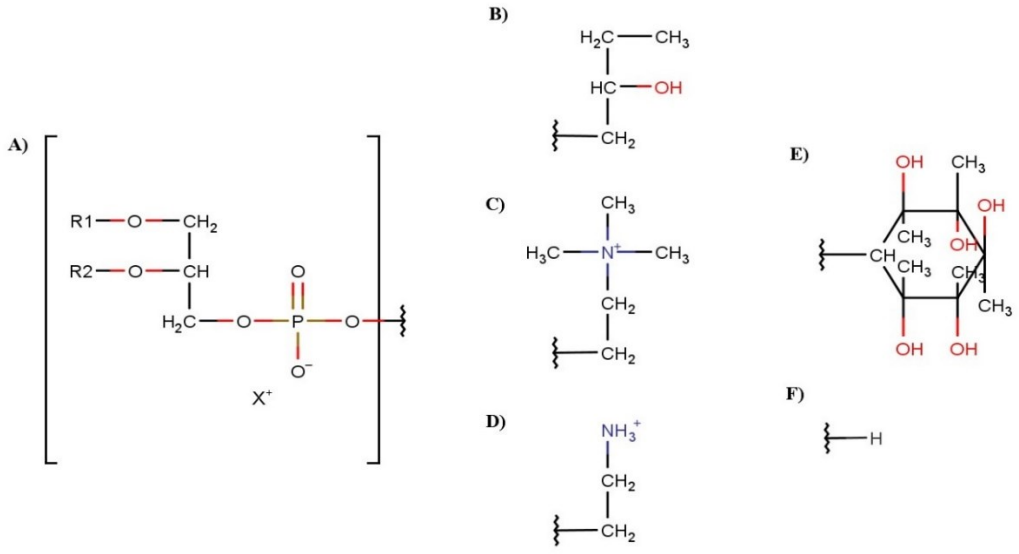

Figure 2. Glycerophospholipids with A) glycerol backbone, fatty acyls (R groups), phosphate group (PO_4^-) and corresponding unique functional moieties forming: B) phosphatidylglycerol (PG), C) phosphatidylcholine (PC), D) phosphatidylethanolamine (PE), E) phosphatidylinositol (PI), F) phosphatidic acid (PA). X^+ represents a charge-stabilizing ion.

A unique class of lipids known as betaine lipids are also found among several microalgal classes, including chlorophytes, cryptophytes, haptophytes, and ochrophytes (Fig. 3; Cañavate et al., 2016; Eichenberger and Gribi, 1997; Guschina and Harwood, 2009; Harwood and Jones, 1989). The major betaine lipids include 1,2-diacylglyceryl-3-O-4'-(N,N,N-trimethyl)-homoserine (Fig. 3B; DGTS), 1,2-diacylglyceryl-3-O-2'-(hydroxymethyl)-(N,N,N-trimethyl)-β-alanine (Fig. 3C; DGTA), 1,2-diacylglyceryl-3-O-carboxy-(hydroxymethyl)-choline (Fig. 3D; DGCC) (Guschina and Harwood, 2009). The specific role of betaine lipids is less clear; however, there is support that betaine lipids primarily act as intermediate acyl carriers within cell cytoplasm (Eichenberger and Gribi, 1997).

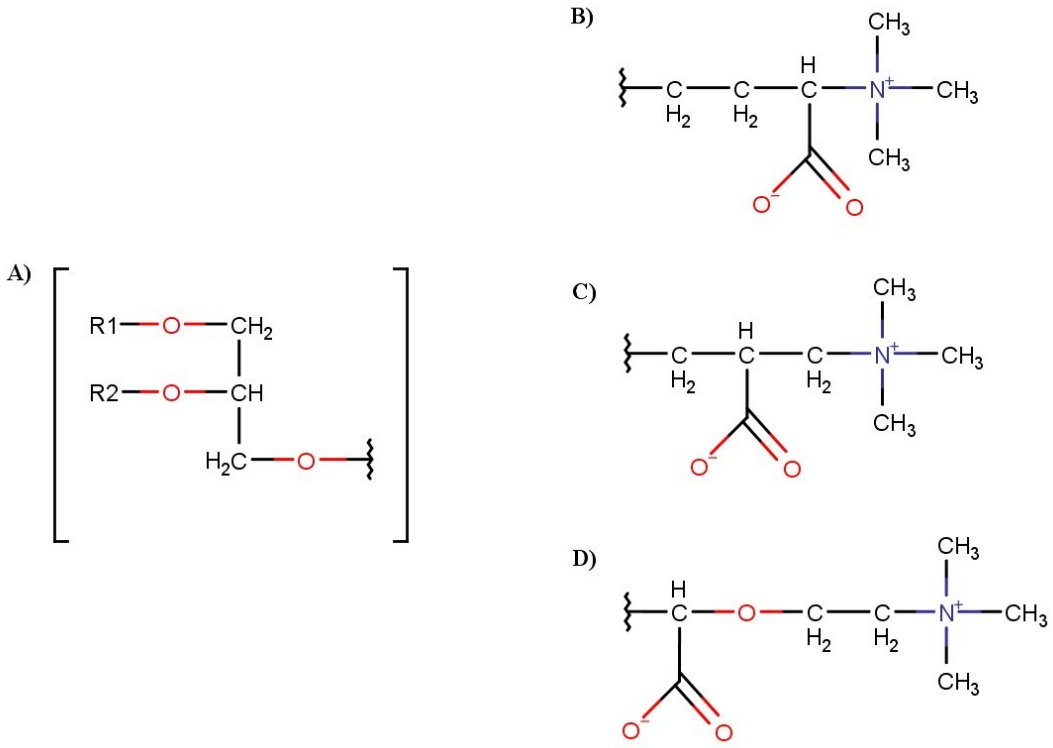

Figure 3. Betaine lipids with A) glycerol backbone, fatty acyls (R groups), and corresponding methyl complex and functional moieties forming: B) 1,2-diacylglyceryl-3-O-4'-(N,N,N-trimethyl)-homoserine (DGTS), C) 1,2-diacylglyceryl-3-O-2'-(hydroxymethyl)-(N,N,N-trimethyl)-β-alanine (DGTA), D) 1,2-diacylglyceryl-3-O-carboxy-(hydroxymethyl)-choline (DGCC).

1.1 GROWTH PHASES AND THEIR INFLUENCE ON FA PRODUCTION

Phytoplankton undergo different growth stages during their lifetime, which can be crucially-influenced by biotic and abiotic factors (Abida et al., 2015). Under normal conditions (e.g. batch growth), phytoplankton first enter a lag phase, then an exponential phase of rapid growth, followed by a stationary phase, and a declining phase (Meyers, 1953). Stationary phase effectively denotes nutrient "starvation" and subsequent reduction in growth rate (MacIntyre and Cullen, 2005). However, under constant nutrient-repletion, phytoplankton can persist in the exponential phase, achieving balanced growth (Bull, 2010). Acclimation to conditions maintaining exponential growth typically requires 7-10 generations (Bull, 2010). To compare photosynthetic efficiencies and biosynthetic profiles, it is critical to achieve balanced or steady-state growth where cell and chlorophyll densities, and resource addition and consumption are constant (Halsey and Jones, 2015). In addition, growth phase has a marked influence on lipid profile. In stationary phase, TAG is accumulated with a simultaneous decrease in polar lipids (relative to total lipid by dry mass) and PUFA (relative to total mass FA) in several microalgae (Guschina and Harwood, 2009; Thompson, 1996). There is strong support in favour of higher glycolipid and PUFA production within exponential phase, suggesting that balanced growth is ideal to compare lipid profiles as well as maximize EPA production (Abida et al., 2015; Alboresi et al., 2015; Guschina and Harwood, 2009; Martin et al., 2014; Meng et al., 2014).

1.2 EFFECT OF TEMPERATURE AND LIGHT ON PLASTIDIAL LIPIDS, EPA, AND CHLOROPHYLL-A (CHL-A)

In general, microalgae tend to accumulate more unsaturated fatty acids at temperatures lower than their optimal range (Guschina and Harwood, 2009). For example, the chlorophyte *Dunaliella salina* showed an increased level of lipid unsaturation with a decrease from 30 °C to 12 °C, with a concomitant increase of chloroplast membrane lipids by 20% (Thompson, 1996). Similar trends have been found in species within a variety of classes including haptophytes *Isochrysis galbana* (Zhu et al., 1997) and *Pavlova lutheri* (Tatsuzawa and Takizawa, 1995), and the diatom

Phaeodactylum tricornutum (Jiang and Gao, 2004). Conversely, Chl:C (θ_{Chl}), at any given irradiance and nutrient-replete conditions, decreases as temperature decreases (Geider et al., 1997). Enzymatic mechanisms are highly-dependent on temperature. A reduced temperature from optima will translate to a constrained growth rate, consequently reducing energy demand and θ_{Chl} (Geider et al., 1997). The relationship of θ_{Chl} with increasing temperature is characterized as an Arrhenius curve and has been demonstrated in a number of species, such as diatoms, ochrophytes, cyanobacteria, dinoflagellates, and haptophytes (Behrenfeld et al., 2005; Geider et al., 1997).

Irradiance can lead to oxidative damage of lipids but is also essential for photosynthesis. In general, low irradiance induces an increased production of plastidial lipids such as MGDG, DGDG, and SQDG, as well as sequestering of EPA within these lipids (Guschina and Harwood, 2009). This has been found in the chlorophyte *Cladophora* spp. (Napolitano, 1994), the rhodophyte *Tichocarpus crinitus* (Khotimchenko and Yakovleva, 2005), and the diatom *P. tricornutum* (Fernández et al., 1999). This makes inherent sense as algae will invest resources in forming plastidial membranes in low light conditions to compensate for lower rate of photosynthesis (per chlorophyll). High irradiance generally causes a decrease in EPA, which has been observed in a number of species including the ochrophyte *Nannochloropsis* sp. (Fabregas et al., 2004), the diatom *P. tricornutum* (Guschina and Harwood, 2009), and the xanthophyte *Monodus subterraneus* (Guschina and Harwood, 2009). Similarly, an increase of irradiance is followed by a concomitant decrease in θ_{Chl}, resembling a logarithmic decline (Geider et al., 1996; Geider et al., 1997; Geider et al., 1998). It is presumed that the down-regulation of θ_{Chl} at high irradiance occurs because light absorption exceeds the maximum capacity to process the light-produced metabolites (Geider et al., 1997). This relationship has been fitted to a wide range of phytoplankton species, where expected and predicted values are consistent (Geider et al., 1997). Additionally, this pattern is consistent across several species including dinoflagellates (Mansurova, 2015), diatoms (Dubinsky and Stambler, 2009; Shoman and Akimov, 2015), the haptophyte *I. galbana* (Dubinsky and Stambler, 2009), the rhodophyte *Porphyridium cruentum* (Dubinsky and Stambler, 2009), the chlorophyte *Scenedesmus guadricauda*

(Dubinsky and Stambler, 2009), and the cyanobacterium *Synechococcus leopliensis* (Dubinsky and Stambler, 2009).

The relative biomass profile (e.g. metabolites) in phytoplankton is constant during balanced growth and therefore, fatty acid abundance increases in direct relation to biomass and chlorophyll (Chl) increase. This phase can be illustrated by specific growth rate or rate of change in biomass using:

$$\frac{dC}{dt} = C \times \mu \;\; or \;\; \frac{dC}{dt} \times \frac{1}{C} = \mu \qquad \text{(Eq. 1)}$$

where,

C = biomass (mg L^{-1})
μ = specific growth rate (d^{-1})

Since the relative amounts of all components are constant in balanced growth, chlorophyll and EPA production, when integrated over a light cycle, must also share the same growth rate calculation:

$$\frac{dChl}{dt} \times \frac{1}{Chl} = \mu = \frac{dEPA}{dt} \times \frac{1}{EPA} \qquad \text{(Eq. 2)}$$

$$\frac{dEPA}{dt} = \frac{dChl}{dt} \times \frac{EPA}{Chl} \qquad \text{(Eq. 3)}$$

where,

Chl = chlorophyll-a concentration (mg g C^{-1})
EPA = EPA concentration (mg g C^{-1})
dChl/dt = Chlorophyll-a production (mg g C^{-1} day^{-1})
dEPA/dt = EPA production (mg g C^{-1} day^{-1})

Thus, in balanced growth, growth rate can predict chlorophyll production since μ x Chl = dChl/dt; any set of conditions that produces the highest rate of chlorophyll production should also coincide with highest EPA production, provided that EPA/Chl varies less than dChl/dt. The advantage of this approach, rather than monitoring EPA

directly, is that chlorophyll and growth rate can be easily and rapidly measured on very small volumes of culture, allowing many cultures to be screened simultaneously. However, accurately predicting EPA production across many cultures and under different growth conditions requires the assumption that the ratio of EPA/Chl is constant. While there is some evidence in the literature to suggest that there is little variation in this ratio (Budge et al., 2014), the validity of this approach relies on a rigorous examination of the relationship between EPA and chlorophyll in different species grown under different irradiances and temperatures.

1.3 EPA-PRODUCING MICROALGAE SPECIES OF INTEREST

Nannochloropsis oculata (*N. oculata*) is a marine phototrophic ochrophyte typically measuring 2-4 μm in diameter (Sharifah and Eguchi, 2011). *Nannochloropsis* spp., including *N. oculata*, have been a subject of intense research within the past decade, due to its ability to concentrate high % EPA (relative to total mass FA) (Sharma and Schenk, 2014). Several studies have aimed to increase omega-3 FA production in *Nannochloropsis* spp. cultivation by modifying growth conditions, including applying a variety of UV radiation types and intensities (Fabregas et al., 2004; Forján et al., 2011; Sharma and Schenk, 2014; Srinivas and Ochs, 2012), nitrogen limitation (Converti et al., 2009; Meng et al., 2014), and carbon supplementation (Hu and Gao, 2006). Among MGDG and DGDG, *N. oculata* also produces extra-chloroplast phospholipids such as PC and the betaine lipid DGTS (Guschina and Harwood, 2009; Servaes et al., 2015).

Pavlova lutheri (*P. lutheri*), a 4-6 μm marine haptophyte, is another high-performing EPA producer (Shah et al., 2014). The effects of growth conditions on FA and lipid profile has also been studied extensively in this species, including temperature and light variation (Carvalho et al., 2009; Guihéneuf and Stengel, 2017; Shah et al., 2014), salinity and pH (Shah et al., 2014), and even random mutagenesis (Meireles et al., 2002). Along with MGDG, DGDG, and SQDG, *P. lutheri* also produces the betaine lipid DGCC (Kato et al., 1995). DGCC and other betaine lipids are theorized to primarily act as acyl

carriers from cytoplasm to the chloroplast (*P. lutheri*, *Ochromonas* sp. (ochrophyte) and *Chroomonas* sp. (cryptophyte); Eichenberger and Gribi, 1997).

T. pseudonana is a marine centric diatom, measuring about 4-6 µm in diameter, with a fully-sequenced genome (Armbrust et al., 2004). Several diatom species have been found to be particularly rich in EPA, with numerous studies on environmental effects on lipid profiles (Sayanova et al., 2017). However, fewer studies have been done with respect to *T. pseudonana*. The effect of carbon dioxide (Sabia et al., 2018), and natural changes during cultivation life cycle (Zhukova, 2004) on lipid profile and EPA have been studied, where both reductions in atmospheric CO_2 concentrations and prolonged batch culturing increased proportions of EPA (relative to total mass FA). *T. pseudonana* is known to also sequester high amounts of SQDG and thylakoid-bound PG, which each contribute ~10% of total lipids (Schaller-Laudel et al., 2017).

Table 1. Review of EPA content in *N. oculata, P. lutheri, and T. pseudonana.* AFDW = ash-free dry weight.

Species	**Lipid content**	**EPA content**	**Reference**
Nannochloropsis oculata	N/A	5-25 mg g^{-1} AFDW	Aussant et al., 2018
	10.9% (of total dry mass)	27.6% (of total FA)	Borges et al., 2016
Pavlova lutheri	129-134 mg g^{-1} AFDW	2-20 mg g^{-1} AFDW	Guihéneuf and Stengel, 2017
	N/A	23.6% (of total FA)	Kato et al., 1995
	15-35% (of total dry mass)	12.1% (of total FA)	Shah et al., 2014
Thalassiosira pseudonana	21-31% (of total dry mass)	12.2% (of total FA)	Sayanova et al., 2017
	N/A	12.9-19.3% (of total FA)	Zhukova, 2004

Localization of EPA within plastidial compartments (correlation with Chl) as well as predictable variation in EPA in response to temperature and irradiance (covariance with Chl) is hypothesized to allow for the development of a rapid EPA prediction tool in microalgae. The overall aim of this research was to evaluate the fundamental use of

EPA/Chl ratio to predict EPA production in three candidate microalgae, *N. oculata*, *P. lutheri*, and *T. pseudonana*. There were three specific objectives:

1. Determine variation in % EPA (relative to total mass FA), cell quotas (EPA:C and θ_{EPA}) and EPA production with temperature and irradiance within a selection of optimal EPA-producing microalgal species (*N. oculata*, *P. lutheri*, *T. pseudonana*).

2. Determine the relationship between EPA and Chl-a within species and treatments.

3. Explore variation in other significant % PUFA (relative to total mass FA), cell quotas, and production, and their relationship with Chl-a.

CHAPTER 2 – METHODS

2.1 MICROALGAL STRAINS AND TREATMENT LEVELS

N. oculata (CCMP525), *P. lutheri* (CCMP1325), and *T. pseudonana* (CCMP1335) were obtained from National Centre for Marine Algae and Microbiota (NCMA Bigelow Laboratory for Ocean Sciences) on January 24, 2019. Strains were grown in an incubator (SANYO versatile environmental test chamber, SANYO Scientific) at 15 °C (low temperature; LT), 20 °C (medium temperature temp; MT), and 25 °C (high temperature; HT). Built-in fluorescent lighting, opaque plastic sheets, and black mesh screens were used to achieve desired light variations of 260 ± 10 (high light; HL), 105 ± 5 (medium light; ML), 22 ± 4 (low light; LL) µmol photons m^{-2} s^{-1} for a given temperature. A Biospherical scalar quantum irradiance sensor (QSL2102) was used to ensure accurate irradiance levels. Additionally, orientation of culture vessels was kept constant and specific to irradiance measurement spots, as irradiance varied with locality within the incubator. Once balanced growth was achieved, cultures were scaled-up to 1 L within 2 L glass flasks and monitored daily to ensure balanced growth was maintained.

2.2 MEDIA PREPARATION

All culture glassware was prepared by thorough washing, overnight soaking in an alkaline cleaner (5% Micro-90, International Products Corp.), followed by overnight soaking in a 1% dilute HCl in de-ionized water bath. Glassware was rinsed thoroughly with de-ionized water between/after soaking.

Stock f/2 media was prepared using the recipe provided by NMCA Bigelow, which references original formulation derived from Guillard and Ryther (1962) and stored in 2 L glass bottles. Tangential-flow-filtered coastal seawater collected at the NRC Ketch Harbour lab served as the seawater base. Media batches were recorded and autoclaved (121.1°C for 45 mins) before storing at 20°C in a media incubator. An aliquot pump was fitted to media bottles for culture media preparation.

2.3 STRAIN MONITORING AND FLUORESCENCE MEASUREMENTS

Daily fluorescence measurements of minimum, maximum, and variable fluorescence (F_0, F_m, F_v) and the dimensionless ratio F_v/F_m were obtained by non-linear fitting of the fluorescence induction curve using Fireworx software (Barnett and Ciochetto, 2017) and chlorophyll fluorescence was determined using a 10-AU fluorometer (Turner designs) following 15-minute dark acclimation of cultures. FIRe readings were processed through MATLAB (R2014a, 8.3.0.532). Daily fluorescence data was input on Excel. Specific growth rate (μ) was estimated using the following equation derived from Brand et al. (1981):

$$\mu = \frac{\ln\left(\frac{V[media]}{V[transfer]}\right) \times \left(\frac{F[Turner]}{t_{-1}}\right)}{t - F_{-1}[Turner]} \qquad \text{(Eq. 4)}$$

where,

μ = specific growth rate (day^{-1})
V[media] = volume of media used (mL)
V[transfer] = volume of inoculate (mL)
t = time of current fluorescence measure (h)
t_{-1} = time of previous fluorescence measure (h)
F[Turner] = current measure of Turner fluorescence (corrected to blank) (F)
F_{-1}[Turner] = previous measure of Turner fluorescence (corrected to blank) (F)

Cumulative fluorescence (F_{cum}) was generated using the following equation:

$$F[cum] = F_{-1}[cum] \times e^{(\mu(t - t_{-1}))} \qquad \text{(Eq. 5)}$$

where,

F[cum] = current cumulative Turner fluorescence (F)
F_{-1}[cum] = previous cumulative Turner fluorescence (F)
μ = specific growth rate (day^{-1})
t = time of current fluorescence measure (h)
t_{-1} = time of previous fluorescence measure (h)

Balanced growth was achieved when growth rate and the ratio of variable to maximum fluorescence (F_v/F_m) was within 10% variation and/or the R^2 value of F_{cum} (logarithmic transformed) reached above 0.995, through 10 generations.

2.4 CULTURE TRANSFERS

The aliquot amount required to maintain balanced growth was calculated using the following equation:

$$V[transfer] = \frac{V[target]/(F[corr] \times Interval \times e^{\left(\frac{\mu}{F[target]}\right)})}{V[target] - (V[target]/(F[corr] \times Interval \times e^{\left(\frac{\mu}{F[target]}\right)}) \times 30} \quad \text{(Eq. 6)}$$

where,

V[transfer] = transfer aliquot required (rounded to nearest mL)
V[target] = volume of fresh media (mL)
F[corr] = Turner fluorescence of sample corrected to blank (F)
Interval = transfer interval (d)
F[target] = target Turner fluorescence desired in inoculated culture (F)
μ = mean specific growth rate (d^{-1})

Aliquots of culture were aseptically transferred to room-temperature pre-autoclaved 30 mL f/2 media in 45 mL tubes within a laminar flow hood. The workspace and nitrile gloves were wiped with 70% ethanol, and a Bunsen burner was lit and placed in the middle of the work area. Culture racks with labelled fresh media tubes were placed no more than 10 cm away from the Bunsen burner, tubes were wiped with 70% ethanol using a Kimwipe, and then the culture tubes were inverted at least 6 times. The culture tube caps and openings were flamed and transfers were done using cotton-tipped graduated plastic pipettes and a pipette dispenser. The new tubes were flamed following transfers and the old tubes were appropriately disposed of. The workspace was wiped with 70% ethanol between treatment racks.

2.5 CELL FILTERING

Harvest timing of scaled-up 1 L cultures was determined by Turner fluorescence readings to ensure that adequate cell densities had been reached. The cultures were kept in exponential-phase growth and target fluorescence for harvest varied in response to temperature. Once cultures reached harvest fluorescence, they were filtered under vacuum pressure below 17 kPa (5" Hg) using plastic graduated funnel towers connected to a vacuum pump and a disposal tank. Each culture replicate flask was swirled manually in a circular fashion before filtering to ensure even cell concentration. Filter towers were rinsed thoroughly with Milli-Q de-ionized water between each sample run. Each treatment harvest was accompanied by an appropriate blank of filtered seawater obtained from Ketch Harbour NRC facility in Halifax, Nova Scotia.

2.6 DATA COLLECTION

2.6.1 Chl-a Determination

Chl-a was measured fluorometrically using the non-acidification method (Welschmeyer, 1994) after extraction in a 3:2 (v/v) mixture of 90% acetone and dimethyl sulfoxide (Shoaf and Liam, 1976). The Turner Designs 10-005R fluorometer was calibrated with purified Chl-a (Sigma Aldrich C6144). The following equation derived from Weschmeyer (1994) was used to quantify Chl-a:

$$Chl-a[sol] = \frac{(F[sample] - F[blank]) \times Cal\ factor \times V[solvent]}{Sens\ \times V[sample]} \quad \text{(Eq. 7)}$$

where,

Chl-a[sol] = chlorophyll-a in solution (μg mL^{-1})
F[sample] = fluorescence value of sample in voltage (V)
F[blank] = fluorescence value of seawater in voltage (V)
Cal factor = Welschmeyer calibration (non-acidified) factor defined as 64.88 μg Chl-a mL^{-1} V^{-1} (Welschmeyer, 1994)
V[solvent] = volume of 3:2 DMSO : 90% acetone (mL)
V[sample] = volume of sample filtered (mL)

Sens = sensitivity levels used (no units)

2.6.2 Cell Count

Cultures were aseptically transferred into cryovials using a 5 mL Eppendorf pipetter along with 25% glutaraldehyde in water at a ratio of 40 uL glutaraldehyde per 1 mL culture. Sample cryovials were quickly submerged in liquid nitrogen and freeze-stored in cryovial containers until analysis.

Flow cytometry was used to determine cell count and bacterial load based off methods used by Gasol and Giorgio (2000). A flow cytometer (BD Accuri C6) fitted with 488 nm solid-state and 640 nm diode fluorescent lasers (FL), side-angle scatter diodes, and standard filters and detectors: green (488 nm x 533/30; FL1), orange (488 nm x 585/40; FL2), red (488 nm x 670 LP; FL3), blue (640 nm x 675/25; FL4) was used to conduct cell analysis, which was connected to a desktop computer (Dell, Optiplex 7010). Pre- and post-analysis set up was performed according to manufacturer specifications. Filtered samples were diluted until total counted events reached over 4,000 but cumulative events per second did not exceed 110. Dilutions were summed to 1 mL for each sample. Bacterial load was quantified using SYBR™ Green staining method where 20 uL of SYBR™ Green I nucleic acid gel stain (10000x concentrate in DMSO, Invitrogen Thermo Fisher Scientific) was added to 1 mL of Milli-Q de-ionized water as a stock solution, and a subsequent 20 uL of stock solution was added to 1 mL of samples, within a dark environment. Working stock solution was cold-stored in the dark. Stained samples were kept in dark conditions for at least 10 mins but no longer than 30 mins before flow cytometry analysis. Re-filtered seawater (using 47 mm nylon filters with pore size of 0.45 um) was run between different treatments, with an additional SYBR™-stained filtered seawater blank run between stained samples. An unstained sample for each treatment was also run to accurately compare and quantify bacterial load. Unstained samples were single-run, while stained samples were run in triplicate.

To quantify cell and bacterial counts, several plots were organized comparing different pigment detections and forward-angle scatter. FL4 detection vs. FL3 detection

plot was used to isolate populations of particulate debris, SYBR™ Green-stained bacteria, and phytoplankton (FL3 does not vary with green fluorescence but FL4 does), and subsequent phytoplankton counts were extracted. Frequency distribution of FL1 gated with removal of phytoplankton population, along with a vertical dividing line (left side indicated as V1-L, right side indicated as V1-R) was used to estimate bacterial populations by overlaying appropriate SYBR™-stained and non-stained cultures and visually placing the divider where stained bacterial and miscellaneous debris population intersected the non-stained population. Phytoplankton cell concentrations (uncorrected) were calculated using the following equation:

$$[Cells] = \frac{Count \times 10^3}{Dilution \times V[inj]} \qquad \text{(Eq. 8)}$$

where,

[Cells] = concentration of phytoplankton cells (cells mL^{-1})
Count = Total cell count of phytoplankton population (gated FL4 vs. FL3 plot)
Dilution = dilution factor of analyzed sample to filtered seawater
V[inj] = volume of sample injected and analyzed through flow cytometer (uL)

Phytoplankton cell concentration of samples were averaged for each respective treatment replicate and corrected by subtraction of the mean concentration found in filtered seawater blanks (using Eq. 8). Bacterial count was calculated using the following equation:

$$[Bacteria] = \frac{([Stained] - [V1 - L\ unstained]) \times 10^3}{Dilution \times V[inj]} \qquad \text{(Eq. 9)}$$

where,

[Bacteria] = concentration of bacterial cells (cells mL^{-1})
[Stained] = Total cell count of stained sample
[V1-L unstained] = Total cell count of V1-L side in unstained sample (gated FL1 frequency plot)
Dilution = dilution factor of analyzed sample to filtered seawater

V[inj] = volume of sample injected and analyzed through flow cytometer (mL)

Bacterial counts were converted to total bacterial carbon using the following equation:

$$Total[C] = [Bacteria] \times Conversion \times 10^{-9} \quad \text{(Eq. 10)}$$

where,

Total [C] = total bacterial carbon concentration (mg C L^{-1})
[Bacteria] = concentration of bacterial cells (cells mL^{-1})
Conversion factor (heterotrophic bacteria) = High-range constant described by Kawasaki et al. (2011) as 20 fg C $cell^{-1}$

Total bacteria carbon concentrations were averaged for each respective treatment replicate and then subtracted from mean total sample carbon concentration to account for respective bacterial contribution.

2.6.3 Carbon Analysis

Samples of 50 mL were poured and measured using graduated filter towers, following even mixing through manual swirling. Subsequently, measured samples were filtered. Filters were frozen in liquid nitrogen and freeze-stored in clean Petri dishes until analysis. Prior to processing, filters were oven-dried at 50 °C overnight and kept in a vacuum-sealed dessicator at room temperature.

To prepare for carbon analysis, sample filters were packed using stainless-steel forceps, a stainless-steel packing mold, and pressed aluminum foil cups (Isomass Scientific Inc. Elemental Microanalysis D1104; 10.5 mm x 9 mm). Packing tools were wiped with 70% ethanol between samples. Empty muffled 25 mm Whatman GF/F glass fibre filters (duplicates) and f/2 media filters (triplicates) were also prepared in the same manner and served as reference blanks. Packed samples were stored in plastic cell culture trays and analyzed on an Elementar (model vario MicroCube) elemental analyzer in the Canada Excellence Research Chair (CERC) in Ocean Science and Technology Research Laboratory using a flash combustion temperature of 1150 °C. Total mass (mg) was

calculated from peak area and % C was determined through comparison to a calibration curve (obtained using carbon standards). Carbon results from f/2 media and empty filter were used to subtract from sample total carbon to obtain total organic carbon (TOC) for each sample replicate.

Carbon concentration was calculated using the following equation:

$$[C] = \frac{m[sample] \times \%C \times 10^3}{V[sample] \times 10^2} \qquad \text{(Eq. 11)}$$

where,

[C] = concentration of total organic carbon (μg L^{-1}; uncorrected)
m[sample] = mass of sample filter (mg)
%C = percentage of analyzed total organic carbon (%)
V[sample] = volume of sample filtered (mL)

The carbon concentration for each sample was then corrected by subtracting mean carbon concentration of f/2 media samples.

2.6.4 FA Collection

Samples of 400 mL of culture were filtered onto muffled 47 mm Whatman GF/C glass fibre filters as one replicate, until the filtrate meniscus was just above the filter. Then approximately 10mL of boiling seawater was introduced and filtered through until samples were just dry (as prolonged vacuum pressure could cause excessive stress to cell structures). Filters were frozen in liquid nitrogen and then submerged in 3 mL of 2:1 chloroform-methanol contained in 10 mL glass round-bottom test tubes, after filtering of all samples had concluded. Sample headspace were purged with nitrogen gas and freeze-stored until analysis.

2.6.5 FA Profiling - Fatty Acid Methyl Esterification (FAME) and Transesterification

All glassware and Teflon caps were triple solvent-rinsed with approximately 1 mL of dichloromethane and dried prior to use. As well, all samples were contained within nitrogen atmosphere prior to capping, where appropriate. A direct transesterification method (modified Hilditch method) outlined by Budge et al. (2006) for microalgae tissues was used. This method simultaneously extracts and methylates acyl lipids within samples via the use of acid and base catalysts, transforming the FA groups into a volatile form for analysis. The chloroform-methanol mixture preserving each sample was first evaporated under a nitrogen evaporator. Once dry, 0.1 mL of C23:0 internal standard (0.06 mg mL $CH_2Cl_2^{-1}$) and 1 mL of sodium hydroxide in high-pressure liquid chromatography (HPLC) grade methanol (20 mg mL^{-1}) was added to each sample, using a micro-syringe and a graduated glass pipette fitted with a rubber pipette bulb respectively. Tubes were vortexed for 10 seconds, sonicated for 3 minutes, and placed on a heat block for 10 mins at 90-100 °C (base-catalyzed transesterification). Once samples were cooled to room temperature, 1 mL of boron trichloride in 12% methanol was transferred to each sample, vortexed for 10 seconds, and heated for 10 mins at 90-100 °C (acid-catalyzed methylation). Once cooled to room temperature, 2 mL of reverse-osmosis (RO) water and n-hexane was added to each sample. Samples were vortexed for 30 seconds and centrifuged at ≥ 100 g for 10 mins. The hexane supernatant was extracted using a disposable glass pipette and placed in a conical 10 mL glass tube. The hexane extraction was repeated, and extracts were combined. 1 mL of RO water was added to the hexane containing the FAME and it was then vortexed lightly and centrifuged at the same speed for 5 mins. The hexane supernatant was pipetted into a second conical 10 mL tube containing ~1 g of anhydrous sodium sulfate to remove any residual water. The resulting purified FAME in hexane was pipetted into a third pre-weighed conical 10 mL test tubes and nitrogen evaporated until the hexane was evaporated completely. The purified FAME was reconstituted in 0.4 mL hexane and vortexed. The FAME was transferred to gas chromatography (GC) vials, sealed using Duraseal, and stored at -20 °C in preparation for gas chromatography using flame ionization detection (GC-FID) analysis.

2.6.6 FA Determination

FA profiles were analyzed by GC-FID using splitless injection, helium as a carrier gas, and a polar capillary column coated with 50% cyanopropyl-methylpolysiloxane (specifically, DB-23; 30 m). GC method properties used were as follows: injector set at 250 °C and detector set at 270 °C, oven ramp - initial oven temperature to 60 °C (0.5 min), 45.0 °C min^{-1} to 150 °C (2 min), 8.0 °C min^{-1} to 220 °C (8.77 min) with total run time of 22.02 min and a flow rate of 0.7 mL min^{-1}. FAME produced from a well-characterized fish oil sample served as an in-house standard. Chromatograms were individually inspected, and peak and baseline modifications were applied manually. Duplicate injections were made at approximately intervals of ten samples (excluding seawater blanks) to assess consistency between injections. FA data expressed as mass percent and ug L^{-1} (calculated in reference to the amount of C23:0 internal standard) were extracted and summarized.

Concentration of EPA and other major fatty acids were calculated using the following equation:

$$[FA] = \frac{\%\ FA}{\%\ C23{:}0} \times \frac{[C23{:}0] \times V[C23{:}0] \times 10^3}{V[sample]} \qquad \text{(Eq. 12)}$$

where,

[FA] = concentration of FA in µg L^{-1} (uncorrected)
% FA = percent of FA out of total FA percent (% w/w)
% C23:0 = percent C23:0 out of total FA percent (% w/w)
[C23:0] = concentration of C23:0 internal standard (mg mL^{-1} CH_2Cl_2)
V[C23:0] = volume of C23:0 internal standard used (mL)
V[sample] = volume of sample filtered (L)

The concentration of FA was then corrected by subtracting the mean concentration of seawater blank data for appropriate FA species.

2.6.7 FA Production Rate Determination

FA production rate was calculated as follows:

$$\frac{dFA}{dt} = [FA] \times \mu \qquad \text{(Eq. 13)}$$

where,

dFA/dt = FA production in (mg gC^{-1} day^{-1})

[FA] = concentration of final corrected FA (µg L^{-1})

µ = mean specific growth rate over the course of balanced growth (d^{-1})

2.7 STATISTICAL ANALYSES

2.7.1 FA profile

Non-parametric multivariate analysis was carried out on fatty acids of major interest, including EPA (20:5n-3), docosahexaenoic acid (DHA; 22:6n-3), and arachidonic acid (ARA; 20:4n-6). Non-parametric multi-dimensional scaling (nMDS) was applied on log transformed FA profiles and compared between species. Permutational analysis of variance (PermANOVA) between species (regardless of conditions) was then carried out, followed by PermANOVA within species (with regards to conditions) if significance was found. If significance was found in both tests, Levene's test (95%) was carried out on data sets. If variances were similar, two-way ANOVAs (95%) and Tukey's honest significant difference (HSD) tests (95%) were carried out on untransformed FA of major interest (arachidonic acid (ARA; 20:4n-6), EPA (20:5n-3), docosahexaenoic acid (DHA; 22:6n-3)) within each species. Kruskal-Wallis (KW; 95%) and Dunn's (95%; no transformation) tests were performed upon data sets that failed Levene's test (95%).

2.7.2 Growth Rate, Phytoplankton/Bacteria Ratio, FA Concentrations, FA Production and FA Ratioed-to-Chl-a

Statistical analyses were primarily focused on data sets within species, with the exception of growth rates, which also compared between species, and phytoplankton/bacteria, which was only compared between species. Levene's test (95%) was performed on all data, followed by two-way ANOVAs (95%) tests and Tukey's HSD test (95%) if variances were homogenous. If variances were heterogenous, then KW tests (95%) and Dunn's (95%; no transformation) tests were used. To compare balanced-growth and scale-up growth data, two-sided Wilcoxon rank sum test (WRST; 99%) was used. One-way ANOVA (95%) was performed on highest EPA production between species. Where appropriate, trendlines were fitted to FA/Chl-a data. All statistical analyses were performed in R studio version 3.5.2. Graphical representations were done through Microsoft Office Excel 365.

CHAPTER 3 - RESULTS

3.1 GROWTH RATE

Unfortunately, not all strains could be grown in all conditions. *N. oculata* did not grow in high temperature-medium light and high temperature-low light treatments. As well, *T. pseudonana* was not successfully grown in low temperature-high light and high temperature-high light treatments. A replicate of *P. lutheri* within high temperature-low light was excluded due to contamination. The majority of balanced growth data were similar to scaled-up growth (Fig. 4, 5, 6). However, the two stages of growth were different at conditions of low temperature-low light (WRST: $W = 667$, $p < 0.001$) in *N. oculata* (Fig. 4); and low temperature-high light (WRST: $W = 11$, $p < 0.001$) and medium temperature-low light (WRST: $W = 525$, $p = 0.006$) in *P. lutheri* (Fig. 5). Of all species, *T. pseudonana* exhibited the highest growth rates in all conditions (Fig. 6; KW: $df = 2$, $X^2_{0.95} = 16.40$, $p < 0.01$), up to ~72% more than *P. lutheri* (LT-ML; Fig. 5). For *N. oculata* and *P. lutheri* (Fig. 4 and Fig. 5), growth rates were similar at given sets of conditions with only a few exceptions (e.g. MT-ML, MT-HL). Highest growth rates for all three cultures were generally found at medium temperature and medium and high light (Fig. 4, 5, 6).

For all species, growth rates differed in response to temperature (*N. oculata*, ANOVA: $df = 2$, $F = 16.94$, $p < 0.001$; *P. lutheri*, ANOVA: $df = 2$, $F = 26.90$, $p < 0.001$; *T. pseudonana*, ANOVA: $df = 2$, $F = 4.17$, $p = 0.020$), and light (*N. oculata*, ANOVA: $df = 2$, $F = 210.38$, $p < 0.001$; *P. lutheri*, ANOVA: $df = 2$, $F = 524.91$, $p < 0.001$; *T. pseudonana*, ANOVA: $df = 2$, $F = 269.91$, $p < 0.001$); there was also a significant light-temperature interaction (*N. oculata*, ANOVA: $df = 2$, $F = 18.32$, $p < 0.001$; *P. lutheri*, ANOVA: $df = 2$, $F = 24.78$, $p < 0.001$; *T. pseudonana*, ANOVA: $df = 2$, $F = 4.25$, $p = 0.018$). For all cultures, at low light, there was little difference in growth rate with increasing temperature (Fig. 4, 5, 6). However, at medium and high light, increasing temperature from low to medium did result in a higher growth rate in *P. lutheri* (Fig. 5) and *T. pseudonana* (Fig. 6). For all cultures, within a light level, growth was either

highest at medium temperature or there was no difference between growth at medium and high temperature (Fig. 4, 5, 6).

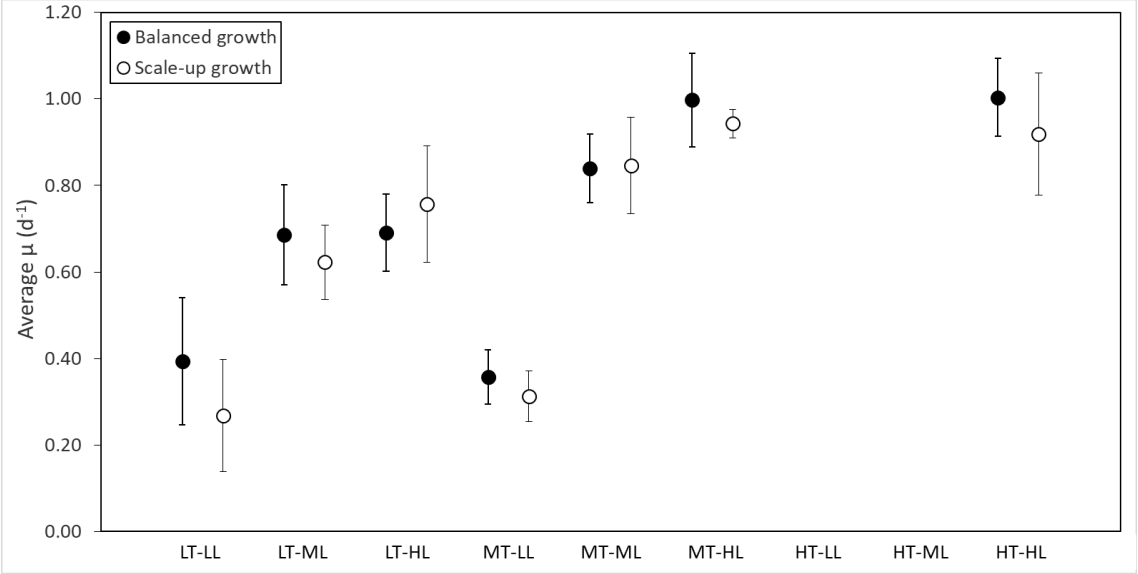

Figure 4. Mean balanced and scaled-up specific growth rate (μ) of *N. oculata* within temperature (LT, MT, HT) and light (LL, ML, HL) treatments (mean ± sd; balanced growth: n = 8 to 19, scale-up growth: n = 4 to 16).

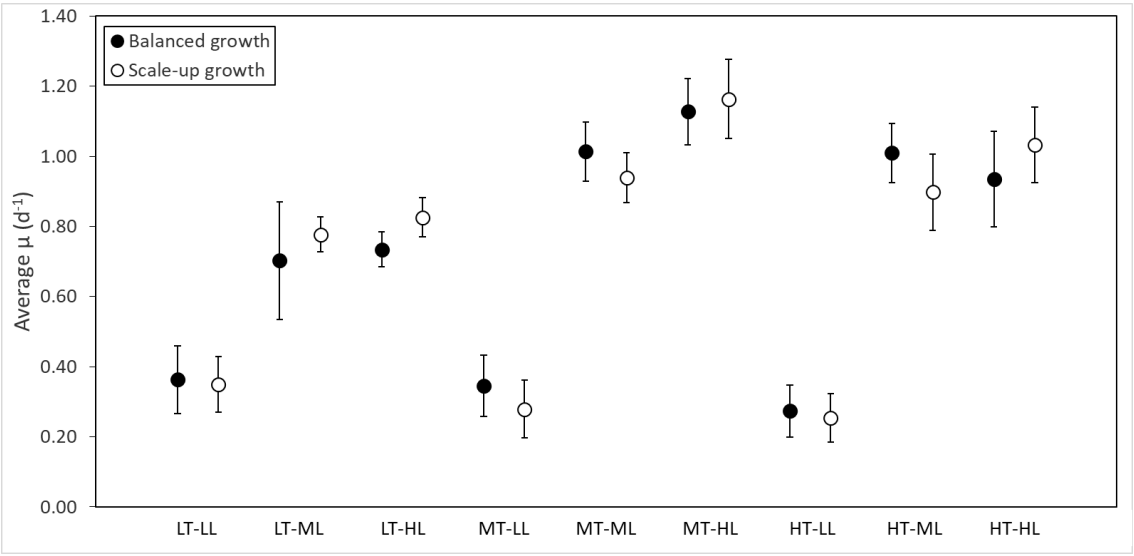

Figure 5. Mean balanced and scaled-up specific growth rate (μ) of *P. lutheri* within temperature (LT, MT, HT) and light (LL, ML, HL) treatments (mean ± sd; balanced growth: n = 8 to 27, scale-up growth: n = 6 to 16).

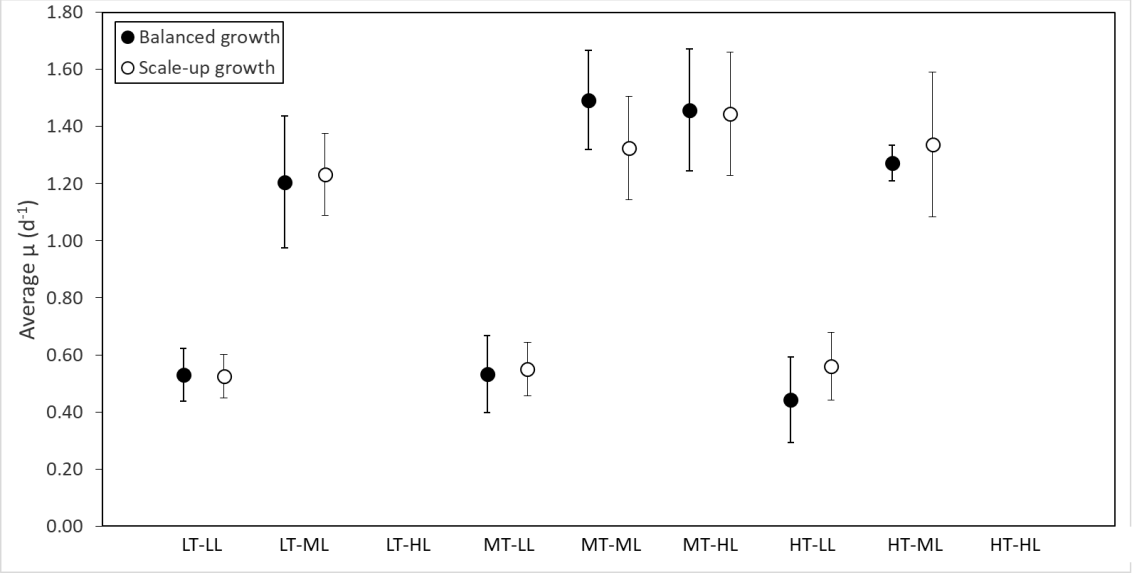

Figure 6. Mean balanced and scaled-up specific growth rate (μ) of *T. pseudonana* within temperature (LT, MT, HT) and light (LL, ML, HL) treatments (mean ± sd; balanced growth: n = 8 to 17, scale-up growth: n = 2 to 12).

3.2 PHYTOPLANKTON-TO-BACTERIA RATIO

A high temperature-low light replicate of *T. pseudonana* was excluded due to an inconclusive bacterial count. Despite efforts, bacterial growth was present in all treatments. However, bacterial load was relatively low compared to phytoplankton load (Fig. 7) and the mean bacterial proportion differed with species (KW: df = 2, $X^2_{0.95}$ = 35.66, $p < 0.01$). The mean phytoplankton/bacteria ratio was ~7.6X higher in *N. oculata* (9.45 ± 5.40) and ~8.9X higher in *T. pseudonana* (10.76 ± 11.35) compared to *P. lutheri* (Fig. 7; 1.82 ± 1.01, Dunn's: $p < 0.01$) but mean ratios between *N. oculata* and *T. pseudonana* did not differ (Fig. 7). Across conditions, the ratio did not differ for *N. oculata*; however, bacterial loads did vary with *P. lutheri* (KW: df = 2, $X^2_{0.95}$ = 21.23, p = 0.01) and *T. pseudonana* (KW: df = 2, $X^2_{0.95}$ = 16.09, p = 0.01). Eight out of eleven significant comparisons in *P. lutheri* and six out of nine comparisons in *T. pseudonana* involved low temperature treatments.

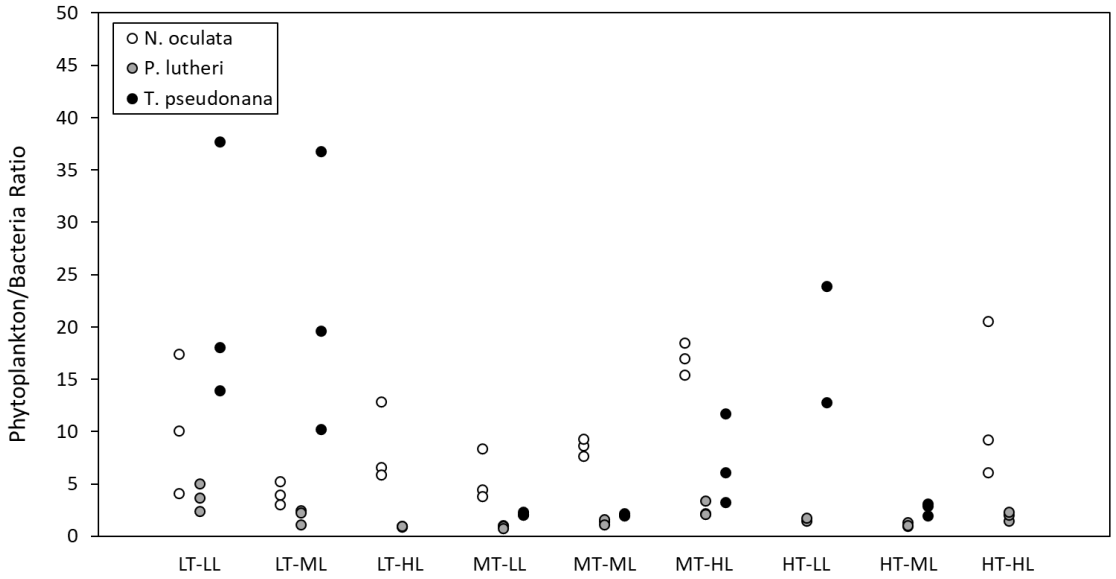

Figure 7. Phytoplankton to bacteria cell ratio of *N. oculata*, *P. lutheri*, and *T. pseudonana* within temperature (LT, MT, HT) and light (LL, ML, HL) treatments.

3.3 FA PROFILES

Fatty acid profile across all three species were dominated by 14:0, 16:0, 16:1n-7, and EPA (Appendix A1, A2, A3) but key differences were apparent. For instance, ARA was only present in *N. oculata*, and moderate amounts of SDA and DHA were found only in *P. lutheri*. Upon MDS of log-transformed FA data (Fig. 8), the FA profiles of *P. lutheri* and *T. pseudonana* appear to be moderately dissimilar, while *N. oculata* is dramatically different from the other two. Non-parametric multivariate analysis confirmed that the fatty acid profiles of the three species were different (PermANOVA: df = 1, Pseudo-F = 53.04, p = 0.001). In *T. pseudonana*, the FA peak resembling 18:4n-3 was found in appreciable amounts in all samples, but these occurrences were determined to be artifacts. These peak values were removed from the data and subsequently renormalized prior to statistical analysis.

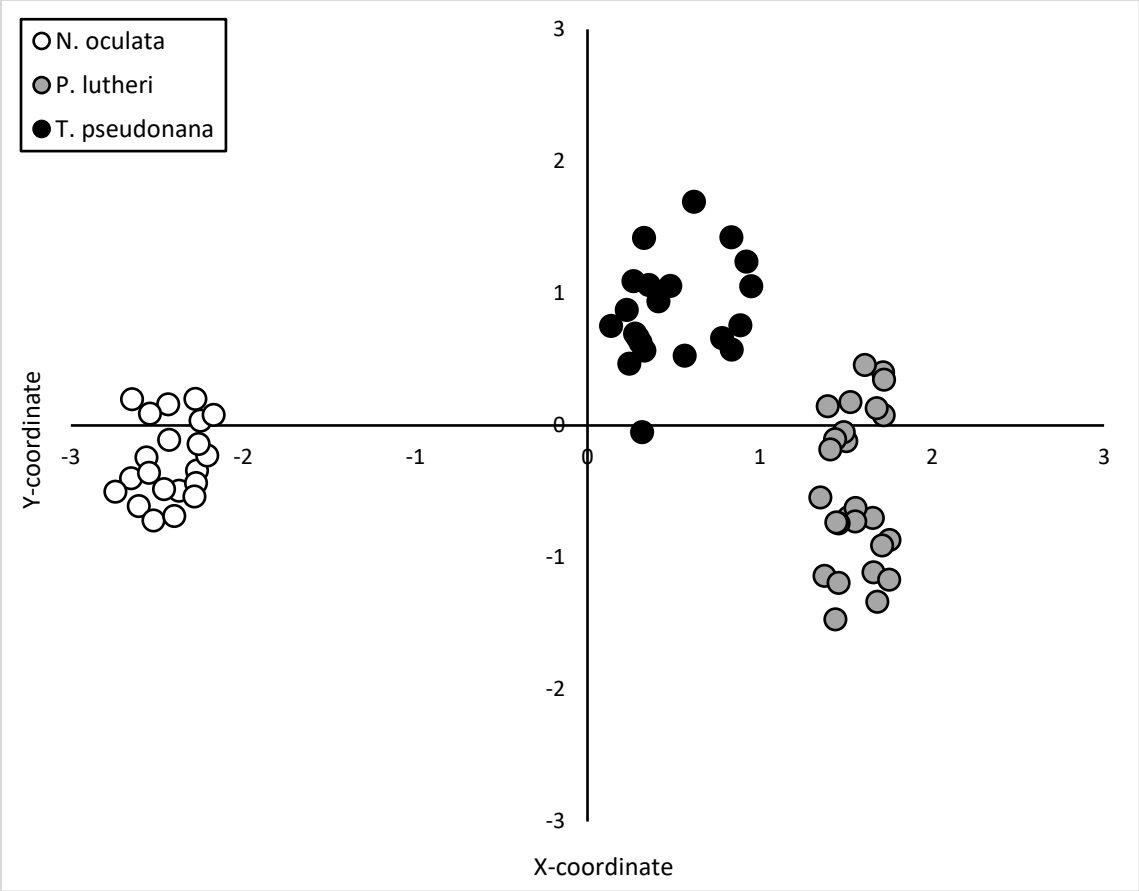

Figure 8. Non-parametric multi-dimensional scaling (nMDS) representation of the FA profile (>0.5% w/w of total FA) of *N. oculata*, *P. lutheri*, and *T. pseudonana*.

N. oculata:

The overall FA distribution of *N. oculata* changed with temperature (PermANOVA: df = 1, Pseudo-F = 1.64 x 10^5, $p < 0.01$) and light (PermANOVA: df = 1, Pseudo-F = 1.27 x 10^6, $p < 0.01$). The interaction of light and temperature was not significant. ANOVA indicated that both % EPA and % ARA (relative to total mass FA) varied with temperature (EPA: df = 2, F = 19.25, $p < 0.001$; ARA: df = 2, F = 110.66, $p < 0.001$) and light (EPA: df = 2, F = 199.05, $p < 0.001$; ARA: df = 2, F = 332.58, $p < 0.001$) with a significant interaction of the two factors (EPA: df = 2, F = 5.81, p = 0.015; ARA: df = 2, F = 12.37, p = 0.001). Highest % EPA and % ARA were observed in the medium temperature-low light group (Fig. 9B; 29.8 ± 0.9%; 5.1 ± 0.1%) and equivalent % EPA

were found in low temperature-low light (Fig. 9A; 27.5 ± 2.2%). Within a light level, there was little change in % EPA with increasing temperature (Fig. 9). However, % ARA were found to consistently increase with increasing temperature (Fig. 9; Tukey's: $p < 0.009$ for comparisons), except between medium temperature and high temperature within high light where there was no difference (Fig. 9B, 9C). Within a given temperature, both % EPA and % ARA usually decreased when light was increased (Fig. 9A, 9B; Tukey's: $p < 0.019$ for comparisons). However, there was no difference in % EPA between medium light and high light within low temperature (Fig. 9A).

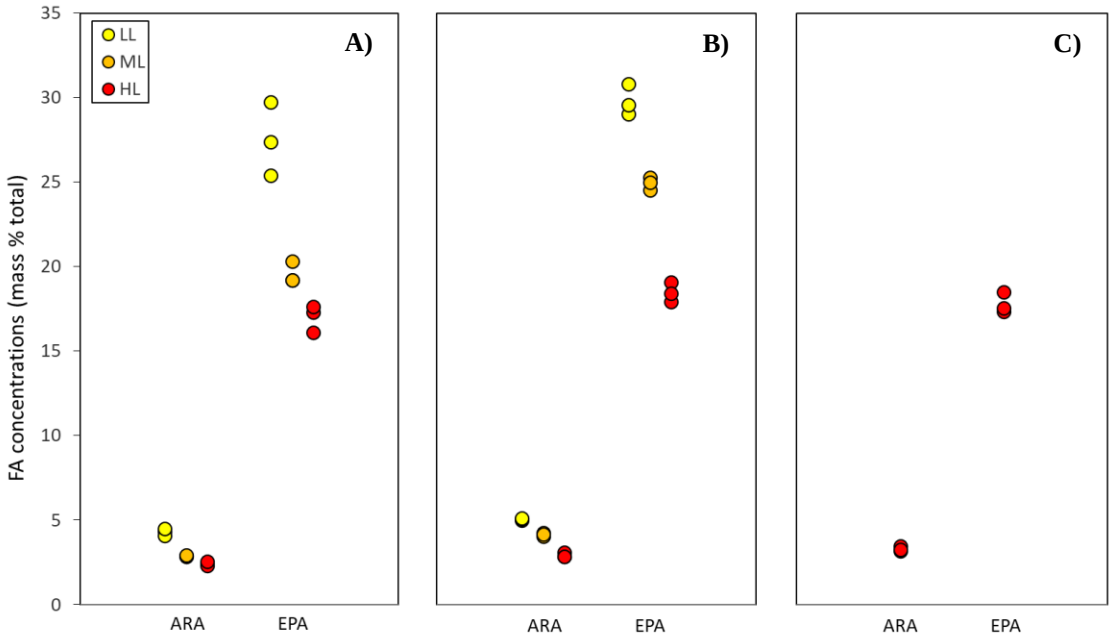

Figure 9. Fatty acid proportions (expressed as mass percent of total FA mass) of major PUFA in *N. oculata* within A) low temperature, B) medium temperature, and C) high temperature, and light (LL, ML, HL) treatments.

P. lutheri:

As with *N. oculata*, the overall FA distribution changed with temperature (PermANOVA: df = 1, Pseudo-F = 3.59×10^3, $p < 0.01$) and light (PermANOVA: df = 1, Pseudo-F = 7.78×10^5, $p < 0.01$), but the interaction of light and temperature was not significant (PermANOVA: df = 1, Pseudo-F = 0.99, p = 0.322). ANOVA revealed that %

EPA and % DHA changed with temperature (EPA: df = 2, F = 71.54, $p < 0.001$; DHA: df = 2, F = 39.99, $p < 0.001$) and light (EPA: df = 2, F = 441.16, $p < 0.001$; DHA: df = 2, F = 30.30, $p < 0.001$); the interaction between the two factors was also significant (EPA: df = 2, F = 21.68, $p < 0.001$; DHA: df = 2, F = 9.44, $p < 0.001$). Similar to *N. oculata,* % EPA was highest at medium temperature (Fig. 10B; 25.3 ± 0.3%) and low temperature (Fig. 10A; 25.0 ± 1.2%) at low light. Highest % DHA was 8.0% and was achieved at low temperature (Fig. 10A) and medium temperature (Fig. 10B) within both medium light and high light (no difference in values at separate conditions).

Within a light level, temperature did not have a consistent effect on major PUFA percent (Fig. 10). For instance, between low temperature (Fig. 10A) and medium temperature (Fig. 10B) in medium light, % EPA increased (17.5 ± 0.2% compared to 22.0 ± 0.3%, Tukey's: $p < 0.001$), but at all three light levels, % EPA was always lower at high temperature (Fig. 10C) compared to medium temperature (Fig. 10B; Tukey's: $p < 0.003$ for comparisons). For DHA, at all three light levels, % DHA were similar between low (Fig. 10A) and medium temperature (Fig. 10B) but were lower at high temperature (Fig. 10C) than at medium temperature, similar to EPA (Tukey's: $p < 0.005$ for comparisons). Within a given temperature, increases in light almost always coincided with a decrease in % EPA (Fig. 10; Tukey's: $p < 0.009$ for comparisons). An exception occurred in high temperature between low light and medium light, where % EPA were the same (Fig. 10C). % DHA across light was much less variable, remaining mostly unchanged across conditions (Fig. 10). However, at medium temperature, the % DHA was lower at low light than at medium or high light (Fig. 10B; Tukey's: $p < 0.001$ for comparisons).

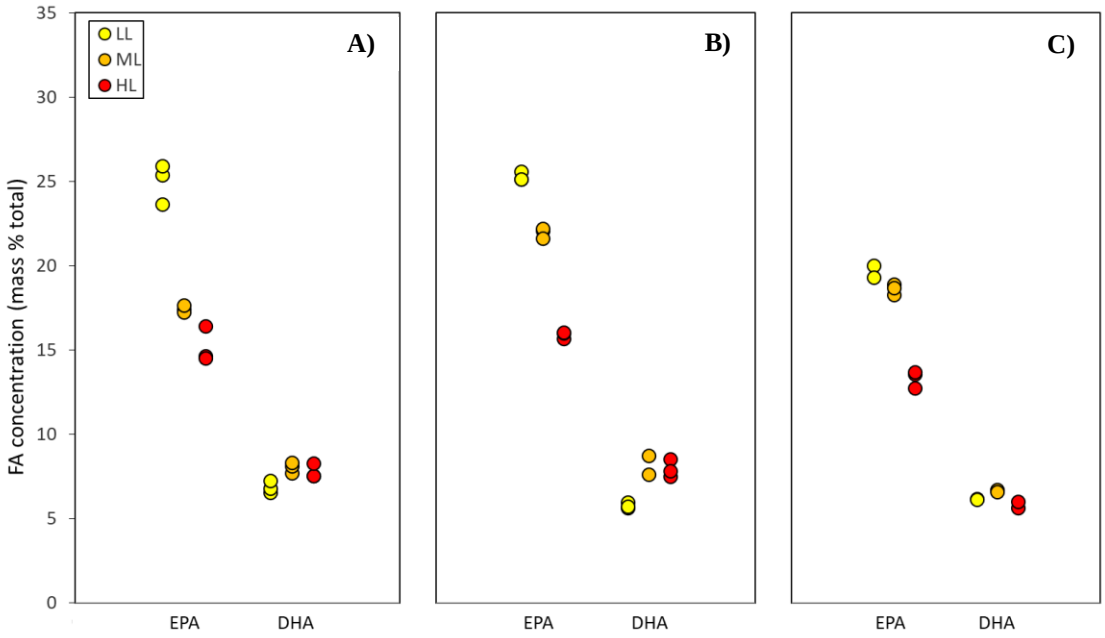

Figure 10. Fatty acid proportions (expressed as mass percent of total FA mass) of major PUFA in *P. lutheri* within A) low temperature, B) medium temperature, and C) high temperature, and light (LL, ML, HL) treatments.

T. pseudonana:

The overall FA profile of *T. pseudonana* varied with temperature (PermANOVA: df = 1, Pseudo-F = 1.15 x 10^3, $p < 0.01$) and light (PermANOVA: df = 1, Pseudo-F = 4.95 x 10^5, $p < 0.01$), and showed a significant interaction (PermANOVA: df = 1, Pseudo-F = 5.51, $p = 0.03$). Like the other two species, % EPA changed with temperature (ANOVA: df = 2, F = 40.36, $p < 0.001$), light (ANOVA: df = 2, F = 493.99, $p < 0.001$), and their interaction (ANOVA: df = 2, F = 42.06, $p < 0.001$). In this species, highest % EPA were achieved at high temperature (Fig. 11C; 20.8 ± 0.4%) and medium temperature (Fig. 11B; 19.6 ± 0.5%, Tukey's: $p = 0.189$) at low light. Again, temperature did not have a consistent effect on % EPA; however, like the other two species, effects of light were more predictable (Fig. 11). In all comparisons, % EPA decreased with increasing light (Fig. 11; Tukey's: $p < 0.002$ for comparisons).

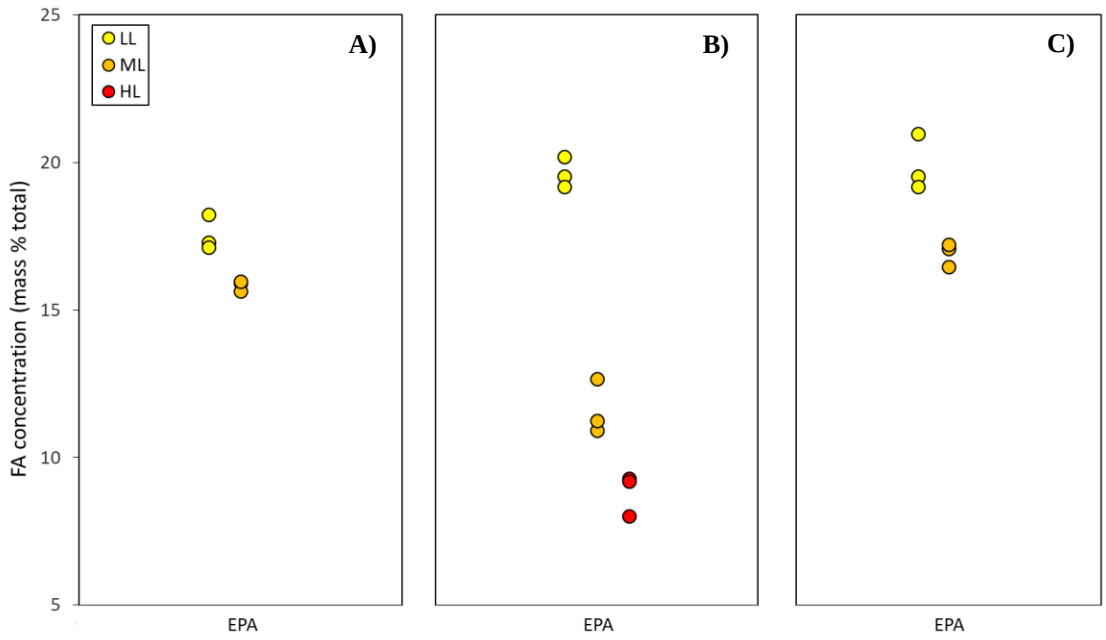

Figure 11. Fatty acid proportions (expressed as mass percent of total FA mass) of major PUFA in *T. pseudonana* within A) low temperature, B) medium temperature, and C) high temperature, and light (LL, ML, HL) treatments.

3.4 FA CONCENTRATION

N. oculata:

When considered relative to mass of carbon, only temperature influenced mean θ_{EPA} and ARA:C (θ_{ARA}) in *N. oculata* (ANOVA: EPA - df = 2, F = 10.48, p = 0.002; ANOVA: ARA - df = 2, F = 4.93, p = 0.024). θ_{EPA} was ~15 mg EPA g C^{-1} lower at medium temperature (Fig. 12B) than low temperature (Fig. 12A; 69.0 vs. 84.2 mg EPA g C^{-1}, Tukey's: p = 0.001). θ_{ARA} was higher at the high temperature (Fig. 12C) than at medium temperature (Fig. 12B; Tukey's: p = 0.048). θ_{EPA} and θ_{ARA} were highest at low temperature with values of 88.4 mg EPA g C^{-1} and 13.9 mg ARA g C^{-1} (Fig. 12A). $\theta_{Chl\text{-}a}$ varied with light (ANOVA: df = 2, F = 242.47, p < 0.001); there was also a significant interaction of temperature and light (ANOVA: df = 2, F = 55.13, p < 0.001). Within a given light, differences were only observed between low (Fig. 12A) and medium temperature (Fig. 12B), where $\theta_{Chl\text{-}a}$ was lower at medium temperature (Tukey's: p < 0.009 for comparisons). Within a given temperature, increasing light almost always

resulted in a sharp decline in $\theta_{Chl\text{-}a}$ (Fig. 12; Tukey's: $p < 0.030$ for comparisons). An exception occurred between low and medium light in low temperature, where $\theta_{Chl\text{-}a}$ were similar (Fig. 12A; 53.5 vs. 48.0 mg Chl-a g C^{-1}).

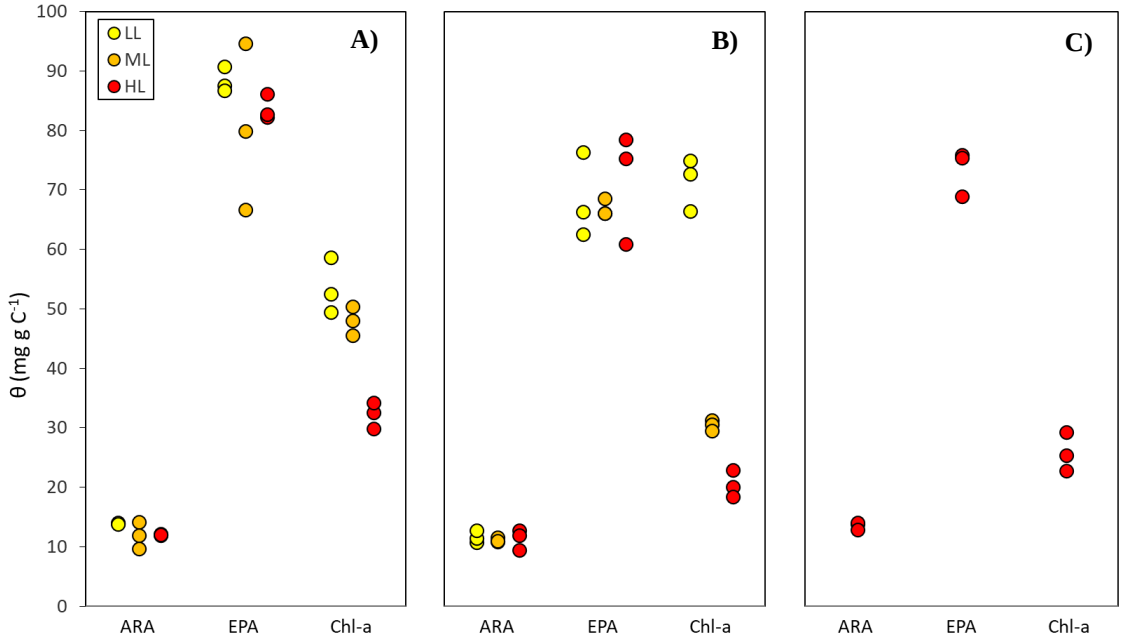

Figure 12. Major FA and Chl-a concentration (θ expressed as mg g C^{-1}) of *N. oculata* within A) low temperature, B) medium temperature, and C) high temperature, and light (LL, ML, HL) treatments.

P. lutheri:

Whereas only temperature influenced PUFA concentration in *N. oculata*, both θ_{EPA} and DHA:C (θ_{DHA}) in *P. lutheri* varied with temperature (ANOVA: EPA - df = 2, F = 38.75, $p < 0.001$; ANOVA: DHA - df = 2, F = 5.33, $p = 0.016$), light (ANOVA: EPA - df = 2, F = 128.37, $p < 0.001$; ANOVA: DHA - df = 2, F = 11.27, $p < 0.001$), and the interaction effect (ANOVA: EPA - df = 2, F = 17.91, $p < 0.001$; ANOVA: DHA - df = 2, F = 4.34, $p = 0.013$). Peak θ_{EPA} occurred at medium temperature-low light (corresponding to maximum EPA proportion) where it averaged 69.8 ± 5.1 mg EPA g C^{-1} (Fig. 13B). On the other hand, highest θ_{DHA} was 19.2 mg DHA g C^{-1} achieved across medium (Fig. 13B) and high temperature (Fig. 13C; no difference in values at separate conditions).

Holding light constant, temperature effects were inconsistent in major PUFA concentrations (Fig. 13). At low and medium light, θ_{EPA} was highest at medium temperature (Fig. 13B). Almost all comparisons had similar θ_{DHA}, except between medium (Fig. 13B) and high temperature (Fig. 13C) in high light, where an increase of ~4.3 mg DHA g C^{-1} was seen (15.9 vs. 20.2 mg EPA g C^{-1}). Within a given temperature, variation in θ_{EPA} with increasing light was more consistent. At low (Fig. 13A) and medium temperature (13B), strong declines in θ_{EPA} occurred with increasing light. The largest difference was at medium temperature between low and high light, where a ~38.0 mg EPA g C^{-1} reduction was observed (Fig. 13B; 31.8 vs. 69.8 mg EPA g C^{-1}). Oddly, while θ_{EPA} changed with light, θ_{DHA} remained relatively constant (Fig. 13A, 13C), with the exception of cultures at medium temperature (Fig. 13B), where θ_{DHA} increased from low to medium light (16.0 vs 21.1 mg DHA g C^{-1}), then decreased by roughly the same amount (21.1 vs. 15.9 mg DHA g C^{-1}). Like θ_{EPA} and θ_{DHA}, θ_{Chl} differed across temperature (ANOVA: $df = 2$, $F = 23.70$, $p < 0.001$) and light (ANOVA: $df = 2$, $F = 796.84$, $p < 0.001$), and also showed a significant interaction (ANOVA: $df = 2$, $F = 84.09$, $p < 0.001$). Significant changes occurred only at low light, where low (Fig. 13A) and medium temperature (Fig. 13B) were significantly higher in $\theta_{Chl\text{-}a}$ than at high temperature (Fig. 13C). Holding temperature constant, $\theta_{Chl\text{-}a}$ dramatically decreased with increasing light at low and medium temperature (Fig. 13B; Tukey's: $p < 0.001$ for comparisons). At high temperature, $\theta_{Chl\text{-}a}$ was equivalent at low and medium light (Fig. 13C).

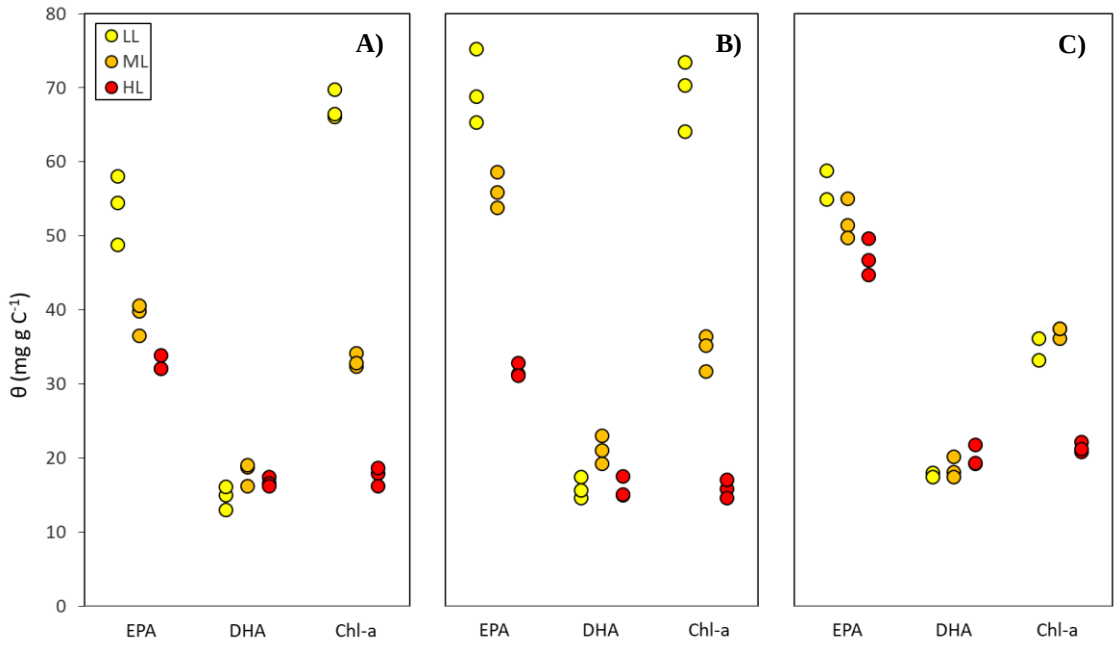

Figure 13. Major FA and Chl-a concentration (θ expressed as mg g C^{-1}) of *P. lutheri* within A) low temperature, B) medium temperature, and C) high temperature, and light (LL, ML, HL) treatments.

T. pseudonana:

Like *P. lutheri*, EPA yield was found to vary with temperature (ANOVA: df = 2, F = 49.80, $p < 0.001$) and light (ANOVA: df = 2, F = 272.41, $p < 0.001$), with a significant interaction of the two (ANOVA: df = 2, F = 20.04, $p < 0.001$). Highest EPA concentration was achieved at high temperature-low light (Fig. 14C; 73.30 ± 4.05 mg EPA g C^{-1}), similar to mass percent (Fig. 11C). At low light, EPA increased with temperature; however, it did not vary with temperature at medium light (Fig. 14A, 14B, 14C; Tukey's: $p < 0.022$ for comparisons). As in *P. lutheri*, light had a consistent influence on EPA concentration within a given temperature with increasing light always coinciding with sharp declines in EPA yield (Fig. 14), of which the greatest differences occurred at medium temperature (Fig. 14B). For instance, EPA concentration was reduced by ~37.2 mg EPA g C^{-1} when high light was compared to low light at medium temperature (Fig. 14B; 57.2 vs. 20.0 mg EPA g C^{-1}). θ_{Chl} was found to only differ with temperature (ANOVA: F = 81.81, $p < 0.001$) and light (ANOVA: F = 633.77, $p < 0.001$). From low to

medium conditions of both light and temperature, mean Chl-a concentration decreased significantly (Fig. 14A, 14B; Tukey's: $p < 0.001$ for comparisons).

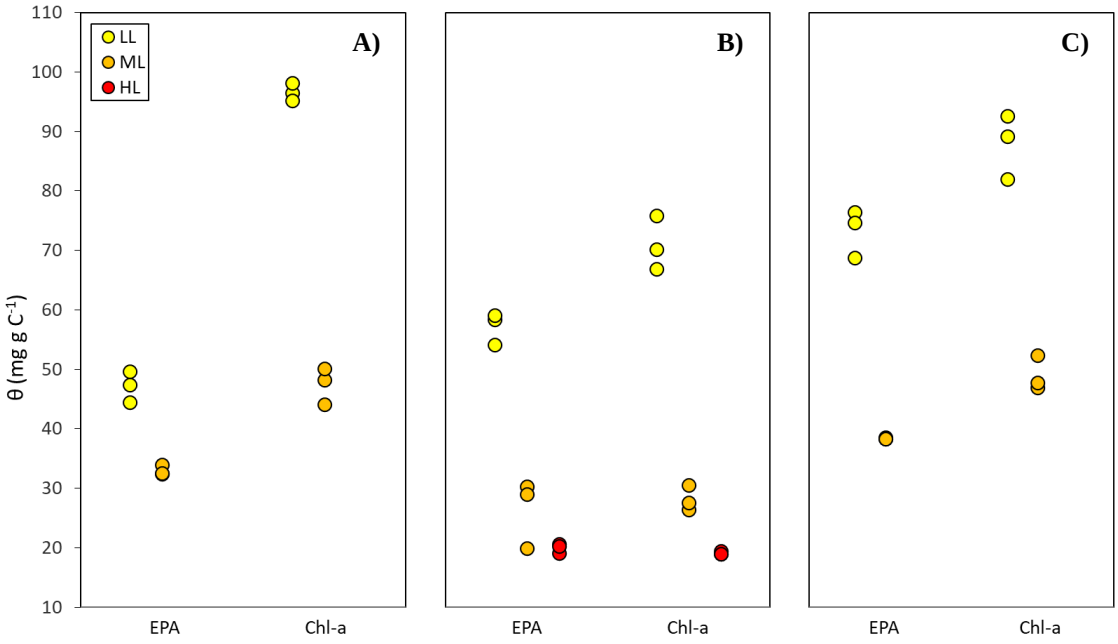

Figure 14. Major FA and Chl-a concentration (θ expressed as mg g C^{-1}) of *T. pseudonana* within A) low temperature, B) medium temperature, and C) high temperature, and light (LL, ML, HL) treatments.

3.5 FA PRODUCTION RATE

N. oculata:

When analyzing FA production rates, ANOVA showed that both EPA and ARA production was significantly affected by temperature (EPA: df = 2, F = 21.73, $p < 0.001$; ARA: df = 2, F = 46.84, $p < 0.001$) and light (EPA: df = 2, F = 77.54, $p < 0.001$; ARA: df = 2, F = 55.74, $p < 0.001$). Means of major FA production rates between both low and medium temperature, and medium and high light were not different (Fig. 15). Maximum EPA production averaged ~51.9 mg EPA g C^{-1} day^{-1} and ARA production averaged ~8.39 mg ARA g C^{-1} day^{-1} for all treatments (Fig. 15).

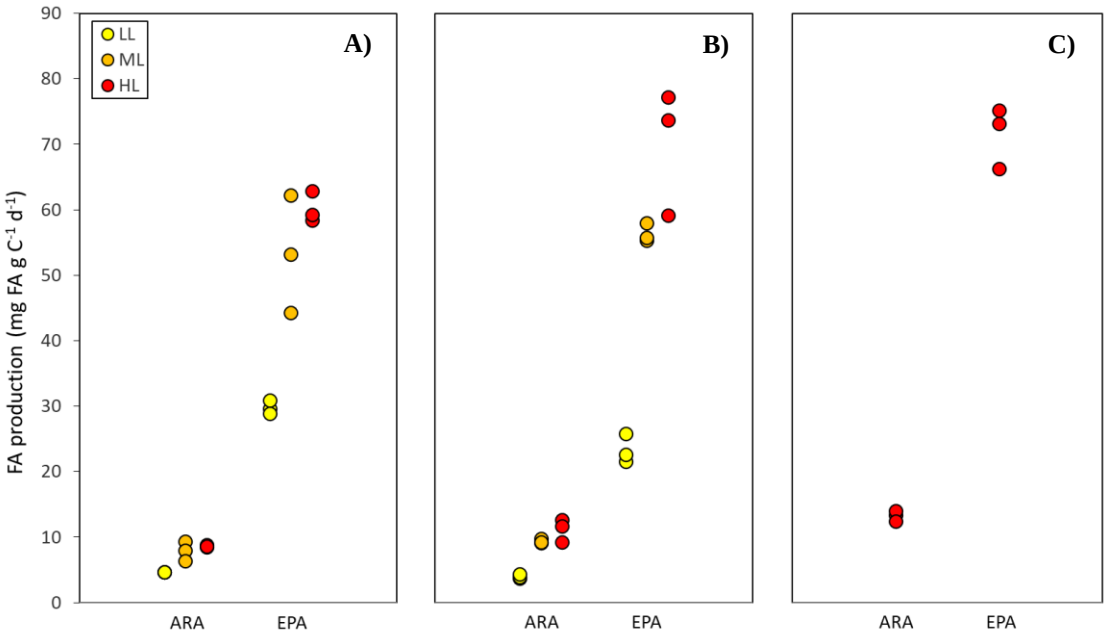

Figure 15. Major FA production (mg FA g C^{-1} day^{-1}) of *N. oculata* within A) low temperature, B) medium temperature, and C) high temperature, and light (LL, ML, HL) treatments.

P. lutheri:

As with mass percent and concentration, both EPA and DHA production were influenced by temperature (ANOVA: df = 2, F = 207.37, $p < 0.001$; ANOVA: df = 2, F = 47.10, $p < 0.001$) and light (ANOVA: df = 2, F = 389.03, $p < 0.001$; ANOVA: df = 2, F = 261.30, $p < 0.001$), with a significant interaction (ANOVA: df = 2, F = 67.11, $p < 0.001$; ANOVA: df = 2, F = 12.76, $p < 0.001$). Highest EPA production rate were reached at medium and high temperature in medium light (Fig. 16B, 16C; MT: 55.1 ± 2.3 mg EPA g C^{-1} day^{-1}; HT: 52.2 ± 2.6 mg EPA g C^{-1} day^{-1}). Maximum DHA production reached ~19.3 mg DHA g C^{-1} day^{-1} attained at medium and high temperature, and medium and high light conditions (Fig. 16B, 16C).

There was no consistent effect of temperature (within a given light) on major FA production. Within low light levels, EPA production rates involving low temperature treatments were not different (Fig. 16). Within medium light, medium and high temperature EPA production rates were not different (Fig. 16B, 16C), while all

comparisons within high light were different (Fig. 16; Tukey's: $p < 0.001$ for comparisons). DHA production rates responded slightly differently to EPA, where low temperature rates in medium and high light were significantly different than the other temperatures (Fig. 16A, 16B, 16C; Tukey's: $p < 0.002$ for comparisons). Conversely, EPA production was consistently the highest in medium light and lowest in low light at all three temperatures (Fig. 16). For DHA, production also increased in medium and high light compared to low light at all three temperatures (Fig. 16).

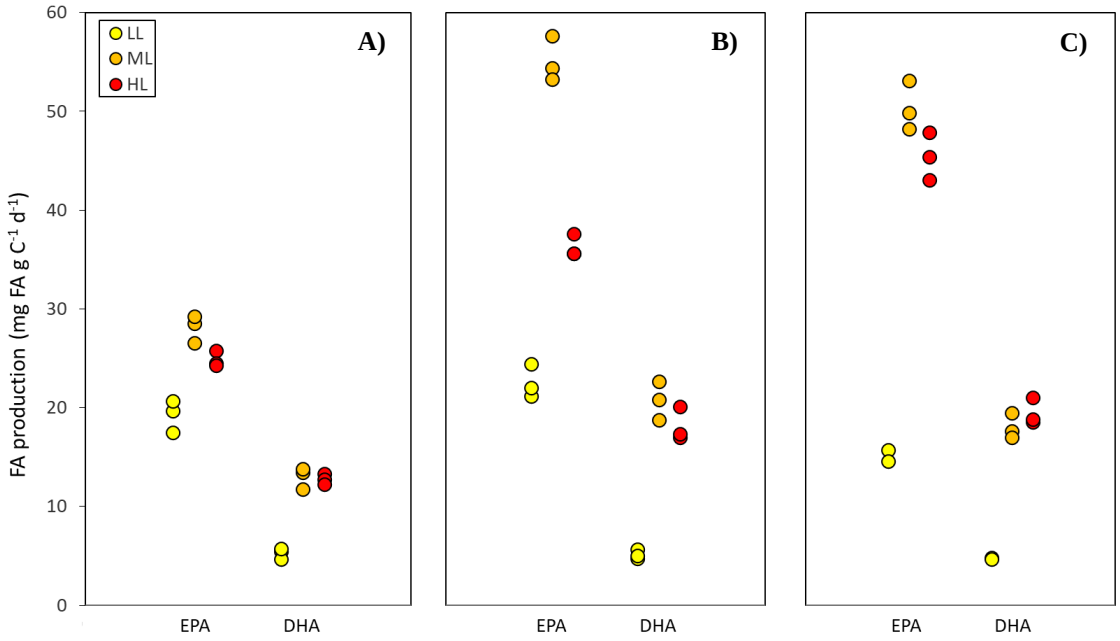

Figure 16. Major FA production (mg FA g C^{-1} day^{-1}) of *P. lutheri* within A) low temperature, B) medium temperature, and C) high temperature, and light (LL, ML, HL) treatments.

T. pseudonana:

EPA production in *T. pseudonana* was found to vary by temperature (ANOVA: df = 2, F = 19.63, $p < 0.001$) and light (ANOVA: df = 2, F = 30.429, $p < 0.001$). Like *N. oculata*, there was no significant interaction between temperature and light. The mean EPA production increased between low and high temperature (Fig. 17A, 17B), and between low and medium light (Fig. 17; Tukey's: $p < 0.001$ for comparisons). EPA

production was highest at medium light, where it averaged ~41.7 mg EPA g C^{-1} day^{-1} (Fig. 17).

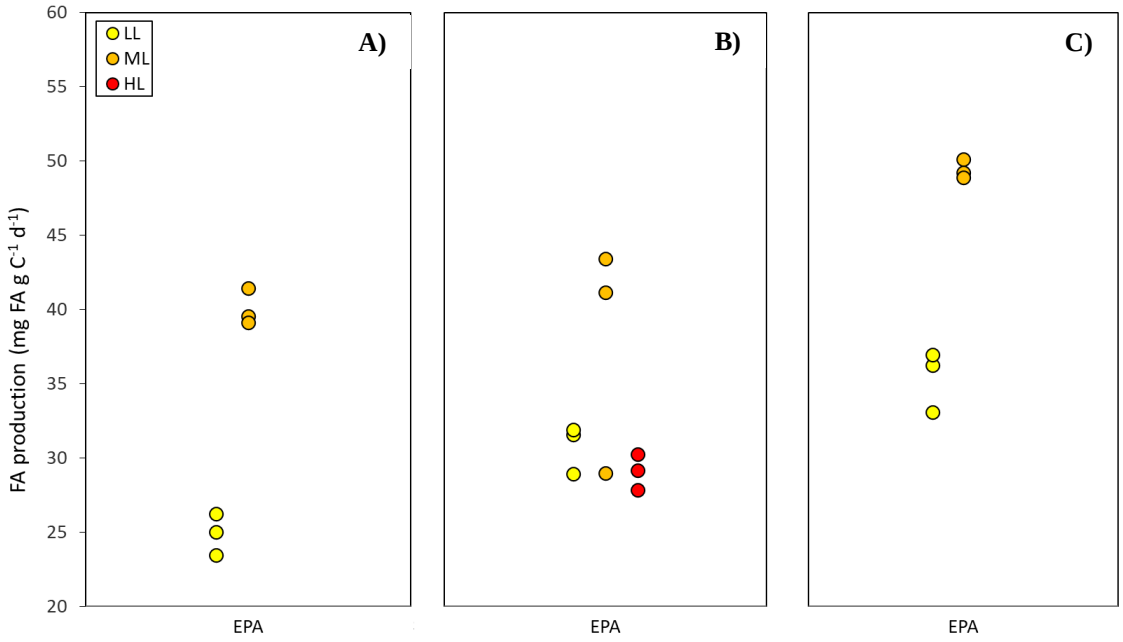

Figure 17. Major FA production (mg FA g C^{-1} day^{-1}) of *T. pseudonana* within A) low temperature, B) medium temperature, and C) high temperature, and light (LL, ML, HL) treatments.

3.6 FA/CHL-A RATIOED

EPA/Chl-a was found to range by ~1 to 4 in *N. oculata* (Fig. 18), ~0.75 to 2.5 in *P. lutheri* (Fig. 19), and ~0.5 to 1.1 in *T. pseudonana* (Fig. 20). ARA/Chl-a ranged from ~0.15 to 0.6 (Fig. 21) and DHA/Chl-a ranged from ~0.2 to 1 (Fig. 22). ANOVA showed that EPA/Chl-a for all three species was significantly different with temperature (*N. oculata*: df = 2, F = 3.80, p = 0.048; *P. lutheri*: df = 2, F = 40.20, p < 0.001; *T. pseudonana*: df = 2, F = 23.44, p < 0.001) and light (*N. oculata*: df = 2, F = 125.20, p < 0.001; *P. lutheri*: df = 2, F = 190.10, p < 0.001; *T. pseudonana*: df = 2, F = 23.02, p < 0.001); there was also a significant interaction of the two (*N. oculata*: df = 2, F = 24.04, p < 0.001; *P. lutheri*: df = 2, F = 13.57, p < 0.001; *T. pseudonana*: df = 2, F = 4.66, p = 0.028). The same was observed for ARA/Chl-a in *N. oculata* (temperature - ANOVA: df = 2, F = 11.75, p = 0.001; light - ANOVA: df = 2, F = 116.56, p < 0.001; interaction -

ANOVA: df = 2, F = 25.62, $p < 0.001$) but DHA/Chl-a in *P. lutheri* varied only by light (ANOVA: df = 2, F = 301.04, $p < 0.001$) and had a significant interaction of temperature and light (ANOVA: df = 2, F = 10.42, $p < 0.001$). Light appeared to have a major and consistent influence on FA/Chl-a across temperature, with high light generating largest ratios across all species (Fig. 18, 19, 20, 21, 22). However, within species, FA/Chl-a across light groups appear more similar in magnitude, regardless of temperature conditions (Fig. 18, 19, 20, 21, 22). In *N. oculata,* within a given light, both EPA/Chl-a and ARA/Chl-a was highest at medium temperature, with the exception of low light where it was lowest (Fig. 18A, 21A; Tukey's: $p < 0.05$ for comparisons). In *P. lutheri*, EPA/Chl-a either remained relatively the same or increased with increasing temperature (Fig. 19A; Tukey's: $p < 0.02$ for all comparisons). In *T. pseudonana*, at low light, EPA/Chl-a increased with increasing temperature (Fig. 20A; Tukey's: $p = 0.002$ for all comparisons). DHA/Chl-a contrasted with the other FA/Chl-a ratios, where the only differences were found between low and high temperature, and medium and high temperature under low light conditions (Fig. 21A; Tukey's: $p \leq 0.001$ for comparisons).

EPA/Chl-a increased with increasing light in both *N. oculata* (Fig. 18B; Tukey's: $p < 0.002$ for all comparisons) and *P. lutheri* (Fig. 19B; Tukey's: $p < 0.007$ for all comparisons), with a couple of exceptions (*N. oculata*: LL to ML in LT, *P. lutheri*: LL to ML in HT). Strong relationships between EPA/Chl-a and light were also found in both species at low and medium temperature (Fig. 18B, 19B; $R^2 > 0.883$); however, the relationship was not found to be as strong at high temperature in *P. lutheri* (Fig. 19B; $R^2 = 0.626$). In *P. lutheri*, EPA/Chl-a ratios were quite similar regardless of temperature (Fig. 19B). In *T. pseudonana*, EPA/Chl-a stayed relatively constant, except between low and high light at medium temperature, where it increased (Tukey's: $p = 0.03$), consistent with a weak relationship between the ratio and light at medium temperature (Fig. 20B; $R^2 = 0.526$). ARA/Chl-a and DHA/Chl-a also increased with increasing light, in a very similar manner to EPA/Chl-a (Fig. 21B, 22B; Tukey's: $p < 0.03$ for comparisons), with one exception in both FA (ARA: LL and ML at LT, DHA: LL and ML at HT). As a result, both FA/Chl-a also exhibited strong relationships with light (Fig. 21B, 22B; $R^2 > 0.814$).

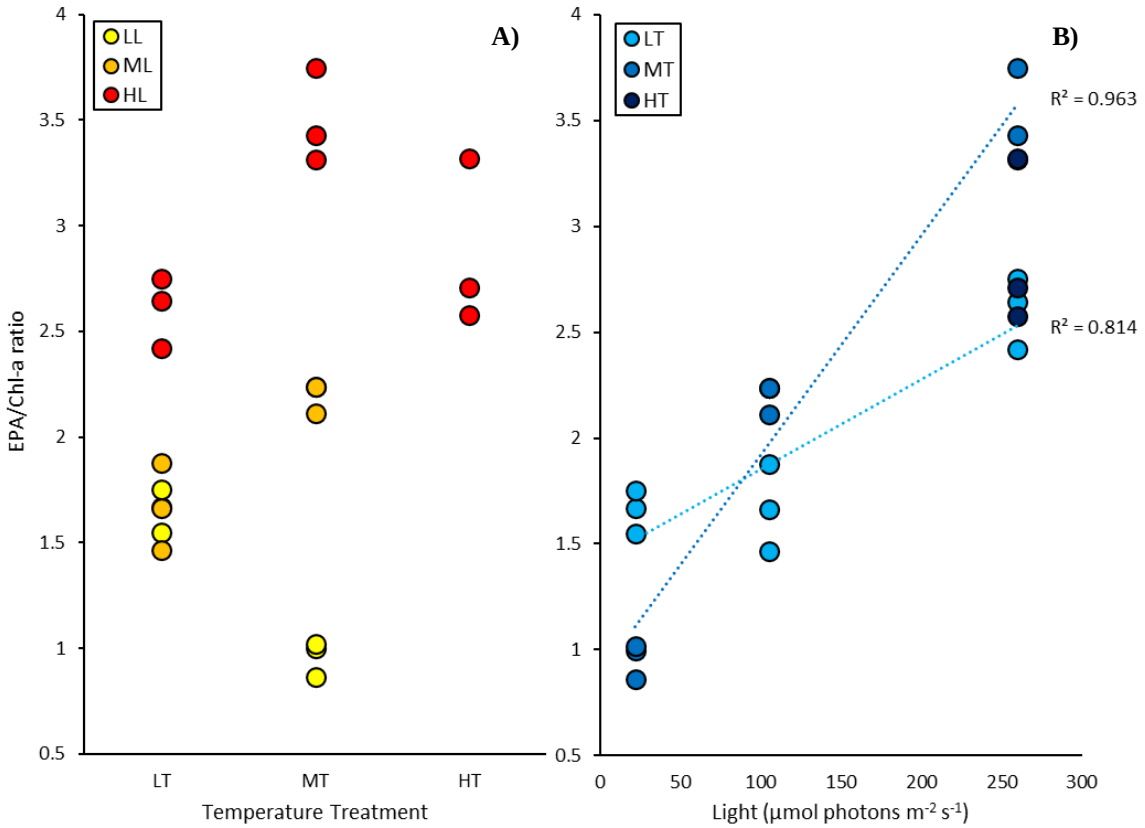

Figure 18. EPA/Chl-a ratio of *N. oculata* within temperature (LT, MT, HT) and light (LL, ML, HL) treatments, showing A) across temperatures (LT, MT, HT) and B) across light (µmol photons m^{-2} s^{-1}).

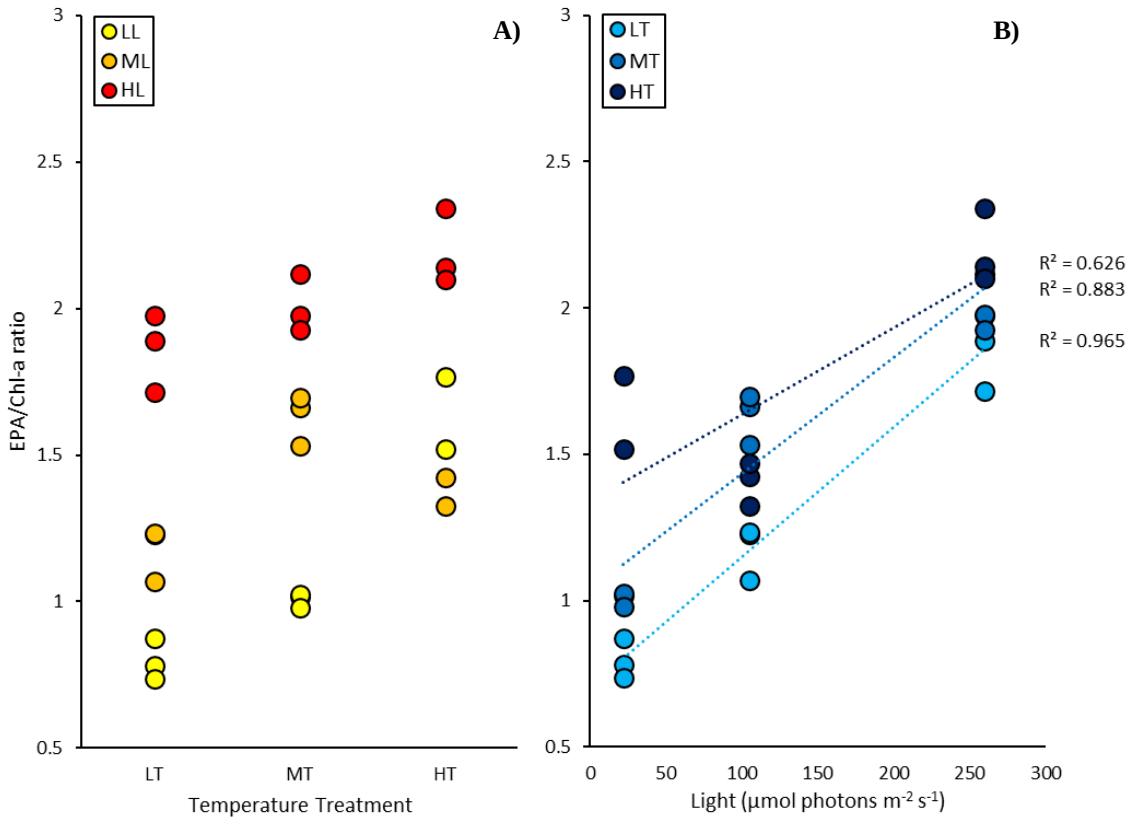

Figure 19. EPA/Chl-a ratio of *P. lutheri* within temperature (LT, MT, HT) and light (LL, ML, HL) treatments, showing A) across temperatures (LT, MT, HT) and B) across light (µmol photons m^{-2} s^{-1}).

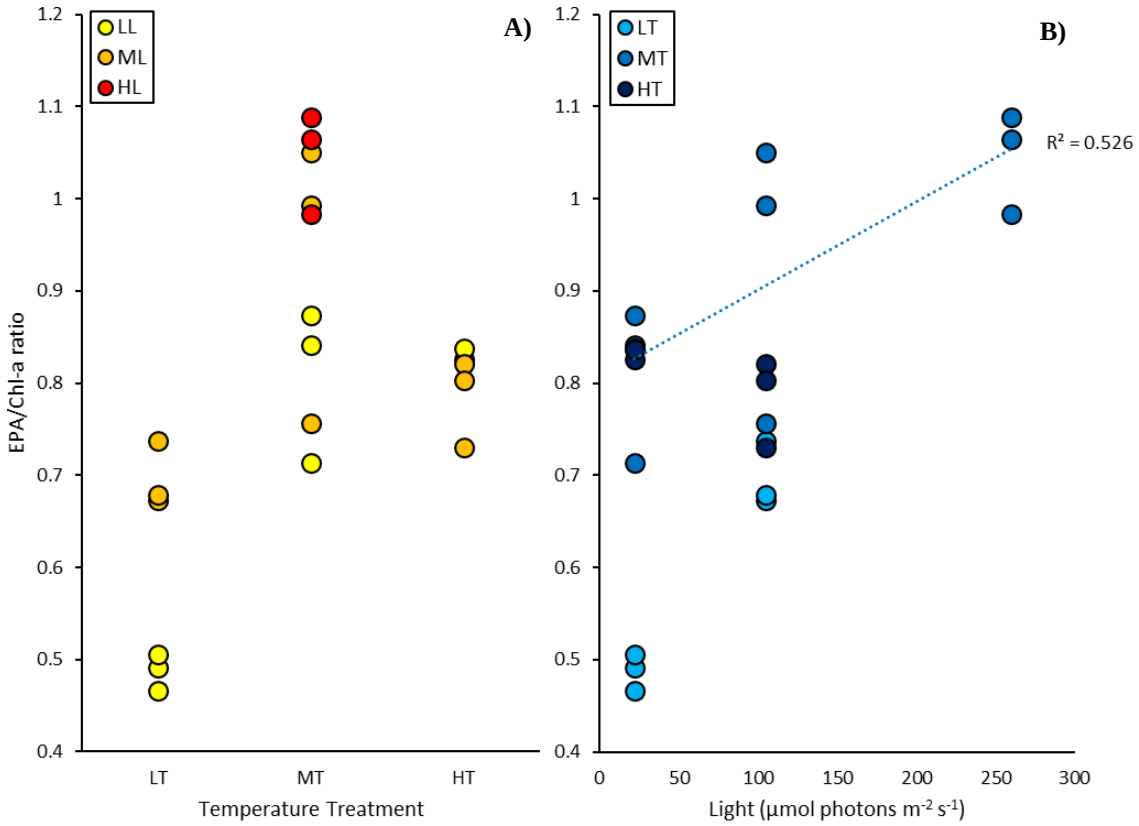

Figure 20. EPA/Chl-a ratio of T. *pseudonana* within temperature (LT, MT, HT) and light (LL, ML, HL) treatments, showing A) across temperatures (LT, MT, HT) and B) across light (µmol photons m^{-2} s^{-1}).

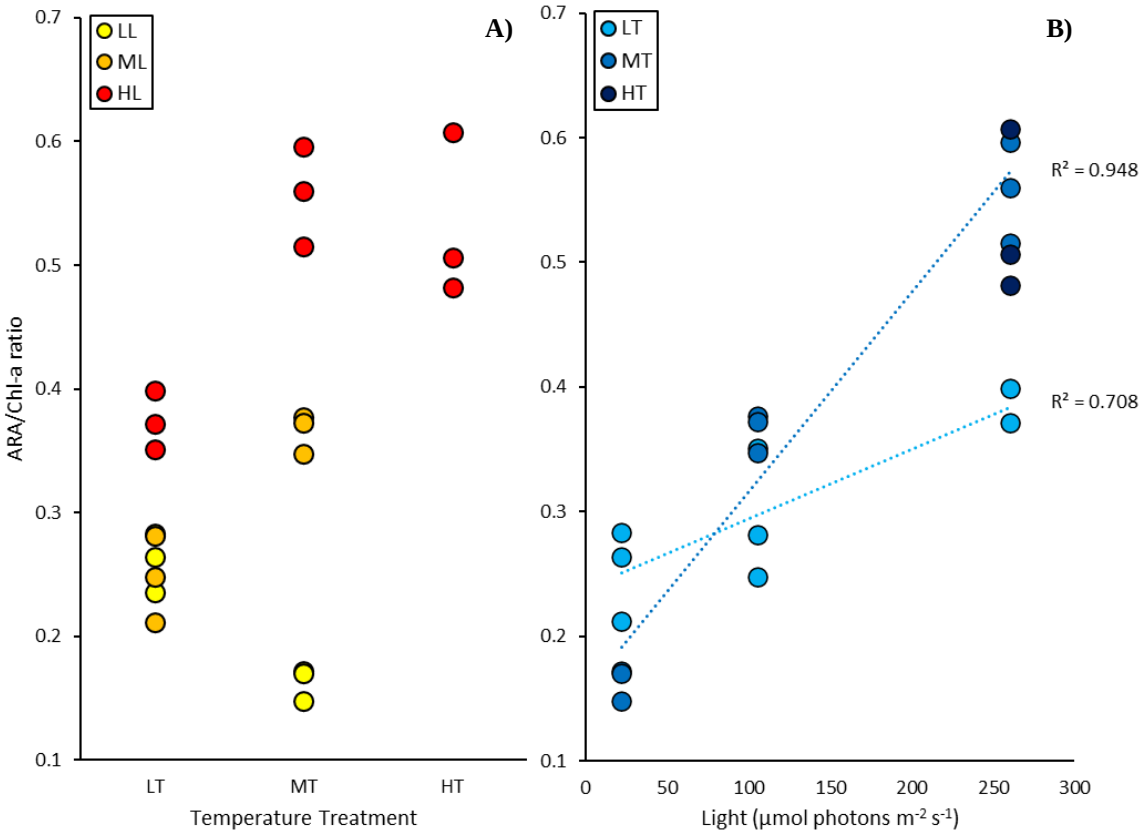

Figure 21. ARA/Chl-a ratio of *N. oculata* within temperature (LT, MT, HT) and light (LL, ML, HL) treatments, showing A) across temperatures (LT, MT, HT) and B) across light (µmol photons m^{-2} s^{-1}).

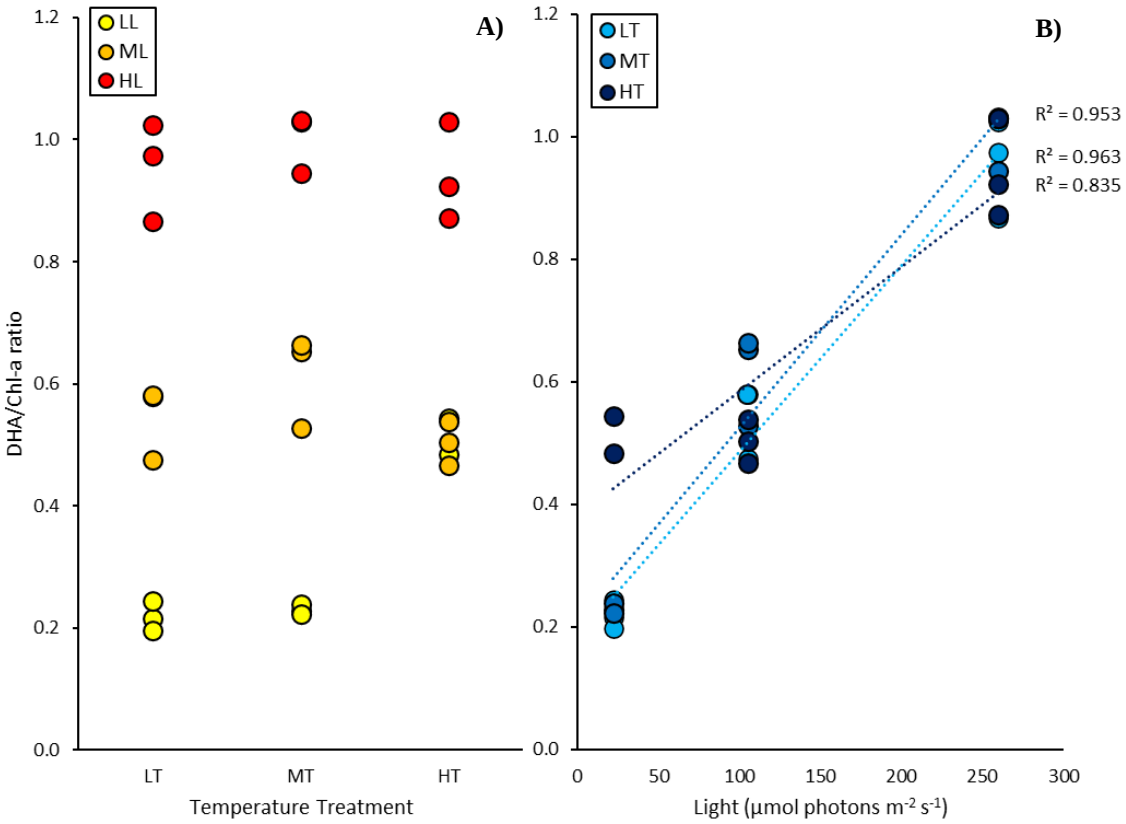

Figure 22. DHA/Chl-a ratio of *P. lutheri* within temperature (LT, MT, HT) and light (LL, ML, HL) treatments, showing A) across temperatures (LT, MT, HT) and B) across light (µmol photons m^{-2} s^{-1}).

CHAPTER 4 – DISCUSSION

4.1 FA/CHL-A RELATIONSHIP

There were two primary focuses within this study. The first was evaluating the potential of EPA/Chl-a as an effective screening tool for optimal EPA-producing strains. Prior to this study, the sequestering of EPA and Chl-a within plastidial membranes as well as predictable behaviour of both constituents suggested that a consistent relationship could be present across species. High light consistently yielded the highest FA/Chl-a among all species. However, EPA/Chl-a was not consistent within or between species in response to temperature and light. Inherent species differences are likely in effect. Nonetheless, considering the ratio does not vary drastically among dissimilar species, the opportunity for a conservative screening tool exists. This tool would provide efficient estimation of EPA based on Chl in steady-state strains. As highest EPA production for each species were somewhat competitive, perhaps an EPA/Chl-a ratio of 1:1 (highest ratio in *T. pseudonana*) could serve as a baseline to quickly eliminate low EPA-producing strains. This research could also form the beginning of the development of an EPA/Chl-a database, to determine whether the ratio is conserved within closely-related species. Research by Aussant et al. (2018) may suggest this, as their cultures of *N. oculata* and *N. salina* appeared to show similarities between total chlorophyll and EPA content in their 8 ºC treatments; however, batch-cultivated methods were used.

For optimal screening of high EPA producing strains, we would suggest the use of LED-fitted photosynthetrons within temperature-controlled incubators, allowing several cultures to be grown at small scale (~10 mL) in triplicate simultaneously. These cultures would be grown until balanced-growth is achieved (Halsey and Jones, 2015; MacIntyre and Cullen, 2005), prior to harvesting for quantification of θ_{Chl}. Assuming a 1:1 EPA/Chl-a ratio, the strains with the highest Chl-a production ($\theta_{Chl} \times \mu$) would be selected for scale-up, where θ_{EPA} could be determined. Traditionally, bioprospecting of oleaginous algal species involves a screening pipeline of sampling, isolation of strains, cultivation, FA profiling, and lastly selection of optimal strains (Minhas et al., 2016; Neofotis et al.,

2016; Steinrucken et al., 2017). Cultivation for FA profiling usually require large aliquots of culture grown to high density, and constant turbidity and aeration (Babetta et al., 2017; Minhas et al., 2016). Additionally, FA profiling itself requires the use of several resources and is time-consuming (Budge et al., 2014). The major advantage of screening by Chl production is that low-producing strains can be removed before larger-scale cultivation and FA profiling by using a small amount of culture, effectively reducing supply and maintenance costs, and making strain selection more efficient.

The success of screening for optimal strains using EPA/Chl-a is crucially-dependent on balanced-growth parameters obtained through semi-continuous culture techniques (Halsey et al., 2015). The choice between semi-continuous and batch growth modes in algae cultivation can have vastly different implications on FA profile. Batch growth entails a one-time inoculation of media grown over a period of time, while semi-continuous growth involves frequent dilutions of inoculum with fresh media (Meyers, 1953; Bull, 2010). The key difference is that batch growth exposes the culture to several growth phases (i.e. lag, exponential, and stationary), changing growth rate and physiology (Meyers, 1953). By definition, stationary phase involves nutrient "starvation" rather than limitation (MacIntyre and Cullen, 2005). In contrast, semi-continuous growth allows for both growth rate and physiology to be maintained and sustained over time (steady-state growth), effectively prolonging the exponential phase (Bull, 2010; Halsey and Jones, 2015).

The proportion of PUFA (relative to total mass FA) tends to decrease under nutrient limitation, but contradiction does exist (Guschina and Harwood, 2009). In some cases, biosynthesis of FA is maintained, where storage is diverted into TAG (Guschina and Harwood, 2009). In fact, cellular EPA (mg mL^{-1} by biovolume) has shown to be upregulated in late stationary compared to exponential phase. This has been reported in several diatoms (*P. tricornutum, T. weissflogii, T. pseudonana*), and in the cryptophyte *Rhodomonas salina* (Boelen et al., 2017). Although EPA concentration is an important measure, comparisons of productivity is more practical from an industry standpoint, as the incorporation of μ can greatly affect the return of investment (ROI) from valuable

lipids. Consequently, Aussant et al. (2018) reported EPA productivity (mg L^{-1} day^{-1}) was lowest at Day 14 compared to Day 5 and 10 in batch growth at 8 ºC, 14 ºC, 20 ºC, and 26 ºC (*N. oculata, N. salina, R. salina, I. galbana, Rhodella violacea* (rhodophyte)*, Rhodella maculata* (rhodophyte)*, Dixionella grisea* (rhodophyte)*, Leptocylindrus danicus* (diatom)). It appears that the concomitant reduction in growth rate in stationary phase likely drives the reduction of FA production in microalgae, which agrees well with our results.

It may be intuitive to one that FA productivity of short-term batch growth (which effectively eliminates PUFA reductions in stationary phases) and semi-continuous growth would be similar. However, Wang et al. (2019) reported that EPA productivity (mg L^{-1} day^{-1}) was lower under pre-stationary batch growth compared to semi-continuous growth in *N. oculata, P. tricornutum,* and *Rhodomonas baltica* (cryptophyte). Indeed, a major advantage of semi-continuous mode is that the culture is usually kept optically-thin, allowing for maximum light availability to cells and discouraging culture self-shading due to a high number of cells (Chisti, 2013; Dubinsky et al., 1989; Shene et al., 2016).

4.2 EFFECT OF LIGHT AND TEMPERATURE ON EPA AND CHL-A (WITH RATIO IMPLIED)

There is a general consensus that microalgae tend to store lower mass percents of unsaturated FA (relative to total mass FA) as temperature and light increases (Guschina and Harwood, 2009). All three cultures here showed the anticipated response to increasing light, where significantly lower proportions (as mass % of total FA) were seen. However, temperature had a much smaller effect on % EPA, and was repeatedly inconsistent, as the lowest temperature treatments rarely yielded the highest % EPA. This was especially distinct in *N. oculata*, where temperature variation did not influence % EPA within a given light. Contradiction does exist in the literature. *N. oculata*, as well as *N. salina*, *R. violacea*, *D. grisea* and *L. danicus* all displayed increases in % EPA after a shift from 8 ºC to 14 ºC after five days (Aussant et al., 2018). *N. salina* was also found to maintain similar % EPA across a temperature range of 13 ºC to 30 ºC (Wagenen et al.,

2012). Additionally, *P. lutheri* appeared to significantly up-regulate % EPA from 8 ºC to 12 ºC in both 40 µmol photons m^{-2} s^{-1} and 200 µmol photons m^{-2} s^{-1} light conditions after seven days, but higher subsequent temperature increases were shown to decrease % EPA (Guihéneuf and Stengel, 2017). This has also been observed in other species such as the diatoms *Achnanthes brevipes* and *Cocconeis peltoides* with a temperature increase from 18ºC to 35 ºC after 24 hours, while temperature increases from 4 ºC to 18 ºC typically showed a reduction in % EPA (Scholz and Liebezeit, 2013), as well as in Antarctic assemblages where temperatures above ambient yielded higher % EPA following initial incubation (Hernando et al., 2018). In addition to this, most studies that describe decreases in PUFA as temperature is increased usually compare large temperature variations (difference of 10 ºC to 18 ºC; Guschina and Harwood, 2009). Although % EPA is a relative measure of EPA, it does not accurately represent yield until normalized to biomass or C (θ_{EPA}). With regards to θ_{EPA}, the expected decreasing trend with increasing temperature and light was not always followed, being particularly apparent in *N. oculata* and *T. pseudonana*. However, this is consistent with previous literature. At high light (200 µmol photons m^{-2} s^{-1}), Guihéneuf and Stengel (2017) showed that changes between 12 ºC and 16 ºC had almost no effect on EPA yield in *P. lutheri,* similar to findings in this study. Sholz and Liebezeit (2013) analyzed five diatom species and increases, decreases, and minimal changes of EPA were observed, particularly from 4 ºC to 18 ºC. Small differences of EPA with a 12 ºC change is especially stark, in contrast to the 5 ºC temperature differences in this study. EPA stability as light increases has been recorded in *Trachydiscus minutus* (ochrophyte) from 470 to 1070 µmol photons m^{-2} s^{-1}, where productivity (mg L^{-1} d^{-1}) and growth rate (d^{-1}) did not statistically differ after nine days (Cepák et al., 2014). However, the light conditions used were much higher than this study and spanned nine days, a time frame which may have pushed the cultures out of semi-continuous growth and into stationary phase. Examples of past research suggests that PUFAs are not as affected by temperature as other factors, and that interspecific variation such as differences in optimal growth temperature, is likely at play. Oddly, % EPA and θ_{EPA} did not behave the same way in response to light in *N. oculata*, indicating that the widely-reported FA proportion does not always accurately reflect EPA concentration.

As EPA and Chl-a have different relationships with light and temperature, it becomes clear that Chl-a production within chloroplast membranes is not directly correlated under changing growth conditions, as previously hypothesized. Increasing light always resulted in an expected decrease in Chl-a, but in some cases EPA did not. As well, the EPA/Chl-a ratio actually increased with increasing light, suggesting that EPA production was not as limited by light as Chl-a. Although literature suggests EPA is primarily concentrated within plastidial glycolipids, significant amounts are also sequestered in other extra-plastidial lipids such as TAG and phospholipids and exposure to changing temperatures and light affects these lipid classes differently. Indeed, extra-plastidial lipids associated with species used in this study can store significant proportions of % EPA. For instance, the betaine lipid DGCC has been found to concentrate up to 34% of total EPA mass proportion in *P. lutheri* (Kato et al., 1995). EPA deposition in PC, which is present in *N. oculata*, has also been shown at ~13.5% EPA in relative proportion to total mass % PC FA (Servaes et al., 2015). *Nannochloropsis* sp. also produces the betaine lipid DGTS, which it upregulates under cold-stress conditions, and may also contain a disproportionate amount of EPA (Murakami et al., 2018; Servaes et al., 2015).

Additionally, concentrations of these glycolipids and extra-plastidial lipids appear to vary inconsistently in response to temperature and inversely in response to light. Relative abundances of betaine lipids, PG, and SQDG increased, while TAG and MGDG decreased when temperature was decreased from 25 ºC to 15 ºC in *P. lutheri* (Guschina and Harwood, 2009). Variation in PG is less significant, as it is also a thylakoid-bound lipid (Guschina and Harwood, 2009). Contrarily, TAG actually increased when temperature was decreased from 20 ºC to 11 ºC in the diatom *Cylindrotheca closterium*, and PUFA proportions in neutral lipids, glycolipids, and phospholipids all increased substantially (control to exponential phase temperature stress; Almeyda et al., 2020). At high light (1000 µmol photons m^{-2} s^{-1}) in *Nannochloropsis gaditana,* % EPA in the glycolipids MGDG and DGDG was higher than at low light (10 and 100 µmol photons m^{-2} s^{-1}); however, PG, phosphatidylethanolamine (PE), and DGTS were all lower at the same high light conditions compared to lower light (Alboresi et al., 2016). A study by

Remmers et al. (2017) also showed that % EPA in TAG (relative to total % FA in TAG) stayed relatively constant, while % EPA in membrane lipids (relative to total % FA in membrane lipids) decreased as light increased (range of 60 to 750 μmol photons m^{-2} s^{-1}) in *P. tricornutum*. In conjunction, TAG yield was considerably reduced as light increased (Remmers et al., 2017). Relative proportions of PC in *T. crinitus* also decreased with increased photosynthetically-available radiation (PAR) from 8-10% to 70-80%, but contrarily, TAG proportions concomitantly increased (Khotimchenko and Yakovleva, 2005). Clearly, the response of extra-plastidial lipids to changing conditions is different than that of plastidial lipids, and the response of plastidial lipids is not consistent among strains. This could explain the inconsistencies of EPA/Chl-a behaviour, particularly if EPA is distributed in both plastidial and extra-plastidial lipids.

Although proposed prediction models cannot be made assuming a constant EPA/Chl-a ratio likely due to the presence and variation of EPA in extra-plastidial lipids, potential for a covariance model between EPA/Chl-a and irradiance may exist. A linear covariance between EPA and Chl-a in response to light confirms that both constituents are responding in somewhat similar ways, particularly in *P. lutheri*. This implies that a similar logarithmic decline of EPA with increasing light may also exist in this species, which is supported by EPA concentration distributions in light treatments within given temperatures. EPA/Chl-a within a given temperature showed a much stronger relationship than within a given light for all species, exhibiting a positive linear function across light. In particular, *P. lutheri* showed the greatest promise for a common relationship for all viable temperatures. There could be potential for a tailored EPA prediction tool specific to this species, with respect to light. Additionally, *N. salina* reportedly had little variation in % EPA across a wide range of temperatures, but the proportion decreased considerably with increasing light, much like *N. oculata* (Wagenen et al., 2012). This suggests that EPA/Chl-a may hold across closely-related species, possibly involving similarities in pigment composition.

4.3 EFFECTS OF PHYSIOLOGICAL DIFFERENCES BETWEEN SPECIES

Photoprotective mechanisms differ between *N. oculata* and the other two species, where both *P. lutheri* and *T. pseudonana* produce highly-efficient photoprotective pigments diadinoxanthin (DD) and diatoxanthin (DT; Anning et al., 2000; Lenning et al., 2003). Photo-oxidation is a key mechanism in PUFA loss (Tejero et al., 2004), so a reduced rate of photo-oxidation through activity of DD and DT could have allowed both species to compete well with *N. oculata* in terms of EPA production. Species also differ in their affinity for carbon utilization. The utilization of carbon for growth and FA production is a direct function of the availability of useable carbon sources with the two main sources of dissolved inorganic carbon (DIC) being carbon dioxide (CO_2) and bicarbonate (Guihéneuf and Stengel, 2013; Huertas and Lubián, 1998). Bicarbonate dominates the supply of DIC in natural seawater (pH of 8.2) where CO_2 diffusion (and bicarbonate dehydration) is slow (Huertas and Lubián, 1998; Matsuda et al., 2017). *N. oculata* has the capacity to uptake both forms, despite a lack of external carbonic anhydrase, where affinity for either is similar but uptake is dependent on their concentration (Hu and Zhou, 2010; Huertas and Lubián, 1998). *P. lutheri* and *T. pseudonana* have also been shown to utilize both CO_2 and bicarbonate (Guihéneuf and Stengel, 2013); bicarbonate supplementation in *P. lutheri* resulted in increased total FA and EPA production (mg L^{-1}; Guihéneuf and Stengel, 2013), while *T. pseudonana* contains a plethora of carbonic anhydrases which allow it to uptake both DIC forms in similar capacity regardless of CO_2 supply (Matsuda et al., 2017; Trimborn et al., 2009). From this, it is likely the growth and FA production rates of *N. oculata* and *T. pseudonana* were not much affected by the presumably low CO_2 supply (since culture aeration was not applied). However, an increased ratio of bicarbonate to CO_2 could have further promoted growth and FA production in *P. lutheri*, as affinity to the particular carbon source is suggested.

4.4 OTHER MAJOR PUFA AND THEIR RELATIONSHIP TO CHL-A

ARA/Chl-a showed similar behaviour to EPA/Chl-a in *N. oculata*, where the fitted trend slope for both ratios were lower at low temperature compared to medium temperature. This indicates that the ratio between ARA and EPA remained quite stable within low temperature (regardless of light) and possibly also fairly similar across low and medium light (regardless of temperature). DHA/Chl-a was quite different in *P. lutheri*. As with EPA/Chl-a, within a light level, temperature had little effect on the FA/Chl-a ratio. In contrast, when temperature treatments were compared across light, an even stronger and more precise positive linear relationship than in EPA/Chl-a was found. *P. lutheri* appears to be a good candidate for the application of a species-specific EPA prediction model using chlorophyll. A linear function is relatively simple and could predict optimal conditions to promote EPA and DHA production in this species.

The similarities of modulation between ARA and EPA in *N. oculata* are likely due to shared lipid classes between the fatty acids. Much like EPA in other species, ARA was the major fatty acid within glycolipids in the chlorophyte *Parietochloris incisa* during exponential phase, while phospholipids and TAG contained lower amounts of ARA (Bigogno et al., 2002; Guschina and Harwood, 2006). On the other hand, DHA was highest in TAG (27%) followed by diphosphatidylglycerol (DPG; 22%) and betaine lipids (21%) in *P. lutheri* cultivated up to stationary phase, which may explain some slight differences in DHA/Chl-a compared to EPA/Chl-a in *P. lutheri* (Meireles et al., 2003). Although DHA does not appear to be concentrated in lipid bodies in the same manner as EPA and ARA, perhaps variation with conditions was driven primarily by DPG (which is presumably thylakoid-bound like PG), while DHA within other lipids (and/or the lipid yields themselves) did not change considerably.

4.5 FA PRODUCTION BEHAVIOUR

The second primary focus of this study was determining actual EPA production within these strains and conditions. Here, FA production is a direct function of both FA

concentration and growth rate. The driving force behind increased production was clearly growth rate, which was particularly apparent across light levels. For example, lower light yielded either similar EPA concentrations (*N. oculata*) or higher EPA concentrations (*P. lutheri, T. pseudonana*) than higher light. However, when growth rate is considered, EPA production in low light had the lowest production rates among the treatments in all species. A similar trend was seen for ARA and DHA as well, but differences were not as large. Despite low light favouring higher PUFA concentration, production remained low due to a greatly diminished growth rate. This suggests that FA concentration is not a good indicator of production.

While higher PUFA production at higher temperature and light was a common theme in our results, the conditions which offered peak EPA production were different across all three species. Most species, used in this study have been evaluated in the past for their EPA content but most studies only include % EPA relative to total FA mass, precluding comparison to the production measurements here. Those that do include concentration/production values are normally standardized by biovolume or biomass (not strictly carbon). Any available concentration or production based on unit mass comparisons obtained from literature will likely underestimate FA relative to carbon mass by roughly ~50%. The concentration of literature estimates can be approximated based on the chemical stoichiometry of major storage compounds and pigments such as typical TAG ($C_{55}H_{98}O_6$), glucose ($C_6H_{12}O_6$), and chlorophyll-a ($C_{55}H_{72}MgN_4O_5$) as well as the chemical formula for the chlorophyte *Neochloris oleoabundans* ($CH_{1.715}O_{0.427}N_{0.148}S_{0.014}P_{0.012}$) where C accounts for roughly 51.2% of total mass (lipid content of ~23%; Murray et al., 2012; Pruvost et al., 2009). With this in mind, and applying a factor of 2 to convert between measurements relative to carbon to those relative to biomass, production and concentration values obtained in this study were found to be higher than past reports. *T. weissflogii,* a related species to *T. pseudonana*, showed EPA productivity of ~18 mg EPA g^{-1} day^{-1} under 100 µmol photons m^{-2} s^{-1} at 25 ºC (Marella and Tiwari, 2020), which was lower than *T. pseudonana* grown at high temperature-medium light (~49 mg EPA g C^{-1} day^{-1}). Unfortunately, EPA production data standardized to dry biomass is quite scarce in the literature, thereby forcing most of our

comparisons to rely on concentrations. As growth rates should be similar within species under similar conditions, comparisons to concentration data is relevant. Yields of ~74-78 mg EPA g C^{-1} in *N. oculata* across low and medium light were much higher than the literature, where it has been shown to sequester up to ~15 mg EPA g^{-1} at 20 ºC under 125 µmol photons m^{-2} s^{-1} (semi-continuous; Shene et al., 2016) and ~12-15 mg EPA g^{-1} under 60 µmol photons m^{-2} s^{-1} across a range of 8 ºC to 26 ºC (Day 5 batch-growth; Aussant et al. 2018). Yields of ~61 mg EPA g C^{-1} at low light and ~37 mg EPA g C^{-1} at high light in *P. lutheri* were also higher than past reports, where under 40 µmol photons m^{-2} s^{-1}, it concentrated up to ~20 mg EPA g^{-1} at 12 ºC, ~19 mg EPA g^{-1} at 18 ºC, and ~13 mg EPA g^{-1} at 28 ºC; and under 200 µmol photons m^{-2} s^{-1}, it concentrated ~10 mg EPA g^{-1} for both 12 ºC and 18 ºC treatments (Guihéneuf and Stengel, 2017). Despite the approximate difference of ~50% between dry biomass and dry carbon taken into account, values from previous studies were consistently lower (up to ~65%) than our results, when similar conditions were compared. When % EPA relative to total FA mass was compared to past results (for closely-related conditions), Borges et al. (2016) reported 27.6% EPA (relative to total mass FA) for *N. oculata* grown at ~19 ºC under ~211 µmol photons m^{-2} s^{-1}, which conversely was higher than our results (~18% EPA at MT-HL). Similar % EPA to our results were reported for both *P. lutheri* grown at 20 ºC under 8 h cycles of 45 µmol photons m^{-2} s^{-1} and 16 h of darkness (~25% EPA at MT-LL compared to 23.6% EPA; Kato et al., 1995) and *T. pseudonana* grown at 20 ºC under ~47 µmol photons m^{-2} s^{-1} (~20% EPA at MT-LL compared to ~13-19% EPA; Zhukova, 2004). However, Shah et al. (2018) reported lower % EPA for *P. lutheri* grown at 28 ºC under 90-130 µmol photons m^{-2} s^{-1} (~19% EPA at HT-ML compared to ~12% EPA). Overestimation of the "true" difference between carbon and dry biomass (using ~50%) could explain consistently higher EPA yield when compared to previous literature. Carbon proportion relative to total biomass could also significantly differ between species. On the other hand, some % EPA (relative to total mass FA) results were consistent with the literature, and while others were higher or lower in comparison, possibly due to differences in methodologies, such as lipid extraction and fatty acyl methylation.

The similarity of EPA production similarities in *N. oculata* and *P. lutheri* is important, as *Nannochloropsis* spp. have been under recent intense focus as a candidate for maximizing EPA production (Pal et al., 2011; Sharma and Schenk, 2015). However, *Nannochloropsis* spp. are known to present issues when it comes to extraction of valuable lipids. *Nannochloropsis* spp. tend to accumulate high proportions of polar lipids, which require additional extraction and fractionating steps to isolate (Yao et al., 2012). As well, its natural robustness against mechanical and chemical stress elevates the expenses of extraction (Zuorro et al., 2016). This same resistance, however, contributes to its ease of culturing. If filtration is used as the primary collection method, investment in special filters with small pore sizes can also be significantly more costly and time-consuming, as *Nannochloropsis spp.* are smaller in cell size (Chua and Schenk, 2017). Unique difficulties in the extraction process should be an important consideration when deciding on strains for EPA induction.

4.6 FUTURE RECOMMENDATIONS

A robust species-specific prediction model was not as strong in *N. oculata* and *T. pseudonana* as it was in *P. lutheri.* However, this may not necessarily mean models do not exist in these species. Both species did not grow at all temperature and light settings, and some trends could not be established due to missing data points. It could be that temperature and light ranges used in this study may have caused inconsistent EPA/Chl-a in those species, particularly at high temperature. The upper limit of culturable temperature for both CCMP525 (*N. oculata*) and CCMP1335 (*T. pseudonana*) was considered to be 25 ºC ([1]NCMA, 2020; [2]NCMA, 2020). However, reductions in the catalytic rate of critical enzymes, notably nitrogen reductase, may have occurred at such high temperature, imposing higher metabolic costs for nitrogen acquisition and subsequently reducing growth efficiency (Gao et al., 2000). Future experiments that test these species between temperatures used in this study is recommended.

Conditions where growth did not occur also affected comparisons of mean EPA and ARA concentrations and production in *N. oculata* and EPA production in *T.*

pseudonana. In some cases, either temperature or light was found to have a significant effect on measurement but the comparison involved a mean of partial data. For example, the effect of temperature on EPA production in *N. oculata* was significant, but the differences lay between the means of low/medium temperature (both with viable growth within all light levels) and high temperature (which only had viable growth at high light). The lack of full data may have produced false-negatives where a significant effect of temperature or light could not be determined simply because missing data prevented the comparison from being made. Future refinement of growth conditions would be useful to reveal missing PUFA interactions with light and temperature.

Growth rates measured during balanced growth and scaling up for harvest were similar in most treatments. However, there were a few groups that did not maintain similar growth rates after scale-up: *N. oculata* (low temperature-low light) and *P. lutheri* (low temperature-high light and medium temperature-low light). Low light tends to upregulate θ_{Chl}, posing the risk of internal self-shading of the culture (Shene et al., 2016). However, the data does not suggest this occurred, as growth rates of scaled-up operations did not appear to taper as harvest time approached (data not shown). As well, low temperature-high light of *P. lutheri* actually had a higher mean growth rate during scale-up than balanced growth. It seems more likely that incubation conditions, such as light, were inconsistent between balanced and scaled-up growth. Timing of scale-up procedures of other cultures within the incubator could have been a factor, as higher or lower density of large culture flasks within sections of the incubator could have had an impact on light. As small changes such as positioning within an incubator can shift cultures out of steady-state, control of all parameters should be strictly monitored and controlled throughout cultivation.

Bacterial load within cultures could have also affected the results obtained in this study, but it is difficult to predict the effect as bacteria can be beneficial or harmful to algae, depending on conditions and species. The interaction can be positive and result in increased tolerance of stressful conditions or it may have a negative effect and induce algal production of bactericidal compounds (and/or bacterial production of algaecides)

and compete with limited resources (Fouilland et al., 2018). For example, some prokaryotes such as cyanobacteria can form a commensal relationship with microalgae by providing limiting nutrients such as iron, boosting growth rate (Ito and Butler, 2005). However, xenic cultures had up to 50% reduced growth rate compared to axenic cultures in *I. galbana* and *Thalassiosira delicatula* (Fouilland et al., 2018). Bacteria can also have a drastic effect on morphology and reduce longevity of diatom cultures (Windler et al., 2014). In this study, *P. lutheri* consistently showed much lower phytoplankton/bacteria ratio, suggesting higher bacterial load than the other two species. It is possible this could have had a marked effect on growth rate of the species, ultimately influencing FA production. Unfortunately, the bacteria obtained in cultures were not identified. However, the lack of fluorescent species within 670 nm LP (FL3) during flow cytometry (data not shown), typically associated with cyanobacteria suggests that cyanobacteria were not present (MacIntyre et al., 2010). Future research should involve only axenic cultures and be maintained bacteria-free throughout the whole study to avoid interference from bacteria. Alternatively, once promising candidates have been identified, determining differences in Chl-a and EPA production between xenic and axenic strains of optimal EPA-producing strains could also be useful, as bacterial contamination is difficult to avoid with large-scale cultivation.

Due to resource and time-constraints, lipid classes were not isolated and individually analyzed in this study. Lipid class analysis would have helped to determine whether EPA yield is, in fact, being stored and varying significantly in extra-plastidial lipids within species and treatments, rather than relying on past literature examples. Additionally, it would be helpful to know if or when EPA storage is diverted to other lipid classes in response to temperature and light conditions in our species, and whether a correlation can be made between certain lipid class EPA and Chl-a. Knowledge of differences in essential FA storage within certain lipid classes is valuable information to commercial industry, as the extent of isolation and extraction processes varies between neutral and polar lipids (Yao et al., 2012).

FA analysis of *T. pseudonana* samples implied that 18:4n-3 was prominent within cells. However, 18:4n-3 has not been isolated from diatoms in past research (Yi et al., 2017). The presence of a noticeable FA peak within the retention time of 18:4n-3 was likely an artifact, perhaps an aldehyde, or a molecular species derived from one during the FAME process. Gas chromatography with mass spectrometry (GC-MS) analysis is necessary to confirm its identity and should be carried out.

Lastly, other classes as well as species closely-related to ones used in this study should be evaluated for their EPA/Chl-a to expand potential applicability of the proposed screening tool and provide a novel database. Widening of viable growth conditions outside our study parameters would also be useful to test the duration of PUFA/Chl-a trends. Furthermore, it may be worthwhile to expand research specifically with regards to ARA and DHA modelling with Chl-a in other high-producing strains. Other nutrient factors should also be addressed, such as nitrogen supplementation or limitation, as well as combinations of stressors (applied simultaneously or sequentially over time).

CHAPTER 5 - CONCLUSION

In general, the patterns of % EPA (relative to total mass FA) in response to light agreed well with the literature in all three species, where it consistently decreased with increasing light. However, responses to temperature were inconsistent. Similarly, θ_{EPA} also decreased with increasing light and was variable across all three species, except *N. oculata*, where changing light generally did not have a significant impact. EPA production appeared to be heavily-influenced by culture growth rate, as the highest production rates were achieved at medium light within medium and high light, despite higher θ_{EPA} (but lowest growth rates) obtained at low light than at medium light. Our results imply that % EPA is not an ideal indicator of EPA production, nor is it a reliable proxy for θ_{EPA}, as temperature and light conditions that offered highest values were different. Maximum EPA/Chl-a values ranged from 1-4 g g^{-1}, inferring that EPA levels vary far more within extra-plastidial lipids than originally anticipated. Despite suggestions that EPA/Chl-a cannot be used to accurately predict optimal EPA-producing strains, it can be useful as a tool to pre-emptively screen out sub-optimal performers prior to scaling-up and FA analysis, cutting down on time and costs. I suggest a preliminary threshold of ~1 EPA/Chl-a (maximum EPA/Chl-a of the lowest EPA producer in this study) would be suitable for screening, with hopes of further refinement of this ratio as a database is expanded. This means that strains exhibiting highest Chl-a production during balanced growth would be ideal candidates for high EPA production, where a 1:1 EPA/Chl-a would predict the lowest achievable production of EPA. Test strains can then be carried through the scaling-up and FA profiling steps or rejected based on the comparison of estimated EPA production to known optimal EPA producers. Additionally, a species-specific model for optimization of EPA production could be possible in *P. lutheri*, as well as prediction models for ARA and DHA.

BIBLIOGRAPHY

Abida, H., Dolch, L., Meï, C., Villanova, V., Conte, M., Block, M. A., Finazzi, G., Bastien, O., Tirichine, L., Bowler, C., Rébeillé, F., Petroutsos, J. J., Maréchal, E. (2015). Membrane glycerolipid remodeling triggered by nitrogen and phosphorus starvation in *Phaeodactylum tricornutum*. *Plant Physiology, 167*, 118–136.

Alboresi, A., Perin, G., Vitulo, N., Diretto, G., Block, M., Jouhet, J., Meneghesso, A., Valle, G., Giuliano, G., Maréchal, E., Morosinotto, T. (2016). Light remodels lipid biosynthesis in *Nannochloropsis gaditana* by modulating carbon partitioning between organelles. *Plant Physiology*, *171*, 2468–2482.

Almeyda, M. D., Bilbao, P. G. S., Popovich, C. A., Constenla, D., Leonardi, P. I. (2020). Enhancement of polyunsaturated fatty acid production under low-temperature stress in *Cylindrotheca closterium*. *Journal of Appl. Phycol., 32*, 989–1001.

Álvarez, P., Pérez, L., Salgueiro, J. L., Cancela, Á., Sánchez, Á., Ortiz, L. (2017). Bioenergy Use from *Pavlova lutheri* Microalgae. *International Journal of Environmental Research*, *11*(3), 281–289.

Anning, T., Macintyre, H. L., Pratt, S. M., Sammes, P. J., Gibb, S., Geider, R. J. (2000). Photoacclimation in the marine diatom *Skeletonema costatum*. *Limnol. Oceanogr., 45*(8), 1807–1817.

Armbrust, E. V., Berges, J. A., Bowler, C., Green, B. J., Martinez, D., Putnam, N. H., Zhou, S., Allen, A. E., Apt, K. E., Bechner, M., Brzezinski, M. A., Chaal, B. K., Chiovitti, A., Davis, A. K., Demarest, J. C., Detter, J. C., Glavina, T., Goodstein, D., Hadi, M. Z., Hellsten, U., Hildebrand, M., Jenkins, B. D., Jurka, J., Kapitonov, V. V., Kröger, N., Lau, W. W. Y., Lane, T. W., Larimer, F. W., Lippmeier, J. C., Lucas, S., Medina, M., Montsant, A., Obornik, M., Parker, M. S., Palenik, B., Pazour, G. J., Richardson, P. M., Rynearson, T. A., Saito, M. A., Schwartz, D. C., Thamatrakoln, K., Valentin, K., Vardi, A., Wilkerson, F. P., Rokhsar, D. S. (2004). The genome of the diatom *Thalassiosira pseudonana*: Ecology, evolution, and metabolism. *Science*, *306*, 79-86.

Asgharpour, M., Rodgers, B., Hestekin, J. A. (2015). Eicosapentaenoic acid from *Porphyridium Cruentum*: increasing growth and productivity of microalgae for pharmaceutical products. *Energies, 8*, 10487-10503.

Aussant, J., Guihéneuf, F., Stengel, D. B. (2018). Impact of temperature on fatty acid composition and nutritional value in eight species of microalgae. *Applied Microbiology and Biotechnology, 102,* 5279–5297.

Barnet, A. & Ciochetto, A. (2017). *Fireworx*. SourceForge, Slashdot Media. Retrieved from: <https://sourceforge.net/projects/fireworx/>.

Behrenfeld, M. J., Boss, E., Siegel, D. A., Shea, D. M. (2005). Carbon-based ocean productivity and phytoplankton physiology from space. *Global Biogeochemical Cycles, 19*, 1-14.

Bigogno, C., Khozin-goldberg, I., Boussiba, S., Vonshak, A., Cohen, Z. (2002). Lipid and fatty acid composition of the green oleaginous alga *Parietochloris incisa*, the richest plant source of arachidonic acid. *Phytochemistry, 60*, 497–503.

Boelen, P., Mastrigt, A., Bovenkamp, H. H., Heeres, H. J., Buma, A. G. J. (2017). Growth phase significantly decreases the DHA-to-EPA ratio in marine microalgae. *Aquaculture International*, *25*, 577–587.

Borges, L., Caldas, S., Montes D'Oca, M. G., Abreu, P. C. (2016). Effect of harvesting processes on the lipid yield and fatty acid profile of the marine microalga *Nannochloropsis oculata*. *Aquaculture Reports*, *4*, 164–168.

Brand, L. E., Guillard, R. L., Murphy, L. S. (1981). A method for the rapid and precise determination of acclimated phytoplankton reproduction rates. *Journal of Plankton Research, 3*, 193-201.

Budge, S. M., Devred, E., Forget, M., Stuart, V., Trzcinski, M. K., Sathyendranath, S. Platt, T. (2014). Estimating concentrations of essential omega-3 fatty acids in the ocean: supply and demand. *ICES J. Mar. Sci*., *71*, 1885-1893.

Bull, A. T. (2010). The renaissance of continuous culture in the post-genomics age. *J. Ind. Microbiol. Biotechnol., 37*, 993–1021.

Cañavate, J. P., Armada, I., Hachero-Cruzado, I. (2017). Polar lipids analysis of cultured phytoplankton reveals significant inter-taxa changes, low influence of growth stage, and usefulness in chemotaxonomy. *Microb. Ecol., 73,* 755–774.

Carvalho, A. P., Monteiro, C. M., Malcata, F. X. (2009). Simultaneous effect of irradiance and temperature on biochemical composition of the microalga *Pavlova lutheri*. *J. Appl. Phycol., 21,* 543–552.

Chisti, Y. (2013). Raceways-based production of algal crude oil. In C. Posten & C. Walter (eds.), *Microalgal Biotechnology: Potential and Production*, 197-216.

Christie, W. W. (2006). *What is a Lipid?*. Scottish Crop Research Institute (and Mylnefield Lipid Analysis), Invergowrie, Dundee, Scotland. Retrieved from: <www.lipidlibrary.co.uk>.

Chua, E. T. % Schenk, P. M. (2017). A biorefinery for *Nannochloropsis*: Induction, harvesting, and extraction of EPA-rich oil and high-value protein. *Bioresource Technology, 244,* 1416-1424.

Converti, A., Casazza, A. A., Ortiz, E. Y., Perego, P., DelBorghi, M. (2009). Effect of temperature and nitrogen concentration on the growth and lipid content of *Nannochloropsis oculata* and *Chlorella vulgaris* for biodiesel production. *Chem Eng Process, 48*(6),1146–1151.

Dolch, L., Rak, C., Perin, G., Tourcier, G., Broughton, R., Leterrier, M., Morosinotto, T., Tellier, F., Faure, J. D., Falconet, D., Jouhet, J., Sayanova, O., Beaudoin, F., Maréchal, E. (2017). A palmitic acid elongase affects eicosapentaenoic acid and plastidial monogalactosyldiacylglycerol levels in *Nannochloropsis*. *Plant Physiology, 173*, 742–759.

Dyall, S. C. (2015). Long-chain omega-3 fatty acids and the brain: a review of the independent and shared effects of EPA, DPA and DHA. *Front. Aging Neurosco., 7,* 52.

Dubinsky, Z., & Stambler, N. (2009). Photoacclimation processes in phytoplankton: mechanisms, consequences, and applications. *Aquatic Microbial Ecology, 56*, 163–176.

Huertas, E., & Lubián, L. M. (1998). Comparative study of dissolved inorganic carbon utilization and photosynthetic responses in *Nannochloris* (Chlorophyceae) and *Nannochloropsis* (Eustigmatophyceae) species. *Canadian Journal of Botany, 76*(6), 1104-1108.

Eichenberger, W., & Gribi, C. (1997). Lipids of *Pavlova lutheri*: Cellular Site and Metabolic Role of DGCC. *Phytochemistry*, *45*(8), 1561-1567.

Fabregas, J., Maseda, A., Dominquez, A., Otero, A. (2004). The cell composition of *Nannochloropsis* sp. changes under different irradiances in semicontinuous culture. *World J. Microbiol. Biotechnol.,* 20, 31-35.

Field, C. B., Behrenfeld, M. J., Randerson, J. T., Falkowski, P. G. (1998). Primary production of biosphere: Integrating terrestrial and oceanic components. *Science*, *281*, 237-240.

Fernández, F. G., Pérez, J. A., Sevilla, J. M., Camacho, F. G., Grima, E. M. (1999). Modeling of eicosapentaenoic acid (EPA) production from *Phaeodactylum tricornutum* cultures in tubular photobioreactors. Effects of dilution rate, tube diameter, and solar irradiance. *Biotechnol. Bioeng.*, *68*, 173-183.

Fouilland, E., Galès, A., Beaugelin, I., Lanouguère, E., Pringault, O., Leboulanger, C. (2018). Chemosphere influence of bacteria on the response of microalgae to contaminant mixtures. *Chemosphere, 211*, 449–455.

Forján, E., Garbayo, I., Henriques, M., Rocha, J., Vega, J., Vílchez, C. (2011). UV-A mediated modulation of photosynthetic efficiency, xanthophyll cycle and fatty acid production of *Nannochloropsis*. *Marine Biotech., 13*(3), 366–375.

Gao, Y., Smith, G. J., Alberte, R. S. (2000). Temperature dependence of nitrate reductase activity in marine phytoplankton: Biochemical analysis and ecological implications. *J. Phycol., 36*, 304-313.

Gasol, J. M. & Giorgio, P. A. D. (2000). Using flow cytometry for counting natural planktonic bacteria and understanding the structure of planktonic bacterial communities. *Scientia Marina*, *64*(2), 197-224.

Geider, R. J., MacIntyre, H. L., Kana, T. M. (1996). A dynamic model of photoadaptation in phytoplankton. *Limnol. Oceanogr., 41*(1), 1-15.

Geider, R. J., MacIntyre, H. L., Kana, T. M. (1997). Dynamic model of phytoplankton growth and acclimation: responses of the balanced growth rate and the chlorophyll a:carbon ratio to light, nutrient-limitation and temperature. *Mar. Ecol. Prog. Ser., 148*, 187-200.

Guihéneuf, F., & Stengel, D. B. (2013). LC-PUFA-enriched oil production by microalgae: accumulation of lipid and triacylglycerols containing n-3 LC-PUFA is triggered by nitrogen limitation and inorganic carbon availability in the marine haptophyte *Pavlova lutheri*. *Mar. Drugs, 11,* 4246–4266.

Guihéneuf, F., & Stengel, D. B. (2017). Interactive effects of light and temperature on pigments and n-3 LC-PUFA-enriched oil accumulation in batch-cultivated *Pavlova lutheri* using high-bicarbonate supply. *Algal Research*, *23*, 113–125.

Guschina, I. A., & Harwood, J. L. (2006). Lipids and lipid metabolism in eukaryotic algae. *Progress in Lipid Research, 45*, 160–186.

Guschina, I. A., & Harwood, J. L. (2009). Algal lipids and effect of the environment on their biochemistry. In M. T. Arts et al. (eds.), *Lipids in Aquatic Ecosystems,* 1–24.

Halsey, K. H., & Jones, B. M. (2015). Phytoplankton strategies for photosynthetic energy allocation. *Annual Review of Marine Science*, *7*(1), 265–297.

Harwood, J. L. & Jones, A. L. (1989). Lipid Metabolism in Algae. *Advances in Botanical Research, 16*, 1-53.

Hu, H. & Gao, K. (2006). Response of growth and fatty acid compositions of *Nannochloropsis* sp. to environmental factors under elevated CO2 concentration. *Biotechnol. Lett.*, *28*, 987-992.

Hu, H., & Zhou, Q. (2010). Regulation of inorganic carbon acquisition by nitrogen and phosphorus levels in the *Nannochloropsis* sp. *World J. Microbiol. Biotechnol., 26,* 957–961.

Ito, Y. & Butler, A. (2005). Structure of synechobactins, new siderophores of the marine cyanobacterium *Synechococcus* sp. PCC 7002. *Limnol. Oceanogr.*, *50*(6), 1918-1923.

Jiang, H. & Gao, K. (2004). Effects of lowering temperature during culture on the production of polyunsaturated fatty acids in the marine diatom *Phaeodactylum tricornutum* (Bacillariophyceae). *J. Phycol., 40*, 651-654.

Kagan, M. L., & Matulka, R. A. (2015). Safety assessment of the microalgae *Nannochloropsis oculata*. *Toxicology Reports, 2*, 617–623.

Kato, M., Hajiro-nakanishi, K., Sano, H., Miyachi, S. (1995). Polyunsaturated fatty acids and betaine lipids from *Pavlova lutheri*. *Plant Cell Physiol., 36*(8), 1607–1611.

Kawasaki, N., Sohrin, R., Ogawa, H., Nagata, T., Benner, R. (2011). Bacterial carbon content and the living and detrital bacterial contributions to suspended particulate organic carbon in the North Pacific Ocean. *Aquatic Microbial Ecology, 62,* 165-176.

Kelly, A. A., Kalisch, B., Hölzl, G., Schulze, S., Thiele, J., Melzer, M., Roston, R. L., Benning, C., Dörmann, P. (2016). Synthesis and transfer of galactolipids in chloroplast envelope membranes of *Arabidopsis thaliana*. *PNAS*, *113*(38), 10714-10719.

Khotimchenko, S. V, & Yakovleva, I. M. (2005). Lipid composition of the red alga *Tichocarpus crinitus* exposed to different levels of photon irradiance. *Phytochemistry, 66*, 73–79.

Kim, S. H., Liu, K. H., Lee, S. Y., Hong, S. J., Cho, B. K., Lee, H., Lee, C. G., Choi, H. K. (2013). Effects of light intensity and nitrogen starvation on glycerolipid, glycerophospholipid, and carotenoid composition in *Dunaliella tertiolecta* culture. *PLOS ONE, 8*(9), e72415.

Lenning, K. Van, Latasa, M., Estrada, M., Sáez, A. G., Medlin, L., Probert, I., Véron, B., Young, J. (2003). Pigment signatures and phylogenetic relationships of the Pavlovophyceae (Haptophyta). *J. Phycol., 39*, 379–389.

MacIntyre, H. L. , Cullen, J. J. (2005). Using cultures to investigate the physiological ecology of microalgae. In R. A. Andersen (ed.) *Algal Culturing Techniques,* Amsterdam: Elsevier, 287–326.

Macintyre, H. L., Lawrenz, E., Richardson, T. L. (1970). Taxonomic discrimination of phytoplankton by spectral fluorescence. In D. J. Suggett et al. (eds.), *Chlorophyll a Fluorescence in Aquatic Sciences, Developments in Applied Phycology 4.*

Mansurova, I. M. (2015). Effect of Light Intensity on the Content of Chlorophyll a, Carbon and Nitrogen in Six Species of Dinophyta from the Black Sea (Crimea). *International Journal on Algae, 17*(4), 363–370.

Marella, K. T., & Tiwari, A. (2020). Bioresource technology marine diatom *Thalassiosira weissflogii* based biorefinery for co-production of eicosapentaenoic acid and fucoxanthin. *Bioresource Technology, 307,* 123245.

Martin, G. J. O., Hill, D. R. A., Olmstead, I. L. D., Bergamin, A., Shears, M. J., Dias, D. A., Kentish, S. E., Scales, P. J., Botte, C. Y., Callahan, D. L. (2014). Lipid profile remodeling in response to nitrogen deprivation in the microalgae *Chlorella* sp . (Trebouxiophyceae) and *Nannochloropsis* sp. (Eustigmatophyceae). *PLOS ONE, 9*(8), e103389.

Matsuda, Y., Hopkinson, B. M., Nakajima, K., Dupont, C. L., Tsuji, Y. (2017). Mechanisms of carbon dioxide acquisition and CO_2 sensing in marine diatoms: a gateway to carbon metabolism. *Phil. Trans. R. Soc. B, 372,* 20160403.

Meireles, L. A., Guedes, A. C., Malcata, F. X. (2002). Increase of the yields of eicosapentaenoic and docosahexaenoic acids by the microalga *Pavlova lutheri* following random mutagenesis. *Biotechnology and Bioengineering, 81*(1), 50-55.

Meireles, L. A., Guedes, A. C., Malcata, F. X. (2003). Lipid class composition of the microalga *Pavlova lutheri*: Eicosapentaenoic and docosahexaenoic acids. *J. Agric. Food Chem.*, *51*(8), 2237-2241.

Meng, Y., Jiang, J., Wang, H., Cao, X., Xue, S., Yang, Q., Wang, W. (2014). The characteristics of TAG and EPA accumulation in *Nannochloropsis oceanica* IMET1 under different nitrogen supply regimes. *Bioresource Technology*, *179,* 483-489.

Meyers, J. (1953) Growth characteristics of algae in relation to the problems of mass culture. In: J. S. Burlew (ed.) *Algae culture. From laboratory to pilot plant.* Carnegie Institution of Washington, Washington, 37–54.

Minhas, K. A., Hodgson, P., Barrow, C. J., Sashidhar, B., Adholeya, A. (2016). The isolation and identification of new microalgal strains producing oil and carotenoid simultaneously with biofuel potential. *Bioresource Technology*, *211*, 556–565.

Murakami, H., Nobusawa, T., Hori, K., Shimojima, M., Ohta, H. (2018). Betaine lipid is crucial for adapting to low temperature and phosphate Deficiency in *Nannochloropsis. Plant Physiology, 177,* 181–193.

Murray, K. E., Shields, J. A., Garcia, N. D., Healy, F. G. (2012). Bioresource technology productivity, carbon utilization, and energy content of mass in scalable microalgae systems. *Bioresource Technology*, *114*, 499–506.

Narayan, B., Miyashita, K., Hosakawa, M. (2006). Physiological effects of eicosapentaenoic acid (EPA) and docosahexaenoic acid (DHA) - a review. *Food Reviews International, 22,* 291-307.

Napolitano, G. E. (1994). The relationship of lipids with light and chlorophyll measurement in freshwater algae and periphyton. *J. Phycol.*, *30*, 943-950.

[1]NCMA. (2020). *CCMP525 Nannochloropsis oculata (Droop) Hibberd.* Bigelow National Center for Marine Algae and Microbiota, Maine, USA. Retrieved from < https://ncma.bigelow.org/ccmp525#.XxXEZ0BFxVY>.

[2]NCMA. (2020). *CCMP1335 Thalassiosira pseudonana (Hustedt) Hasle et Heimdal.* Bigelow National Center for Marine Algae and Microbiota, Maine, USA. Retrieved from < https://ncma.bigelow.org/ccmp1335#.XxXFYUBFxVY>.

Neofotis, P., Huang, A., Sury, K., Chang, W., Joseph, F., Gabr, A., Twary, S., Qiu, W., Holguin, O., Polle, J. E. W. (2016). Characterization and classification of highly productive microalgae strains discovered for biofuel and bioproduct generation. *Algal Research*, *15*, 164–178.

Pal, D., Khozin-Goldberg, I., Cohen, Z., Boussiba, S. (2011). The effect of light, salinity, and nitrogen availability on lipid production by *Nannochloropsis* sp. *Appl. Microbiol. Biotechnol., 90,* 1429–1441.

Pruvost, J., Vooren, G. Van, Cogne, G., Legrand, J. (2009). Investigation of biomass and lipids production with *Neochloris oleoabundans* in photobioreactor. *Bioresource Technology*, *100*, 5988–5995.

Remmers, I. M., & Martens, D. E. (2017). Dynamics of triacylglycerol and EPA production in *Phaeodactylum tricornutum* under nitrogen starvation at different light intensities. *PLOS ONE, 12*(4), e0175630.

Sabia, A., Clavero, E., Pancaldi, S., Rovira, J. S. (2018). Effect of different CO_2 concentrations on biomass, pigment content, and lipid production of the marine diatom *Thalassiosira pseudonan*a. *Applied microbiology and Biotechnology, 102,* 1945–1954.

Sayanova, O., Mimouni, V., Ulmann, L., Morant-Manceau, A., Pasquet, V., Schoefs, B., Napier, J. A. (2017). Modulation of lipid biosynthesis by stress in diatoms. *Philosophical Transactions of the Royal Society B: Biological Sciences*, *372*, 20160407.

Servaes, K., Maesen, M., Prandi, B., Sforza, S., Elst, K. (2015). Polar lipid profile of *Nannochloropsis oculata* determined using a variety of lipid extraction procedures. *Journal of Agricultural and Food Chemistry, 63,* 3931-3941.

Sforza, E., Calvaruso, C., Meneghesso, A., Morosinotto, T., Bertucco, A. (2015). Effect of specific light supply rate on photosynthetic efficiency of *Nannochloropsis salina* in a continuous flat plate photobioreactor. *Applied Microbiology and Biotechnology*, *99,* 8309–8318.

Shah, S. M. U., ., Radziah, C. C., Ibrahim, S., Latiff, F., Othman, M. F., Abdullah, M. A. (2014). Effects of photoperiod, salinity and pH on cell growth and lipid content of *Pavlova lutheri*. *Ann. Microbiol., 64,* 157–164.

Sharifah, E. N., & Eguchi, M. (2011). The phytoplankton *Nannochloropsis oculata* enhances the ability of *Roseobacter* Clade Bacteria to inhibit the growth of fish pathogen *Vibrio anguillarum*. *PLOS ONE, 6*(10), e26756.

Sharma, K., & Schenk, P. M. (2015). Rapid induction of omega-3 fatty acids (EPA) in *Nannochloropsis* sp. by UV-C radiation. *Biotechnology and Bioengineering, 112*(6), 1243–1249.

Shene, C., Chisti, Y., Vergara, D., Burgos-Díaz, C., Rubilar, M., Bustamante, M. (2016). Production of eicosapentaenoic acid by *Nannochloropsis oculata*: Effects of carbon dioxide and glycerol. *Journal of Biotechnology*, *239*, 47–56.

Shoman, N. Y., & Akimov, A. (2015). The Combined Influence of Light Intensity and Temperature on Organic Carbon to Chlorophyll a Ratio in Three Species of Marine Bacillariophyta. *International Journal on Algae*, *17*(1), 82–93.

Srinivas, R., & Ochs, C. (2012). Effect of UV-A irradiance on lipid accumulation in *Nannochloropsis oculata*. *Photochem. Photobiol., 88*(3), 684–689.

Steinrücken, P., Erga, R. S., Mjøs, S. A., Kleivdal, H., Prestegard, K. S. (2017). Bioprospecting North Atlantic microalgae with fast growth and high polyunsaturated fatty acid (PUFA) content for microalgae-based technologies. *Algal Research*, *26*, 392–401.

Schaller-Laudel, S., Latowski, D., Jemiola-Rzemińska, M., Strzałka, K., Daum, S., Bacia, K., Wilhelm, C., Goss, R. (2017). Influence of thylakoid membrane lipids on the structure of aggregated light-harvesting complexes of the diatom *Thalassiosira pseudonana* and the green alga *Mantoniella squamata*. *Physiologia Plantarum, 160,* 339–358.

Shoaf, W. T. & Lium, B. W. (1976). Improved extraction of chlorophyll a and b from algae using dimethyl sulfoxide. *Limnology and Oceanography*, *21*, 926-928.

Subramanian, S., Barry, A. N., Pieris, S., Sayre, R. T. (2013). Comparative energetics and kinetics of autotrophic lipid and starch metabolism in chlorophytic microalgae: implications for biomass and biofuel production. *Biotechnology for Biofuels*, *6*(1), 150.

Sugimoto, K., Tsuzuki, M., Sato, N. (2009). Regulation of synthesis and degradation of sulfolipid under sulfur-starved conditions and its physiological significance in *Chlamydomonas reinhardtii*. *New Phytologist*, *185*, 676-686.

Tatsuzawa, H. & Takizawa, E. (1995). Changes in lipid and fatty acid composition of *Pavlova lutheri*. *Phytochemistry,* 40, 397-400.

Tejero, I., González-Lafont, A., Lluch, J. M., Eriksson, L. A. (2004). Photo-oxidation of lipids by singlet oxygen: a theoretical study. *Chemical Physics Letters, 398*, 336–342.

Thompson, G.A. (1996). Lipids and membrane function in green algae. *Biochem. Biophys. Acta,* 1302, 17-45.

Trimborn, S., Wolf-gladrow, D., Richter, K., Rost, B. (2009). The effect of pCO_2 on carbon acquisition and intracellular assimilation in four marine diatoms. *Journal of Experimental Marine Biology and Ecology*, *376*(1), 26–36.

Wagenen, J. Van, Miller, T. W., Hobbs, S., Hook, P., Crowe, B., Huesemann, M. (2012). Effects of light and temperature on fatty acid production in *Nannochloropsis Salina*. *Energies, 5,* 731–740.

Wang, X., Fosse, H. K., Li, K., Chauton, M. S., Vadstein, O., Reitan, K. I. (2019). Influence of nitrogen limitation on lipid accumulation and EPA and DHA content in four marine microalgae for possible use in aquafeed. *Frontiers in Marine Science, 6,* 95.

Welschmeyer, N. A. (1994). Fluorometric analysis of chlorophyll a in the presence of chlorophyll b and pheopigments. *Limnol. Oceanogr.*, *39*(8), 1985-1992.

Windler, M., Bova, D., Kryvenda, A., Straile, D., Gruber, A., Kroth, P. G. (2014). Influence of bacteria on cell size development and morphology of cultivated diatoms. *Phycological Research, 62,* 269-281.

Yao, L., Gerde, J. A., Wang, T. (2012). Oil extraction from microalga *Nannochloropsis* sp. with isopropyl alcohol. *J. Am. Oil Chem. Soc., 89,* 2279-2287.

Yi, Z., Xu., M., Di, X., Brynjolfsson, S., Fu, W. (2017). Exploring valuable lipids in diatoms. *Frontiers of Marine Science, 4,* 17.

Yoder, J. A. (1979). Effect of temperature on light-limited growth and chemical composition of *Skeletonema costatum* (Bacillariophyceae). *J. Phycol., 15,* 362-370.

Zhukova, N. V. (2004). Changes in the lipid composition of *Thalassiosira pseudonana* during its life cycle. *Russian Journal of Plant Physiology, 51*(5), 778–783.

Zienkiewicz K., Du, Z. Y., Ma, W., Vollheyde, K., Benning, C. (2016). Stress-induced neutral lipid biosynthesis in microalgae – molecular, cellular and physiological insights. *Biochimica et Biophysica Acta*, *1861,* 1269-1281.

Zuorro, A., Maffei, G., Lavecchia, R. (2016). Optimization of enzyme-assisted lipid extraction from *Nannochloropsis* microalgae. *Journal of the Taiwan Institute of Chemical Engineers*, *67*, 106–114.

APPENDIX A

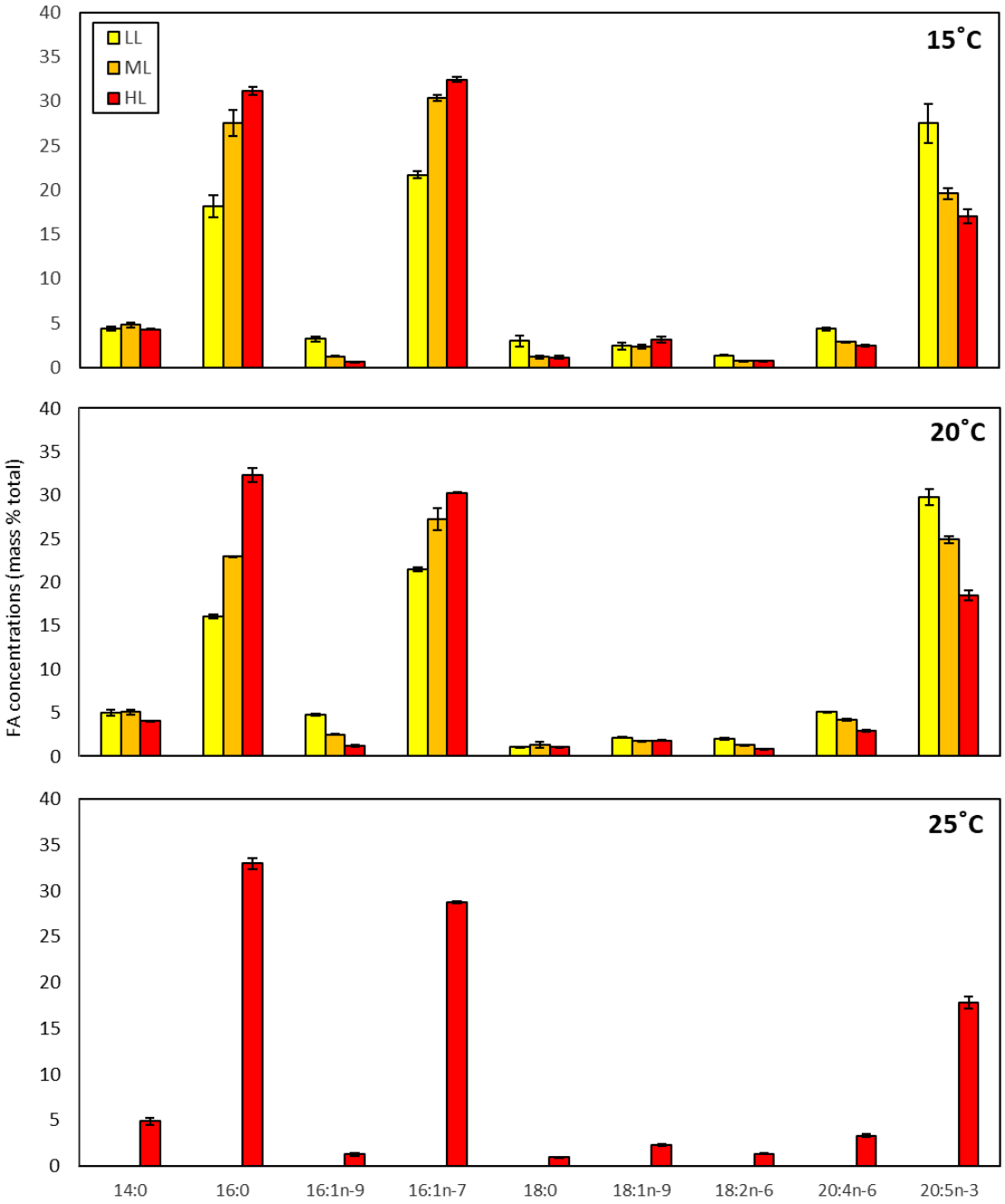

Appendix A1. Fatty acid composition (expressed as FA mass percent of total FA mass percent) of *N. oculata* in the three temperature treatments (LT, MT, HT) and light treatments (LL, ML, HL) (mean ± sd, n=3).

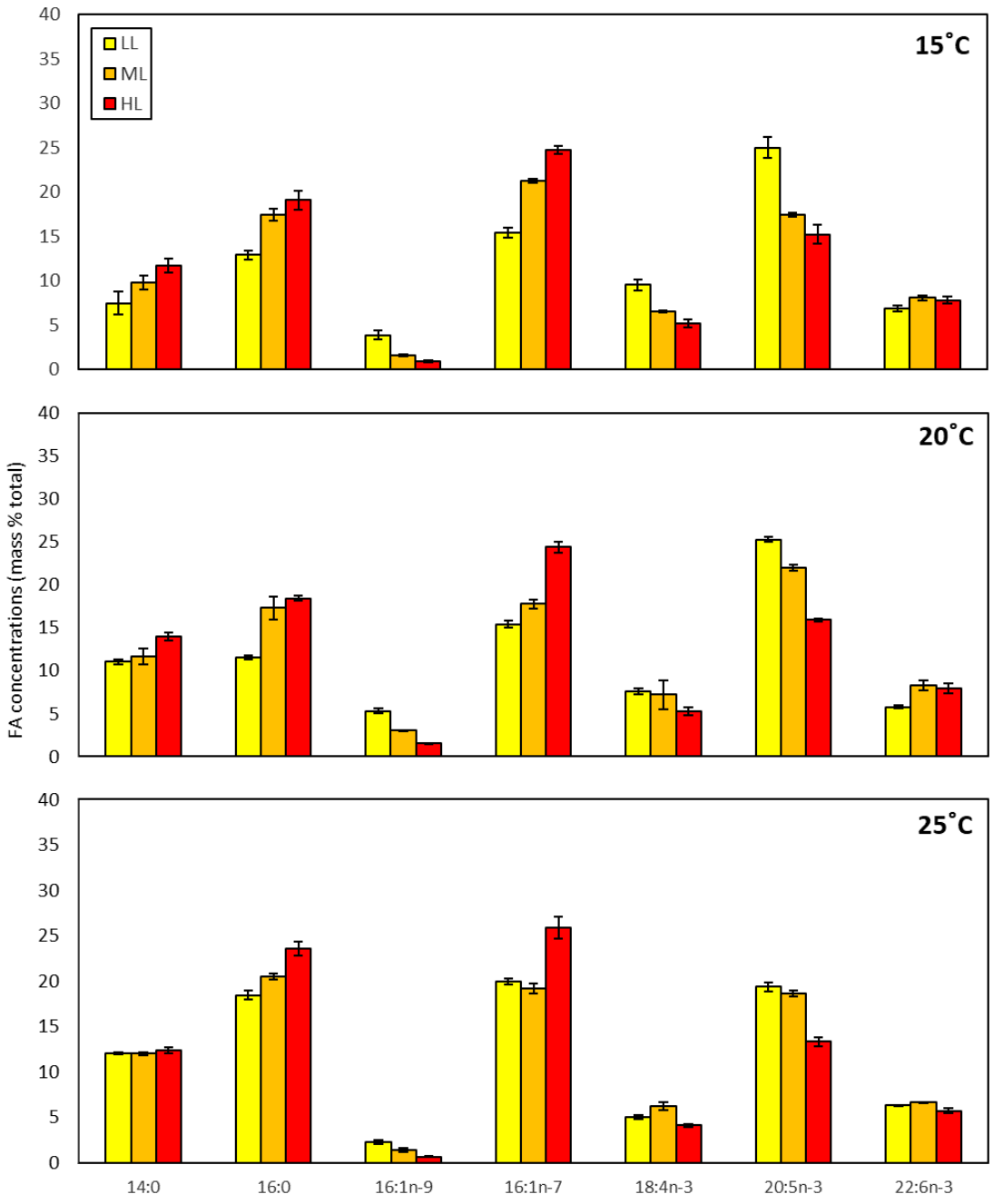

Appendix A2. Fatty acid composition (expressed as FA mass percent of total FA mass percent) of *P. lutheri* in the three temperature treatments (LT, MT, HT) and light treatments (LL, ML, HL) (mean ± sd, n=3; HT-LL mean ± sd, n=2).

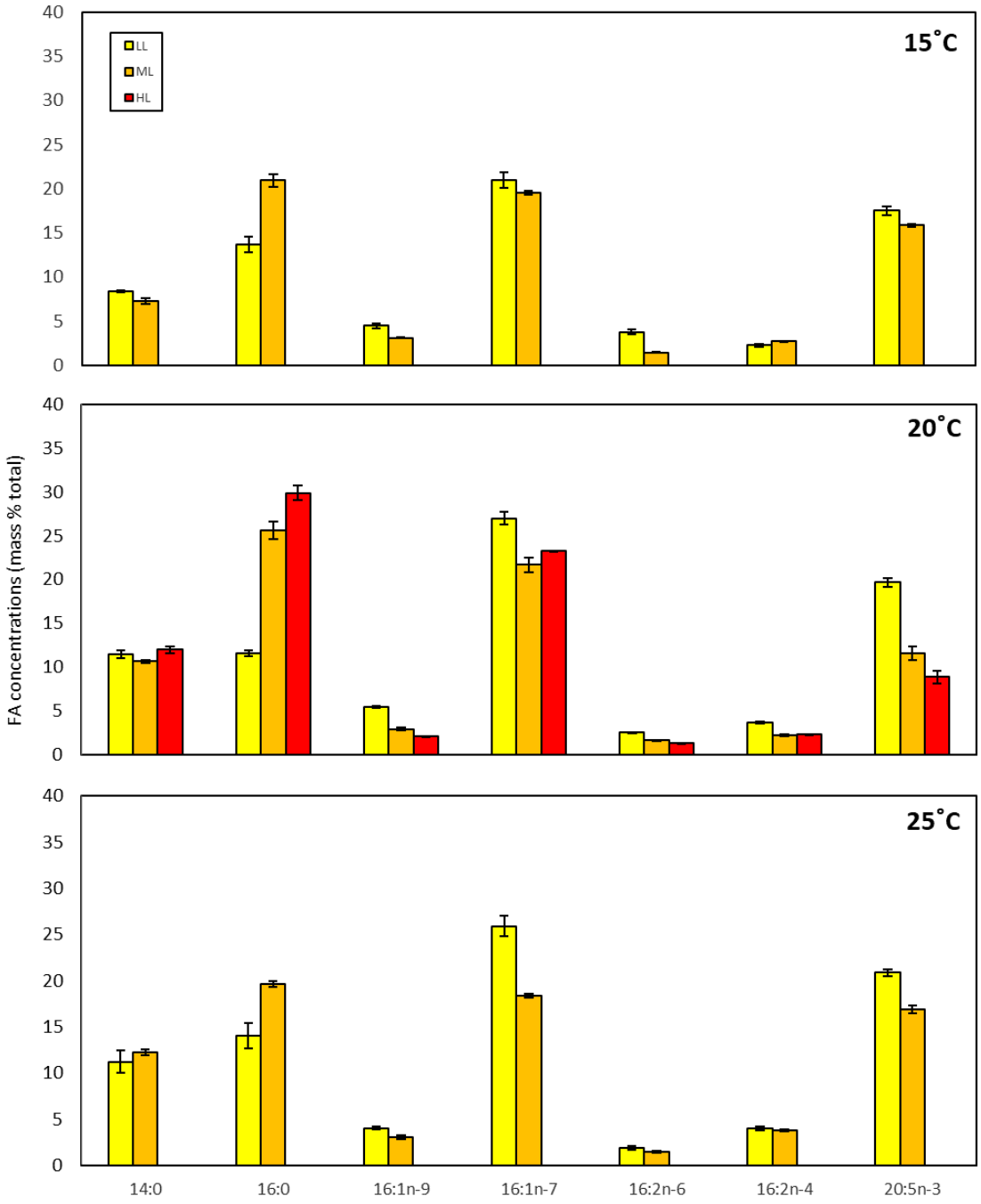

Appendix A3. Fatty acid composition (expressed as FA mass percent of total FA mass percent) of *T. pseduonana* in the three temperature treatments (LT, MT, HT) and light treatments (LL, ML, HL) (mean ± sd, n=3).

APPENDIX B

Appendix B1. Turner and FIRe fluorescence measurements of *N. oculata* during balanced and triplicate scaled-up growth at LT-HL.

Species	Tube#	T[Turner]	Bl[Turner]	Corr F[Turner]	mu	F_cum	Fv/Fm	F0	Fm	Fv
No25	122	35.1	0.264	34.836	0.696	4.741E+13	0.423	647.379	1122.224	474.844
No25	122	9.08	0.245	8.835	0.667	8.417E+13	0.421	170.426	294.581	124.155
No25	122	16.9	0.250	16.650	0.638	1.586E+14	0.402	341.295	570.645	229.350
No25	122	33.4	0.266	33.134	0.686	3.157E+14	0.447	566.431	1023.407	456.977
No25	122	11.0	0.238	10.762	0.816	7.177E+14	0.550	167.915	373.202	205.287
No25	122	23.8	0.272	23.528	0.724	1.569E+15	0.511	428.848	877.066	448.218
No25	122	10.5	0.262	10.238	0.602	2.914E+15	0.537	181.957	392.887	210.930
No25	122	25.5	0.261	25.239	0.790	7.183E+15	0.501	459.734	921.301	461.567
No25	122	38.4	0.277	38.123	0.582	1.085E+16	0.488	946.713	1848.446	901.734
No25	122	13.0	0.253	12.747	0.822	2.539E+16	0.521	196.376	409.888	213.512
No25	122	23.1	0.269	22.831	0.581	4.548E+16	0.484	552.403	1071.293	518.891
No25	1222	4.07	0.264	3.806	0.917	1.137E+17	0.448	1112.630	2015.165	902.535
No25	1222	7.74	0.276	7.464	0.626	2.230E+17	0.551	116.030	258.185	142.155
No25	1222	17.7	0.267	17.433	0.716	5.209E+17	0.450	365.095	664.202	299.108
No25	1222	39.6	0.269	39.331	1.132	1.175E+18	0.502	871.243	1749.117	877.873
No25	1222	0.646	0.144	0.502	-0.811	5.150E+17	0.608	17.452	44.497	27.045
No25	1222	1.15	0.146	1.004	0.696	1.030E+18	0.376	51.371	82.361	30.990
No25	1222	2.51	0.142	2.368	0.855	2.429E+18	0.617	90.721	236.651	145.930
No25	1222	5.29	0.136	5.154	0.642	5.288E+18	0.459	228.974	423.126	194.152
No25	1222	10.3	0.134	10.166	0.684	1.043E+19	0.501	502.674	1006.633	503.959
No25	1223	3.84	0.264	3.576	0.854	1.069E+17	0.610	53.940	138.326	84.386
No25	1223	7.46	0.276	7.184	0.648	2.147E+17	0.474	126.024	239.654	113.630
No25	1223	17.0	0.267	16.733	0.714	5.000E+17	0.488	331.804	648.608	316.803
No25	1223	32.2	0.269	31.931	0.899	9.542E+17	0.487	707.165	1379.662	672.498
No25	1223	0.695	0.144	0.551	-0.576	5.310E+17	0.490	26.590	52.114	25.524
No25	1223	1.40	0.146	1.254	0.825	1.208E+18	0.620	46.679	122.893	76.213
No25	1223	2.53	0.142	2.388	0.642	2.301E+18	0.529	106.639	226.456	119.817
No25	1223	5.57	0.136	5.434	0.679	5.237E+18	0.467	247.174	463.708	216.534
No25	1223	10.4	0.134	10.266	0.641	9.894E+18	0.479	476.775	914.816	438.042
No25	1224	3.63	0.264	3.366	0.794	1.006E+17	0.637	56.989	156.933	99.944
No25	1224	7.26	0.276	6.984	0.678	2.087E+17	0.451	135.648	246.927	111.279
No25	1224	16.1	0.267	15.833	0.691	4.731E+17	0.513	312.270	641.723	329.453
No25	1224	33.9	0.269	33.631	1.048	1.005E+18	0.514	726.150	1493.441	767.291
No25	1224	0.718	0.144	0.574	-0.587	5.532E+17	0.589	20.673	50.254	29.581
No25	1224	1.31	0.146	1.164	0.709	1.122E+18	0.560	47.885	108.786	60.902
No25	1224	2.32	0.142	2.178	0.624	2.099E+18	0.460	103.017	190.859	87.842
No25	1224	5.33	0.136	5.194	0.717	5.006E+18	0.512	221.247	453.220	231.973
No25	1224	10.9	0.134	10.766	0.734	1.038E+19	0.475	534.087	1018.276	484.189

Appendix B2. Turner and FIRe fluorescence measurements of *N. oculata* during balanced and triplicate scaled-up growth at LT-ML.

Species	Tube#	T[Turner]	Bl[Turner]	Corr F[Turner]	mu	F_cum	Fv/Fm	F0	Fm	Fv
No25	132	7.43	0.266	7.164	0.808	2.333E+12	0.523	160.942	337.369	176.427
No25	132	13.2	0.279	12.921	0.594	4.208E+12	0.475	246.511	469.542	223.031
No25	132	26.1	0.267	25.833	0.679	8.413E+12	0.548	410.207	907.929	497.722
No25	132	43.7	0.268	43.432	0.520	1.414E+13	0.445	1022.120	1840.350	818.230
No25	132	10.1	0.264	9.836	0.922	3.524E+13	0.629	139.976	377.640	237.664
No25	132	19.7	0.261	19.439	0.606	6.964E+13	0.600	329.952	825.399	495.447
No25	132	39.4	0.264	39.136	0.693	1.402E+14	0.476	753.209	1438.587	685.378
No25	132	12.8	0.262	12.538	0.661	2.666E+14	0.629	175.514	472.859	297.345
No25	132	26.2	0.261	25.939	0.636	5.516E+14	0.500	505.070	1009.876	504.806
No25	132	41.4	0.277	41.123	0.651	8.744E+14	0.502	1094.407	2198.195	1103.789
No25	132	14.3	0.253	14.047	0.842	2.091E+15	0.540	226.464	492.261	265.798
No25	132	26.5	0.269	26.231	0.622	3.904E+15	0.469	645.873	1216.950	571.077
No25	1322	8.63	0.264	8.366	0.649	7.472E+15	0.552	162.904	363.786	200.882
No25	1322	15.4	0.276	15.124	0.550	1.351E+16	0.485	288.234	559.955	271.721
No25	1322	35.2	0.267	34.933	0.707	3.120E+16	0.464	795.232	1483.068	687.836
No25	1322	51.2	0.269	50.931	0.525	4.549E+16	0.502	1091.503	2192.462	1100.959
No25	1322	1.54	0.144	1.396	-0.206	3.687E+16	0.519	69.029	143.459	74.431
No25	1322	2.73	0.146	2.584	0.618	6.824E+16	0.616	103.329	268.752	165.424
No25	1322	5.12	0.142	4.978	0.653	1.315E+17	0.522	246.975	516.200	269.224
No25	1322	9.99	0.136	9.854	0.563	2.602E+17	0.536	486.372	1048.709	562.337
No25	1323	9.48	0.264	9.216	0.746	8.231E+15	0.540	183.442	398.983	215.542
No25	1323	16.9	0.276	16.624	0.548	1.485E+16	0.499	292.182	583.310	291.129
No25	1323	38.4	0.267	38.133	0.701	3.406E+16	0.501	781.430	1566.369	784.939
No25	1323	53.9	0.269	53.631	0.475	4.790E+16	0.514	1101.474	2264.134	1162.660
No25	1323	1.46	0.144	1.316	-0.315	3.476E+16	0.518	61.427	127.376	65.949
No25	1323	2.52	0.146	2.374	0.592	6.270E+16	0.564	109.045	249.947	140.903
No25	1323	5.19	0.142	5.048	0.752	1.333E+17	0.526	237.142	500.300	263.158
No25	1323	10.7	0.136	10.564	0.609	2.790E+17	0.503	489.941	985.157	495.216
No25	1324	9.21	0.264	8.946	0.716	7.990E+15	0.513	198.416	407.224	208.808
No25	1324	16.4	0.276	16.124	0.547	1.440E+16	0.433	343.969	606.665	262.695
No25	1324	38.0	0.267	37.733	0.718	3.370E+16	0.529	740.999	1573.998	832.999
No25	1324	53.2	0.269	52.931	0.471	4.727E+16	0.484	1194.832	2316.968	1122.136
No25	1324	1.48	0.144	1.336	-0.288	3.528E+16	0.528	59.774	126.532	66.758
No25	1324	2.69	0.146	2.544	0.646	6.719E+16	0.510	120.574	246.113	125.539
No25	1324	5.29	0.142	5.148	0.702	1.360E+17	0.548	233.682	517.532	283.850
No25	1324	10.6	0.136	10.464	0.585	2.764E+17	0.517	476.100	985.361	509.262

Appendix B3. Turner and FIRe fluorescence measurements of *N. oculata* during balanced and triplicate scaled-up growth at LT-LL.

Species	Tube#	T[Turner]	Bl[Turner]	Corr F[Turner]	mu	F cum	Fv/Fm	F0	Fm	Fv
No25	142	11.2	0.264	10.936	0.486	1.686E+06	0.480	245.991	472.654	226.662
No25	142	15.3	0.267	15.033	0.370	2.317E+06	0.605	86.096	218.226	132.129
No25	142	19.7	0.267	19.433	0.232	2.996E+06	0.522	360.261	754.172	393.911
No25	142	30.8	0.267	30.533	0.399	4.707E+06	0.531	517.516	1102.342	584.826
No25	142	38.6	0.266	38.334	0.317	5.909E+06	0.480	836.584	1609.996	773.412
No25	142	50.5	0.279	50.221	0.272	7.742E+06	0.518	856.975	1776.655	919.680
No25	142	15.9	0.267	15.633	0.763	1.687E+07	0.517	267.793	554.207	286.414
No25	142	19.4	0.268	19.132	0.202	2.064E+07	0.594	335.220	825.850	490.630
No25	142	27.7	0.264	27.436	0.364	2.961E+07	0.505	541.089	1093.104	552.015
No25	142	39.8	0.261	39.539	0.325	4.267E+07	0.518	716.553	1487.828	771.275
No25	142	9.85	0.264	9.586	0.371	6.206E+07	0.561	153.536	349.846	196.310
No25	142	12.6	0.245	12.355	0.295	7.999E+07	0.551	213.524	475.608	262.084
No25	142	18.1	0.250	17.850	0.371	1.156E+08	0.514	336.594	692.530	355.936
No25	142	29.2	0.266	28.934	0.481	1.873E+08	0.469	589.702	1109.864	520.162
No25	142	50.2	0.238	49.962	0.542	3.235E+08	0.502	929.513	1866.853	937.339
No25	142	15.6	0.272	15.328	0.708	6.947E+08	0.489	355.941	696.425	340.484
No25	142	19.6	0.262	19.338	0.339	9.842E+08	0.493	367.147	724.543	357.396
No25	142	26.9	0.261	26.639	0.280	1.356E+09	0.449	580.994	1054.949	473.955
No25	142	34.7	0.277	34.423	0.362	1.752E+09	0.516	901.337	1861.499	960.162
No25	1422	8.34	0.253	8.087	0.332	2.470E+09	0.540	112.727	245.185	132.458
No25	1422	11.9	0.269	11.631	0.362	3.552E+09	0.576	211.157	498.441	287.284
No25	1422	15.5	0.264	15.236	0.270	4.653E+09	0.504	339.777	685.207	345.430
No25	1422	21.7	0.276	21.424	0.317	6.542E+09	0.457	423.247	779.825	356.578
No25	1422	32.7	0.267	32.433	0.350	9.904E+09	0.484	720.799	1395.606	674.807
No25	1422	26.9	0.269	26.631	-0.274	8.132E+09	0.485	541.514	1051.638	510.124
No25	1422	0.781	0.144	0.637	-0.284	6.089E+09	0.605	23.155	58.646	35.491
No25	1422	1.05	0.146	0.904	0.351	8.642E+09	0.482	44.328	85.624	41.296
No25	1422	1.33	0.142	1.188	0.272	1.136E+10	0.511	60.935	124.570	63.635
No25	1422	1.74	0.136	1.604	0.248	1.533E+10	0.580	68.853	163.984	95.131
No25	1422	2.22	0.134	2.086	0.265	1.994E+10	0.493	125.951	248.237	122.285
No25	1422	3.02	0.138	2.882	0.334	2.755E+10	0.440	169.312	302.466	133.154
No25	1422	3.80	0.132	3.668	0.289	3.506E+10	0.490	198.717	389.357	190.640
No25	1422	4.99	0.148	4.842	0.282	4.629E+10	0.533	233.711	500.586	266.875
No25	1422	6.83	0.136	6.694	0.266	6.399E+10	0.514	435.981	897.870	461.889
No25	1422	9.69	0.140	9.550	0.350	9.129E+10	0.508	601.175	1220.749	619.574
No25	1423	7.80	0.253	7.547	0.265	2.305E+09	0.619	94.402	247.673	153.271
No25	1423	11.0	0.269	10.731	0.351	3.277E+09	0.542	232.284	507.000	274.717
No25	1423	14.7	0.264	14.436	0.297	4.408E+09	0.543	274.668	601.579	326.911
No25	1423	19.0	0.276	18.724	0.242	5.718E+09	0.403	401.655	672.707	271.052
No25	1423	27.9	0.267	27.633	0.329	8.438E+09	0.464	606.485	1131.103	524.617
No25	1423	26.1	0.269	25.831	-0.094	7.888E+09	0.484	534.637	1036.158	501.521
No25	1423	0.655	0.144	0.511	-0.471	4.885E+09	0.468	29.141	54.731	25.591
No25	1423	0.836	0.146	0.690	0.301	6.596E+09	0.584	25.755	61.947	36.192
No25	1423	1.07	0.142	0.928	0.295	8.871E+09	0.433	63.471	111.954	48.483
No25	1423	1.37	0.136	1.234	0.235	1.180E+10	0.467	65.374	122.629	57.255
No25	1423	1.74	0.134	1.606	0.265	1.535E+10	0.455	92.137	169.027	76.890
No25	1423	2.32	0.138	2.182	0.316	2.086E+10	0.514	106.770	219.804	113.034
No25	1423	2.88	0.132	2.748	0.277	2.627E+10	0.501	141.231	283.294	142.063
No25	1423	3.74	0.148	3.592	0.272	3.434E+10	0.499	186.636	372.334	185.698

No25	1423	5.18	0.136	5.044	0.279	4.822E+10	0.486	296.497	577.019	280.523
No25	1423	7.07	0.140	6.930	0.313	6.625E+10	0.473	398.353	756.239	357.886
No25	1423	9.35	0.135	9.215	0.260	8.809E+10	0.461	514.851	955.835	440.983
No25	1424	7.79	0.253	7.537	0.264	2.302E+09	0.528	561.744	1189.435	627.690
No25	1424	10.9	0.269	10.631	0.343	3.246E+09	0.544	1346.059	2950.179	1604.120
No25	1424	14.4	0.264	14.136	0.285	4.317E+09	0.522	286.742	599.782	313.040
No25	1424	19.3	0.276	19.024	0.276	5.809E+09	0.476	370.897	707.549	336.652
No25	1424	28.6	0.267	28.333	0.336	8.652E+09	0.498	601.224	1198.542	597.318
No25	1424	24.6	0.269	24.331	-0.212	7.430E+09	0.522	467.654	979.354	511.700
No25	1424	0.739	0.144	0.595	-0.319	5.373E+09	0.581	23.342	55.728	32.387
No25	1424	0.983	0.146	0.837	0.342	7.558E+09	0.550	39.692	88.278	48.586
No25	1424	1.33	0.142	1.188	0.349	1.073E+10	0.531	60.988	130.109	69.120
No25	1424	1.79	0.136	1.654	0.273	1.494E+10	0.471	85.877	162.474	76.597
No25	1424	2.27	0.134	2.136	0.258	1.929E+10	0.547	109.211	241.079	131.868
No25	1424	3.01	0.138	2.872	0.306	2.594E+10	0.530	154.203	327.771	173.568
No25	1424	4.07	0.132	3.938	0.379	3.556E+10	0.522	201.607	422.081	220.474
No25	1424	5.38	0.148	5.232	0.288	4.725E+10	0.517	259.354	537.159	277.805
No25	1424	7.78	0.136	7.644	0.311	6.903E+10	0.481	425.572	820.379	394.807
No25	1424	10.5	0.140	10.360	0.300	9.356E+10	0.488	585.363	1143.406	558.044

Appendix B4. Turner and FIRe fluorescence measurements of *N. oculata* during balanced and triplicate scaled-up growth at MT-HL.

Species	Tube#	T[Turner]	Bl[Turner]	Corr F[Turner]	mu	F cum	Fv/Fm	F0	Fm	Fv
No25	152	15.9	0.271	15.629	1.164	1.163E+06	0.452	359.806	656.691	296.885
No25	152	41.6	0.269	41.331	0.976	3.076E+06	0.514	795.622	1638.657	843.035
No25	152	21.6	0.272	21.328	0.958	1.111E+07	0.530	415.085	883.310	468.225
No25	152	45.2	0.278	44.922	1.067	2.341E+07	0.480	899.343	1731.159	831.816
No25	152	16.3	0.258	16.042	0.949	5.851E+07	0.477	314.339	600.946	286.607
No25	152	39.7	0.277	39.423	0.952	1.438E+08	0.447	758.432	1372.550	614.118
No25	152	17.7	0.259	17.441	1.096	4.453E+08	0.518	306.242	635.020	328.778
No25	152	40.4	0.265	40.135	0.816	1.025E+09	0.416	781.149	1338.081	556.932
No25	1522	14.9	0.262	14.638	0.938	2.803E+09	0.521	303.600	633.700	330.099
No25	1522	38.0	0.268	37.732	0.944	7.225E+09	0.506	441.573	893.765	452.192
No25	1522	98.9	0.499	98.401	0.965	1.884E+10	0.453	1940.735	3549.814	1609.079
No25	1522	3.02	0.132	2.888	-0.135	1.682E+10	0.539	135.952	294.930	158.978
No25	1522	14.8	0.139	14.661	0.993	8.537E+10	0.514	709.148	1458.934	749.786
No25	1523	16.0	0.262	15.738	1.005	3.013E+09	0.554	272.257	610.689	338.433
No25	1523	40.6	0.268	40.332	0.938	7.723E+09	0.548	374.177	828.461	454.284
No25	1523	104	0.499	103.501	0.949	1.982E+10	0.437	1866.604	3318.071	1451.468
No25	1523	2.91	0.132	2.778	-0.242	1.618E+10	0.495	133.889	265.320	131.431
No25	1523	12.1	0.139	11.961	0.893	6.965E+10	0.499	572.440	1141.980	569.540
No25	1524	14.9	0.262	14.638	0.938	2.803E+09	0.464	319.954	597.061	277.107
No25	1524	37.1	0.268	36.832	0.920	7.052E+09	0.535	410.152	882.392	472.241
No25	1524	91.0	0.499	90.501	0.905	1.733E+10	0.396	1705.799	2824.010	1118.212
No25	1524	2.57	0.132	2.438	-0.237	1.420E+10	0.477	121.645	232.560	110.914

No25	1524	11.2	0.139	11.061	0.925	6.441E+10	0.547	494.058	1089.706	595.648

Appendix B5. Turner and FIRe fluorescence measurements of *N. oculata* during balanced and triplicate scaled-up growth at MT-ML.

Species	Tube#	T[Turner]	Bl[Turner]	Corr F[Turner]	mu	F_cum	Fv/Fm	F0	Fm	Fv
No25	162	28.1	0.257	27.843	0.744	2.961E+05	0.509	550.902	1122.750	571.848
No25	162	13.2	0.261	12.939	0.901	9.631E+05	0.552	224.947	501.953	277.006
No25	162	21.8	0.258	21.542	0.699	1.603E+06	0.534	399.287	856.098	456.811
No25	162	8.18	0.271	7.909	0.974	4.121E+06	0.641	126.548	352.329	225.781
No25	162	18.5	0.269	18.231	0.838	9.499E+06	0.516	385.094	794.950	409.856
No25	162	15.3	0.272	15.028	0.890	3.132E+07	0.554	282.316	632.952	350.637
No25	162	27.2	0.278	26.922	0.835	5.611E+07	0.551	508.956	1132.876	623.920
No25	162	8.83	0.258	8.572	0.830	1.251E+08	0.497	171.637	341.299	169.662
No25	162	20.0	0.277	19.723	0.882	2.877E+08	0.547	342.218	755.629	413.410
No25	162	45.6	0.259	45.341	0.807	6.615E+08	0.510	917.301	1870.254	952.953
No25	1622	15.1	0.265	14.835	0.661	1.299E+09	0.471	312.674	591.290	278.615
No25	1622	0.660	0.131	0.529	0.049	1.369E+09	0.657	18.449	53.839	35.390
No25	1622	1.42	0.124	1.296	0.893	3.355E+09	0.620	52.367	137.639	85.272
No25	1622	3.49	0.127	3.363	0.960	8.705E+09	0.532	170.715	364.653	193.938
No25	1622	6.71	0.132	6.578	0.798	1.703E+10	0.494	353.492	698.449	344.957
No25	1622	15.8	0.129	15.671	0.853	4.056E+10	0.520	830.668	1732.053	901.385
No25	1623	15.2	0.265	14.935	0.667	1.307E+09	0.517	288.302	596.436	308.134
No25	1623	0.633	0.131	0.502	-0.006	1.299E+09	0.688	19.507	62.495	42.988
No25	1623	1.42	0.124	1.296	0.945	3.355E+09	0.606	62.868	159.479	96.610
No25	1623	3.45	0.127	3.323	0.948	8.601E+09	0.475	185.338	352.752	167.414
No25	1623	7.03	0.132	6.898	0.869	1.785E+10	0.496	348.542	691.689	343.148
No25	1623	16.5	0.129	16.371	0.850	4.237E+10	0.506	783.606	1585.003	801.397
No25	1624	15.3	0.265	15.035	0.674	1.316E+09	0.505	290.110	585.553	295.443
No25	1624	0.592	0.131	0.461	-0.091	1.193E+09	0.593	21.310	52.420	31.111
No25	1624	1.29	0.124	1.166	0.925	3.018E+09	0.507	61.302	124.257	62.956
No25	1624	2.94	0.127	2.813	1.020	8.307E+09	0.510	141.895	289.325	147.429
No25	1624	5.59	0.132	5.458	0.789	1.612E+10	0.506	275.411	557.181	281.769
No25	1624	12.8	0.129	12.671	0.828	3.742E+10	0.522	595.392	1245.981	650.589

Appendix B6. Turner and FIRe fluorescence measurements of *N. oculata* during balanced and triplicate scaled-up growth at MT-LL.

Species	Tube#	T[Turner]	Bl[Turner]	Corr F[Turner]	mu	F_cum	Fv/Fm	F0	Fm	Fv
No25	172	20.2	0.259	19.941	0.355	8.222E+04	0.504	377.696	760.922	383.227
No25	172	26.5	0.265	26.235	0.269	1.082E+05	0.440	541.093	967.034	425.942
No25	172	37.9	0.262	37.638	0.336	1.552E+05	0.468	822.460	1546.039	723.579
No25	172	14.5	0.268	14.232	0.412	2.347E+05	0.468	753.790	1418.174	664.384
No25	172	21.7	0.253	21.447	0.413	3.537E+05	0.473	427.970	811.541	383.572
No25	172	28.6	0.277	28.323	0.331	4.671E+05	0.536	156.106	336.122	180.016
No25	172	40.3	0.264	40.036	0.340	6.603E+05	0.483	824.549	1593.392	768.843

No25	172	14.2	0.264	13.936	0.386	9.959E+05	0.510	297.500	606.790	309.290
No25	172	20.3	0.272	20.028	0.350	1.431E+06	0.514	438.270	902.274	464.005
No25	172	28.3	0.263	28.037	0.345	2.004E+06	0.453	695.730	1272.852	577.122
No25	172	38.2	0.270	37.930	0.275	2.711E+06	0.506	844.617	1710.189	865.572
No25	172	16.3	0.261	16.039	0.520	4.585E+06	0.506	308.990	625.532	316.542
No25	172	20.7	0.271	20.429	0.276	5.840E+06	0.519	422.421	878.180	455.759
No25	172	31.0	0.264	30.736	0.403	8.786E+06	0.499	662.067	1321.386	659.319
No25	172	42.5	0.269	42.231	0.317	1.207E+07	0.468	947.016	1779.266	832.250
No25	172	11.1	0.265	10.835	0.468	2.168E+07	0.556	170.553	384.277	213.724
No25	172	14.0	0.255	13.745	0.303	2.750E+07	0.488	299.794	585.530	285.736
No25	172	20.8	0.271	20.529	0.394	4.108E+07	0.468	469.521	882.721	413.199
No25	172	31.6	0.271	31.329	0.340	6.269E+07	0.436	686.454	1217.373	530.919
No25	172	40.6	0.266	40.334	0.357	8.071E+07	0.457	878.533	1618.220	739.688
No25	172	55.2	0.273	54.927	0.310	1.099E+08	0.476	1252.895	2391.739	1138.844
No25	1722	12.9	0.265	12.635	0.326	1.517E+08	0.554	216.400	485.406	269.006
No25	1722	18.7	0.231	18.469	0.322	2.217E+08	0.471	192.159	363.082	170.923
No25	1722	24.9	0.262	24.638	0.430	2.958E+08	0.498	474.730	944.868	470.138
No25	1722	33.5	0.263	33.237	0.217	3.990E+08	0.477	611.864	1170.144	558.280
No25	1722	0.709	0.132	0.577	-0.634	2.049E+08	0.405	37.948	63.786	25.837
No25	1722	0.928	0.130	0.798	0.327	2.833E+08	0.523	35.451	74.271	38.820
No25	1722	1.14	0.126	1.014	0.332	3.600E+08	0.402	62.109	103.828	41.719
No25	1722	1.59	0.130	1.460	0.361	5.184E+08	0.458	83.325	153.853	70.528
No25	1722	2.14	0.133	2.007	0.331	7.126E+08	0.489	106.600	208.424	101.824
No25	1722	5.99	0.137	5.853	0.330	2.078E+09	0.482	309.043	596.488	287.445
No25	1722	8.66	0.141	8.519	0.349	3.025E+09	0.481	469.485	905.339	435.854
No25	1722	10.1	0.130	9.970	0.220	3.540E+09	0.473	522.667	991.510	468.843
No25	1722	13.6	0.127	13.473	0.314	4.783E+09	0.490	697.361	1367.827	670.467
No25	1723	12.6	0.265	12.335	0.301	1.481E+08	0.454	266.847	488.312	221.465
No25	1723	19.1	0.231	18.869	0.360	2.265E+08	0.522	169.068	353.735	184.667
No25	1723	23.5	0.262	23.238	0.311	2.790E+08	0.513	459.933	944.655	484.723
No25	1723	32.9	0.263	32.637	0.246	3.918E+08	0.494	571.046	1128.742	557.696
No25	1723	0.716	0.132	0.584	-0.605	2.073E+08	0.413	37.667	64.115	26.448
No25	1723	0.963	0.130	0.833	0.358	2.957E+08	0.484	40.940	79.315	38.376
No25	1723	1.20	0.126	1.074	0.352	3.813E+08	0.489	58.969	115.418	56.449
No25	1723	1.63	0.130	1.500	0.331	5.326E+08	0.446	80.583	145.335	64.752
No25	1723	2.28	0.133	2.147	0.373	7.623E+08	0.488	112.376	219.437	107.061
No25	1723	5.72	0.137	5.583	0.295	1.982E+09	0.469	301.023	567.234	266.211
No25	1723	8.27	0.141	8.129	0.349	2.886E+09	0.457	453.683	835.979	382.296
No25	1723	9.16	0.130	9.030	0.147	3.206E+09	0.452	494.002	901.141	407.139
No25	1723	12.6	0.127	12.473	0.337	4.428E+09	0.472	655.088	1239.967	584.880
No25	1724	12.3	0.265	12.035	0.276	1.445E+08	0.483	228.032	440.720	212.688
No25	1724	18.5	0.231	18.269	0.354	2.193E+08	0.438	190.560	339.009	148.449
No25	1724	22.4	0.262	22.138	0.287	2.658E+08	0.497	413.804	823.039	409.234
No25	1724	30.4	0.263	30.137	0.224	3.618E+08	0.453	573.056	1047.046	473.991
No25	1724	0.612	0.132	0.480	-0.662	1.804E+08	0.510	25.904	52.853	26.948
No25	1724	0.809	0.130	0.679	0.349	2.552E+08	0.544	29.318	64.299	34.980
No25	1724	0.977	0.126	0.851	0.313	3.198E+08	0.404	51.391	86.165	34.774
No25	1724	1.31	0.130	1.180	0.323	4.435E+08	0.507	63.833	129.582	65.749
No25	1724	1.78	0.133	1.647	0.347	6.190E+08	0.459	83.391	154.279	70.888
No25	1724	5.20	0.137	5.063	0.346	1.903E+09	0.534	246.903	529.380	282.477
No25	1724	7.33	0.141	7.189	0.326	2.702E+09	0.600	305.290	764.079	458.789
No25	1724	8.15	0.130	8.020	0.153	3.014E+09	0.476	437.345	834.608	397.263
No25	1724	11.3	0.127	11.173	0.346	4.199E+09	0.452	583.822	1065.660	481.837

Appendix B7. Turner and FIRe fluorescence measurements of *N. oculata* during balanced and triplicate scaled-up growth at HT-HL.

Species	Tube#	T[Turner]	Bl[Turner]	Corr F[Turner]	mu	F_cum	Fv/Fm	F0	Fm	Fv
No25	182	16.5	0.266	16.234	1.086	2.857E+03	0.519	280.033	581.961	301.928
No25	182	41.2	0.260	40.940	0.894	7.205E+03	0.478	719.955	1380.476	660.521
No25	182	11.9	0.277	11.623	1.108	2.250E+04	0.506	221.709	449.108	227.399
No25	182	24.4	0.262	24.138	0.892	4.673E+04	0.455	462.395	848.942	386.548
No25	182	9.72	0.269	9.451	1.008	1.281E+05	0.600	141.872	354.275	212.404
No25	182	26.0	0.272	25.728	1.005	3.487E+05	0.540	398.121	866.331	468.210
No25	182	10.6	0.258	10.342	1.099	9.811E+05	0.517	199.646	412.917	213.272
No25	182	29.4	0.265	29.135	0.932	2.764E+06	0.498	535.698	1066.678	530.980
No25	1822	19.8	0.254	19.546	0.813	6.953E+06	0.490	404.156	792.235	388.079
No25	1822	0.726	0.125	0.601	-0.127	6.153E+06	0.545	26.610	58.501	31.891
No25	1822	1.52	0.127	1.393	0.984	1.426E+07	0.428	83.476	145.950	62.474
No25	1822	4.32	0.124	4.196	0.931	4.296E+07	0.584	197.626	475.100	277.474
No25	1822	11.3	0.130	11.170	0.829	1.144E+08	0.490	562.529	1103.535	541.006
No25	1823	19.2	0.254	18.946	0.785	6.740E+06	0.491	408.583	802.719	394.136
No25	1823	0.728	0.125	0.603	-0.091	6.173E+06	0.662	23.900	70.739	46.839
No25	1823	1.67	0.127	1.543	1.100	1.580E+07	0.556	73.792	166.216	92.423
No25	1823	5.66	0.124	5.536	1.079	5.667E+07	0.530	251.382	535.005	283.623
No25	1823	17.6	0.130	17.470	0.973	1.788E+08	0.547	846.109	1869.437	1023.328
No25	1824	15.8	0.254	15.546	0.611	5.530E+06	0.508	317.218	644.665	327.447
No25	1824	0.717	0.125	0.592	0.041	5.753E+06	0.490	28.282	55.474	27.192
No25	1824	1.56	0.127	1.433	1.035	1.392E+07	0.604	58.085	146.510	88.425
No25	1824	4.79	0.124	4.666	0.997	4.534E+07	0.538	217.133	469.650	252.517
No25	1824	13.4	0.130	13.270	0.885	1.289E+08	0.519	629.767	1309.734	679.967

Appendix B8. Turner and FIRe fluorescence measurements of *P. lutheri* during balanced and triplicate scaled-up growth at LT-HL.

Species	Tube#	T[Turner]	Bl[Turner]	Corr F[Turner]	mu	F_cum	Fv/Fm	F0	Fm	Fv
Pl25	122	20.2	0.261	19.939	0.745	8.251E+12	0.336	497.519	748.794	251.275
Pl25	122	40.1	0.264	39.836	0.685	1.648E+13	0.357	895.955	1393.191	497.237
Pl25	122	11.6	0.245	11.355	0.802	3.289E+13	0.452	239.794	437.671	197.877
Pl25	122	23.2	0.250	22.95	0.709	6.648E+13	0.393	548.358	903.080	354.722
Pl25	122	10.6	0.266	10.334	0.758	1.422E+14	0.465	216.228	404.219	187.991
Pl25	122	22.1	0.238	21.862	0.744	3.008E+14	0.407	461.485	777.952	316.468
Pl25	122	46.1	0.272	45.828	0.685	6.306E+14	0.491	997.180	1957.624	960.444
Pl25	122	8.52	0.266	8.254	0.667	1.249E+15	0.468	168.586	316.716	148.130
Pl25	122	20.2	0.267	19.933	0.779	3.017E+15	0.441	406.614	727.355	320.741
Pl25	122	11.1	0.248	10.852	0.813	7.117E+15	0.399	236.573	393.632	157.059
Pl25	122	17.5	0.265	17.235	0.694	1.130E+16	0.419	385.570	663.337	277.767
Pl25	1222	28.3	0.261	28.039	0.832	3.311E+16	0.360	649.854	1016.139	366.285
Pl25	1222	0.760	0.145	0.615	-0.611	2.148E+16	0.479	32.812	62.998	30.186
Pl25	1222	1.66	0.140	1.520	0.874	5.308E+16	0.478	88.304	169.130	80.826

Pl25	1222	3.72	0.140	3.580	0.854	1.250E+17	0.443	223.083	400.660	177.577
Pl25	1222	10.1	0.136	9.964	0.748	3.480E+17	0.484	559.029	1083.095	524.066
Pl25	1223	26.5	0.261	26.239	0.807	3.205E+16	0.400	575.370	958.390	383.020
Pl25	1223	0.720	0.145	0.575	-0.612	2.077E+16	0.630	25.162	68.059	42.897
Pl25	1223	1.69	0.140	1.550	0.958	5.599E+16	0.460	88.268	163.516	75.248
Pl25	1223	3.69	0.140	3.550	0.826	1.282E+17	0.445	198.623	357.830	159.207
Pl25	1223	10.2	0.136	10.064	0.762	3.636E+17	0.415	568.887	971.908	403.021
Pl25	1224	25.8	0.261	25.539	0.783	3.109E+16	0.400	555.528	926.533	371.005
Pl25	1224	0.666	0.145	0.521	-0.714	1.875E+16	0.454	33.201	60.800	27.600
Pl25	1224	1.39	0.140	1.250	0.846	4.500E+16	0.451	74.277	135.225	60.948
Pl25	1224	2.96	0.140	2.820	0.811	1.015E+17	0.455	158.789	291.092	132.303
Pl25	1224	8.73	0.136	8.594	0.815	3.094E+17	0.428	489.935	856.476	366.541

Appendix B9. Turner and FIRe fluorescence measurements of *P. lutheri* during balanced and triplicate scaled-up growth at LT-ML.

Species	Tube#	T[Turner]	Bl[Turner]	Corr F[Turner]	mu	F_cum	Fv/Fm	F0	Fm	Fv
Pl25	132	12.5	0.264	12.236	0.875	4.165E+13	0.599	184.478	459.738	275.260
Pl25	132	26.7	0.261	26.439	0.685	8.999E+13	0.391	630.338	1035.373	405.035
Pl25	132	5.66	0.264	5.396	0.200	1.102E+14	0.624	72.612	193.058	120.446
Pl25	132	10.4	0.245	10.155	0.734	2.074E+14	0.505	212.684	429.704	217.021
Pl25	132	23.1	0.250	22.850	0.817	4.666E+14	0.409	528.956	895.572	366.616
Pl25	132	6.82	0.266	6.554	0.695	9.369E+14	0.486	131.235	255.303	124.068
Pl25	132	13.8	0.238	13.562	0.722	1.939E+15	0.428	305.782	534.391	228.609
Pl25	132	30.7	0.272	30.428	0.748	4.350E+15	0.387	773.548	1261.661	488.113
Pl25	132	11.3	0.266	11.034	0.759	9.464E+15	0.327	284.384	422.300	137.916
Pl25	132	26.4	0.267	26.133	0.762	2.241E+16	0.386	603.596	982.603	379.007
Pl25	132	12.5	0.248	12.252	0.758	4.992E+16	0.350	290.293	446.483	156.190
Pl25	132	19.5	0.265	19.235	0.677	7.837E+16	0.424	440.999	765.170	324.171
Pl25	1322	34.2	0.261	33.939	0.748	2.060E+17	0.380	761.762	1227.938	466.177
Pl25	1322	0.713	0.145	0.568	-0.993	1.019E+17	0.407	41.772	70.459	28.687
Pl25	1322	1.53	0.140	1.390	0.865	2.495E+17	0.385	96.401	156.875	60.474
Pl25	1322	3.18	0.140	3.040	0.780	5.456E+17	0.450	182.408	331.812	149.403
Pl25	1322	9.51	0.136	9.374	0.787	1.682E+18	0.487	660.102	1286.499	626.398
Pl25	1323	30.1	0.261	29.839	0.711	1.964E+17	0.404	652.564	1094.264	441.700
Pl25	1323	0.728	0.145	0.583	-0.774	1.135E+17	0.505	32.635	65.906	33.271
Pl25	1323	1.44	0.140	1.300	0.775	2.531E+17	0.498	73.693	146.800	73.107
Pl25	1323	3.06	0.140	2.920	0.806	5.685E+17	0.472	168.247	318.928	150.680
Pl25	1323	8.65	0.136	8.514	0.748	1.657E+18	0.406	579.855	975.656	395.801
Pl25	1324	31.3	0.261	31.039	0.720	1.986E+17	0.385	705.042	1147.182	442.140
Pl25	1324	0.71	0.145	0.565	-0.874	1.069E+17	0.419	34.537	59.461	24.923
Pl25	1324	1.53	0.140	1.390	0.870	2.630E+17	0.469	77.547	145.976	68.429
Pl25	1324	3.08	0.140	2.940	0.747	5.563E+17	0.441	180.847	323.599	142.752
Pl25	1324	8.96	0.136	8.824	0.768	1.670E+18	0.409	550.813	931.496	380.682

Appendix B10. Turner and FIRe fluorescence measurements of *P. lutheri* during balanced and triplicate scaled-up growth at LT-LL.

Species	Tube#	T[Turner]	Bl[Turner]	Corr F[Turner]	mu	F cum	Fv/Fm	F0	Fm	Fv
Pl25	142	35.4	0.253	35.147	0.462	3.049E+04	0.568	613.454	1420.145	806.691
Pl25	142	49.3	0.258	49.042	0.333	4.255E+04	0.591	164.312	401.952	237.640
Pl25	142	13.4	0.253	13.147	0.521	7.984E+04	0.582	708.652	1695.693	987.042
Pl25	142	17.9	0.260	17.640	0.322	1.071E+05	0.443	327.073	587.308	260.235
Pl25	142	26.9	0.253	26.647	0.359	1.618E+05	0.419	501.247	862.741	361.494
Pl25	142	34.7	0.251	34.449	0.262	2.092E+05	0.471	747.360	1411.660	664.301
Pl25	142	10.9	0.263	10.637	0.511	3.068E+05	0.369	229.740	363.890	134.151
Pl25	142	15.9	0.252	15.648	0.386	4.514E+05	0.446	295.463	532.913	237.450
Pl25	142	24.2	0.256	23.944	0.340	6.907E+05	0.394	523.423	863.921	340.498
Pl25	142	33.2	0.264	32.936	0.340	9.500E+05	0.362	690.886	1083.126	392.240
Pl25	142	42.1	0.267	41.833	0.278	1.207E+06	0.426	306.226	533.348	227.121
Pl25	142	11.3	0.267	11.033	0.414	1.909E+06	0.383	246.540	399.819	153.279
Pl25	142	19.3	0.267	19.033	0.482	3.294E+06	0.446	339.953	614.068	274.115
Pl25	142	23.0	0.266	22.734	0.247	3.935E+06	0.472	460.740	873.217	412.477
Pl25	142	31.9	0.279	31.621	0.332	5.473E+06	0.420	571.285	984.598	413.313
Pl25	142	45.4	0.267	45.133	0.349	7.811E+06	0.417	790.207	1354.948	564.740
Pl25	142	56.3	0.268	56.032	0.216	9.698E+06	0.379	1288.221	2075.730	787.509
Pl25	142	14.1	0.264	13.836	0.553	1.676E+07	0.456	260.939	479.304	218.365
Pl25	142	18.6	0.261	18.339	0.250	2.222E+07	0.311	495.260	718.732	223.472
Pl25	142	24.4	0.264	24.136	0.272	2.924E+07	0.428	533.267	932.432	399.164
Pl25	142	34.2	0.245	33.955	0.396	4.114E+07	0.368	802.002	1268.780	466.778
Pl25	1422	11.6	0.250	11.350	0.228	5.156E+07	0.465	233.895	437.541	203.646
Pl25	1422	15.7	0.136	15.564	0.315	7.071E+07	0.343	361.562	550.303	188.741
Pl25	1422	0.379	0.122	0.257	-0.791	3.189E+07	0.567	17.160	39.649	22.489
Pl25	1422	0.577	0.140	0.437	0.492	5.423E+07	0.563	24.304	55.657	31.353
Pl25	1422	0.717	0.139	0.578	0.273	7.173E+07	0.297	49.307	70.109	20.802
Pl25	1422	1.03	0.143	0.887	0.378	1.101E+08	0.456	59.737	109.760	50.023
Pl25	1422	1.59	0.143	1.447	0.464	1.796E+08	0.490	97.302	190.618	93.317
Pl25	1422	2.10	0.139	1.961	0.456	2.434E+08	0.513	120.435	247.319	126.883
Pl25	1422	2.97	0.150	2.820	0.352	3.500E+08	0.440	176.279	314.820	138.541
Pl25	1422	4.64	0.140	4.500	0.358	5.584E+08	0.413	295.822	503.645	207.823
Pl25	1422	5.92	0.144	5.776	0.344	7.168E+08	0.520	360.612	750.980	390.368
Pl25	1422	8.18	0.146	8.034	0.266	9.970E+08	0.482	610.143	1178.018	567.875
Pl25	1423	11.5	0.250	11.250	0.219	5.111E+07	0.390	268.632	440.545	171.913
Pl25	1423	15.2	0.136	15.064	0.291	6.844E+07	0.462	302.987	562.821	259.834
Pl25	1423	0.395	0.122	0.273	-0.698	3.388E+07	0.448	23.555	42.642	19.086
Pl25	1423	0.567	0.140	0.427	0.414	5.299E+07	0.454	34.388	62.939	28.551
Pl25	1423	0.827	0.139	0.688	0.466	8.538E+07	0.528	42.018	89.067	47.049
Pl25	1423	1.17	0.143	1.027	0.354	1.274E+08	0.408	76.938	129.992	53.054
Pl25	1423	1.78	0.143	1.637	0.442	2.031E+08	0.447	104.423	188.729	84.306
Pl25	1423	2.10	0.139	1.961	0.271	2.434E+08	0.361	148.852	233.021	84.169
Pl25	1423	3.24	0.150	3.090	0.441	3.835E+08	0.490	182.445	357.679	175.234
Pl25	1423	5.29	0.140	5.150	0.391	6.391E+08	0.392	354.149	582.199	228.051
Pl25	1423	6.62	0.144	6.476	0.316	8.037E+08	0.412	403.695	686.102	282.407
Pl25	1423	8.75	0.146	8.604	0.229	1.068E+09	0.407	602.976	1017.058	414.082
Pl25	1424	11.6	0.250	11.350	0.228	5.156E+07	0.604	160.845	406.457	245.613
Pl25	1424	15.7	0.136	15.564	0.315	7.071E+07	0.460	296.253	548.679	252.426
Pl25	1424	0.424	0.122	0.302	-0.630	3.748E+07	0.228	26.058	33.735	7.676
Pl25	1424	0.570	0.140	0.430	0.327	5.336E+07	0.350	35.640	54.830	19.190
Pl25	1424	0.817	0.139	0.678	0.445	8.414E+07	0.247	58.998	78.386	19.387

Pl25	1424	1.15	0.143	1.007	0.349	1.250E+08	0.283	105.290	146.859	41.569
Pl25	1424	1.68	0.143	1.537	0.401	1.907E+08	0.414	98.907	168.821	69.914
Pl25	1424	2.06	0.139	1.921	0.335	2.384E+08	0.455	116.153	213.104	96.951
Pl25	1424	2.65	0.150	2.500	0.255	3.102E+08	0.401	175.634	293.381	117.747
Pl25	1424	4.14	0.140	4.000	0.360	4.964E+08	0.390	277.627	455.466	177.839
Pl25	1424	5.62	0.144	5.476	0.433	6.796E+08	0.434	339.962	600.703	260.741
Pl25	1424	8.37	0.146	8.224	0.328	1.021E+09	0.365	581.964	916.291	334.327

Appendix B11. Turner and FIRe fluorescence measurements of *P. lutheri* during balanced and triplicate scaled-up growth at MT-HL.

Species	Tube#	T[Turner]	Bl[Turner]	Corr F[Turner]	mu	F_cum	Fv/Fm	F0	Fm	Fv
Pl25	152	33.6	0.277	33.323	1.141	1.337E+09	0.364	753.347	1184.818	431.471
Pl25	152	15.5	0.259	15.241	1.128	4.280E+09	0.470	293.574	554.379	260.805
Pl25	152	40.5	0.265	40.235	0.951	1.130E+10	0.430	881.146	1546.302	665.156
Pl25	152	20.1	0.262	19.838	1.155	3.900E+10	0.409	477.149	807.344	330.195
Pl25	152	10.6	0.268	10.332	1.289	1.422E+11	0.429	748.572	1310.928	562.356
Pl25	152	31.5	0.253	31.247	1.114	4.300E+11	0.427	630.615	1100.444	469.828
Pl25	152	12.1	0.277	11.823	1.159	1.139E+12	0.438	555.723	989.355	433.632
Pl25	152	35.8	0.264	35.536	1.082	3.423E+12	0.454	675.243	1236.388	561.145
Pl25	1522	18.2	0.264	17.936	1.039	1.037E+13	0.396	418.600	692.579	273.979
Pl25	1522	0.325	0.136	0.189	0.060	1.103E+13	0.629	6.190	16.675	10.485
Pl25	1522	0.755	0.127	0.628	1.231	3.666E+13	0.779	15.201	68.750	53.550
Pl25	1522	2.30	0.131	2.169	1.130	1.266E+14	0.429	159.119	278.768	119.649
Pl25	1522	12.7	0.129	12.571	1.185	7.338E+14	0.509	679.842	1383.252	703.411
Pl25	1523	17.7	0.264	17.436	1.013	1.008E+13	0.436	388.706	688.818	300.112
Pl25	1523	0.310	0.136	0.174	0.008	1.016E+13	0.479	7.933	15.233	7.300
Pl25	1523	0.728	0.127	0.601	1.270	3.508E+13	0.577	29.101	68.813	39.713
Pl25	1523	2.32	0.131	2.189	1.178	1.278E+14	0.393	156.288	257.438	101.149
Pl25	1523	13.4	0.129	13.271	1.215	7.747E+14	0.409	789.376	1335.514	546.138
Pl25	1524	17.4	0.264	17.136	0.997	9.904E+12	0.398	415.379	690.530	275.151
Pl25	1524	0.330	0.136	0.194	0.130	1.132E+13	0.497	10.019	19.909	9.890
Pl25	1524	0.864	0.127	0.737	1.368	4.302E+13	0.414	45.466	77.571	32.105
Pl25	1524	3.01	0.131	2.879	1.242	1.681E+14	0.367	214.380	338.932	124.552
Pl25	1524	14.7	0.129	14.571	1.094	8.505E+14	0.416	846.777	1449.888	603.112

Appendix B12. Turner and FIRe fluorescence measurements of *P. lutheri* during balanced and triplicate scaled-up growth at MT-ML.

Species	Tube#	T[Turner]	Bl[Turner]	Corr F[Turner]	mu	F_cum	Fv/Fm	F0	Fm	Fv
Pl25	162	55.7	0.258	55.442	0.890	1.719E+03	0.481	1188.522	2288.934	1100.412
Pl25	162	17.9	0.269	17.631	1.082	3.826E+03	0.430	410.910	721.344	310.433
Pl25	162	56.2	0.259	55.941	1.023	1.214E+04	0.428	1495.069	2613.808	1118.739
Pl25	162	14.1	0.264	13.836	1.068	3.303E+04	0.432	320.713	565.050	244.337
Pl25	162	37.7	0.257	37.443	0.934	8.938E+04	0.427	918.673	1602.138	683.465
Pl25	162	15.7	0.269	15.431	1.147	2.578E+05	0.446	317.392	573.230	255.838
Pl25	162	38.5	0.257	38.243	0.965	6.390E+05	0.468	785.899	1476.769	690.870
Pl25	162	20.5	0.261	20.239	1.000	2.367E+06	0.451	382.800	697.382	314.583

Pl25	1622	6.38	0.258	6.122	0.817	4.296E+06	0.592	99.058	242.676	143.618
Pl25	1622	16.1	0.271	15.829	0.981	1.111E+07	0.445	357.400	644.268	286.868
Pl25	1622	39.7	0.269	39.431	0.916	2.767E+07	0.415	871.766	1489.390	617.624
Pl25	1622	1.80	0.127	1.673	0.169	3.472E+07	0.413	114.139	194.496	80.357
Pl25	1622	3.49	0.134	3.356	0.997	6.965E+07	0.404	257.182	431.370	174.189
Pl25	1622	7.86	0.124	7.736	0.865	1.605E+08	0.471	533.475	1009.250	475.776
Pl25	1622	18.7	0.132	18.568	0.927	3.853E+08	0.491	1146.041	2253.159	1107.118
Pl25	1623	6.37	0.258	6.112	0.815	4.289E+06	0.430	126.791	222.579	95.788
Pl25	1623	16.1	0.271	15.829	0.982	1.111E+07	0.476	321.514	614.071	292.557
Pl25	1623	39.9	0.269	39.631	0.921	2.781E+07	0.401	852.066	1422.926	570.860
Pl25	1623	1.84	0.127	1.713	0.183	3.555E+07	0.454	106.413	194.916	88.503
Pl25	1623	3.73	0.134	3.596	1.063	7.463E+07	0.367	271.326	428.840	157.514
Pl25	1623	8.56	0.124	8.436	0.883	1.751E+08	0.410	584.841	990.723	405.882
Pl25	1623	21.7	0.132	21.568	0.994	4.476E+08	0.392	1364.648	2243.449	878.801
Pl25	1624	6.63	0.258	6.372	0.872	4.472E+06	0.636	83.216	228.425	145.209
Pl25	1624	16.6	0.271	16.329	0.971	1.146E+07	0.501	353.675	708.870	355.194
Pl25	1624	41.3	0.269	41.031	0.925	2.879E+07	0.411	855.927	1454.205	598.278
Pl25	1624	1.80	0.127	1.673	0.140	3.472E+07	0.436	127.426	225.895	98.470
Pl25	1624	3.64	0.134	3.506	1.060	7.276E+07	0.392	246.156	404.878	158.721
Pl25	1624	8.73	0.124	8.606	0.930	1.786E+08	0.411	591.117	1004.327	413.210
Pl25	1624	21.7	0.132	21.568	0.973	4.476E+08	0.409	1344.973	2277.314	932.340

Appendix B13. Turner and FIRe fluorescence measurements of *P. lutheri* during balanced and triplicate scaled-up growth at MT-LL.

Species	Tube#	T[Turner]	Bl[Turner]	Corr F[Turner]	mu	F_cum	Fv/Fm	F0	Fm	Fv
Pl25	172	42.4	0.253	42.147	0.389	1.110E+06	0.416	1051.596	1800.509	748.913
Pl25	172	8.99	0.277	8.713	0.440	1.606E+06	0.542	184.747	403.796	219.050
Pl25	172	12.6	0.264	12.336	0.342	2.274E+06	0.498	229.598	457.372	227.774
Pl25	172	18.2	0.264	17.936	0.351	3.306E+06	0.384	430.754	699.478	268.724
Pl25	172	6.27	0.272	5.998	0.447	5.251E+06	0.503	126.831	255.262	128.431
Pl25	172	9.02	0.263	8.757	0.388	7.666E+06	0.398	241.848	401.608	159.760
Pl25	172	12.0	0.270	11.730	0.266	1.027E+07	0.393	292.039	481.480	189.441
Pl25	172	17.9	0.261	17.639	0.404	1.544E+07	0.380	401.968	648.150	246.182
Pl25	172	23.8	0.271	23.529	0.329	2.060E+07	0.382	550.880	891.062	340.182
Pl25	172	32.5	0.264	32.236	0.311	2.822E+07	0.374	768.539	1226.982	458.442
Pl25	172	44.2	0.269	43.931	0.308	3.846E+07	0.400	1076.396	1794.392	717.996
Pl25	172	12.5	0.265	12.235	0.534	7.498E+07	0.367	258.337	408.162	149.825
Pl25	172	14.3	0.255	14.045	0.176	8.607E+07	0.388	338.446	553.175	214.729
Pl25	172	20.9	0.271	20.629	0.378	1.264E+08	0.411	489.556	831.820	342.264
Pl25	172	30.6	0.271	30.329	0.310	1.859E+08	0.393	698.050	1149.772	451.723
Pl25	172	37.1	0.266	36.834	0.274	2.257E+08	0.381	909.182	1467.869	558.686
Pl25	172	49.8	0.273	49.527	0.297	3.035E+08	0.401	1184.169	1978.307	794.139
Pl25	172	11.5	0.265	11.235	0.467	4.819E+08	0.411	253.573	430.876	177.302
Pl25	172	16.5	0.231	16.269	0.314	6.979E+08	0.363	223.373	350.697	127.324
Pl25	172	20.2	0.262	19.938	0.303	8.553E+08	0.292	541.880	764.953	223.074
Pl25	172	25.4	0.263	25.137	0.168	1.078E+09	0.459	567.009	1048.119	481.110
Pl25	172	55.9	0.269	55.631	0.388	2.386E+09	0.440	1266.052	2260.636	994.584
Pl25	1722	17.7	0.265	17.435	0.061	2.493E+09	0.400	365.003	608.174	243.171
Pl25	1722	24.2	0.265	23.935	0.314	3.422E+09	0.447	462.707	837.387	374.680
Pl25	1722	30.9	0.261	30.639	0.257	4.381E+09	0.407	721.032	1214.884	493.852
Pl25	1722	82.4	0.386	82.014	0.304	1.173E+10	0.438	1825.573	3248.039	1422.465

Pl25	1722	1.81	0.141	1.669	-0.569	6.358E+09	0.421	112.795	194.911	82.116
Pl25	1722	2.33	0.130	2.200	0.386	8.381E+09	0.453	159.149	291.155	132.006
Pl25	1722	3.28	0.127	3.153	0.376	1.201E+10	0.418	217.008	372.568	155.560
Pl25	1722	3.94	0.122	3.818	0.190	1.454E+10	0.393	281.660	463.871	182.210
Pl25	1722	6.55	0.134	6.416	0.377	2.444E+10	0.488	438.049	855.798	417.750
Pl25	1722	7.89	0.132	7.758	0.209	2.955E+10	0.391	589.514	967.315	377.801
Pl25	1722	10.5	0.129	10.371	0.394	3.951E+10	0.396	671.668	1111.776	440.107
Pl25	1722	15.4	0.127	15.273	0.260	5.818E+10	0.501	1071.379	2146.122	1074.743
Pl25	1723	18.7	0.265	18.435	0.138	2.636E+09	0.409	381.938	646.619	264.681
Pl25	1723	24.6	0.265	24.335	0.275	3.480E+09	0.393	486.663	802.372	315.708
Pl25	1723	31.2	0.261	30.939	0.250	4.424E+09	0.419	679.927	1169.914	489.987
Pl25	1723	81.7	0.386	81.314	0.298	1.163E+10	0.353	1806.938	2793.104	986.167
Pl25	1723	1.78	0.141	1.639	-0.578	6.244E+09	0.397	110.782	183.811	73.029
Pl25	1723	2.27	0.130	2.140	0.373	8.152E+09	0.371	145.840	231.727	85.886
Pl25	1723	2.96	0.127	2.833	0.293	1.079E+10	0.360	215.734	336.996	121.262
Pl25	1723	3.88	0.122	3.758	0.281	1.432E+10	0.405	270.363	454.597	184.234
Pl25	1723	6.16	0.134	6.026	0.343	2.296E+10	0.409	414.288	701.310	287.021
Pl25	1723	8.18	0.132	8.048	0.318	3.066E+10	0.440	550.794	984.293	433.500
Pl25	1723	9.91	0.129	9.781	0.265	3.726E+10	0.412	627.980	1067.746	439.766
Pl25	1723	15.5	0.127	15.373	0.304	5.856E+10	0.378	1023.269	1646.110	622.842
Pl25	1724	17.6	0.265	17.335	0.053	2.479E+09	0.385	373.720	608.103	234.382
Pl25	1724	22.6	0.265	22.335	0.251	3.194E+09	0.463	406.278	756.170	349.893
Pl25	1724	28.8	0.261	28.539	0.255	4.081E+09	0.446	615.234	1110.743	495.509
Pl25	1724	76.5	0.386	76.114	0.302	1.088E+10	0.366	1754.022	2768.070	1014.048
Pl25	1724	1.58	0.141	1.439	-0.637	5.482E+09	0.354	111.028	171.781	60.753
Pl25	1724	1.93	0.130	1.800	0.313	6.857E+09	0.456	117.871	216.664	98.793
Pl25	1724	2.66	0.127	2.533	0.356	9.649E+09	0.402	187.428	313.595	126.166
Pl25	1724	3.39	0.122	3.268	0.253	1.245E+10	0.354	262.247	406.152	143.905
Pl25	1724	5.08	0.134	4.946	0.301	1.884E+10	0.408	337.788	570.929	233.141
Pl25	1724	6.97	0.132	6.838	0.356	2.605E+10	0.410	479.424	812.209	332.785
Pl25	1724	8.71	0.129	8.581	0.308	3.269E+10	0.392	585.000	962.784	377.784
Pl25	1724	11.8	0.127	11.673	0.207	4.447E+10	0.387	805.988	1315.105	509.117

Appendix B14. Turner and FIRe fluorescence measurements of *P. lutheri* during balanced and triplicate scaled-up growth at HT-HL.

Species	Tube#	T[Turner]	Bl[Turner]	Corr F[Turner]	mu	F_cum	Fv/Fm	F0	Fm	Fv
Pl25	182	10.4	0.254	10.146	1.116	1.432E+07	0.388	238.065	389.015	150.950
Pl25	182	7.64	0.268	7.372	1.109	4.161E+07	0.270	192.961	264.269	71.309
Pl25	182	17.0	0.265	16.735	0.960	9.446E+07	0.377	355.096	569.732	214.637
Pl25	182	11.4	0.265	11.135	0.827	2.514E+08	0.363	250.578	393.073	142.495
Pl25	182	20.8	0.263	20.537	0.760	4.637E+08	0.377	391.880	628.856	236.976
Pl25	182	12.1	0.265	11.835	1.007	1.269E+09	0.472	281.298	532.604	251.306
Pl25	182	30.0	0.267	29.733	0.799	3.189E+09	0.402	614.045	1026.758	412.713
Pl25	182	19.0	0.270	18.730	1.012	9.541E+09	0.413	263.069	448.025	184.956
Pl25	182	44.1	0.258	43.842	0.822	2.233E+10	0.401	638.506	1066.667	428.161
Pl25	1822	0.716	0.129	0.587	0.939	5.980E+10	0.648	25.268	71.829	46.561
Pl25	1822	1.40	0.129	1.271	1.118	1.295E+11	0.370	86.993	138.003	51.010
Pl25	1822	3.99	0.130	3.860	1.103	3.933E+11	0.419	232.949	401.161	168.212
Pl25	1822	12.7	0.129	12.571	0.919	1.281E+12	0.426	742.625	1294.865	552.240
Pl25	1823	0.705	0.129	0.576	0.921	5.868E+10	0.556	28.423	64.039	35.616

Pl25	1823	1.40	0.129	1.271	1.145	1.295E+11	0.459	75.826	140.236	64.410
Pl25	1823	4.23	0.130	4.100	1.163	4.177E+11	0.410	274.354	464.683	190.328
Pl25	1823	14.5	0.129	14.371	0.976	1.464E+12	0.385	850.783	1383.999	533.215
Pl25	1824	0.690	0.129	0.561	0.896	5.716E+10	0.575	27.315	64.290	36.975
Pl25	1824	1.37	0.129	1.241	1.149	1.264E+11	0.437	76.885	136.458	59.573
Pl25	1824	3.95	0.130	3.820	1.117	3.892E+11	0.410	237.650	403.015	165.365
Pl25	1824	13.0	0.129	12.871	0.946	1.311E+12	0.408	742.503	1253.330	510.826

Appendix B15. Turner and FIRe fluorescence measurements of *P. lutheri* during balanced and triplicate scaled-up growth at HT-ML.

Species	Tube#	T[Turner]	Bl[Turner]	Corr F[Turner]	mu	F_cum	Fv/Fm	F0	Fm	Fv
Pl25	192	26.3	0.269	26.031	0.876	1.543E+05	0.435	541.766	958.520	416.754
Pl25	192	11.4	0.272	11.128	1.100	4.618E+05	0.460	210.211	389.602	179.390
Pl25	192	26.4	0.258	26.142	0.908	1.085E+06	0.367	734.896	1160.695	425.799
Pl25	192	11.4	0.265	11.135	0.983	3.235E+06	0.405	249.912	420.081	170.169
Pl25	192	9.68	0.254	9.426	1.074	1.095E+07	0.493	195.419	385.822	190.402
Pl25	192	7.04	0.268	6.772	1.098	3.148E+07	0.387	167.577	273.548	105.971
Pl25	192	16.1	0.265	15.835	0.994	7.361E+07	0.428	340.066	594.899	254.833
Pl25	192	13.9	0.265	13.635	1.044	2.535E+08	0.508	251.827	511.687	259.861
Pl25	1922	6.53	0.263	6.267	0.676	4.370E+08	0.707	8.347	28.460	20.113
Pl25	1922	15.7	0.265	15.435	0.901	1.076E+09				
Pl25	1922	0.761	0.127	0.634	0.068	1.163E+09	0.521	38.763	80.927	42.165
Pl25	1922	2.13	0.121	2.009	1.065	3.686E+09	0.472	125.222	237.367	112.145
Pl25	1922	5.62	0.130	5.490	0.972	1.007E+10	0.417	378.406	648.989	270.584
Pl25	1922	14.2	0.129	14.071	0.898	2.582E+10	0.462	992.457	1846.383	853.926
Pl25	1923	6.87	0.263	6.607	0.741	4.607E+08	0.463	117.642	218.994	101.353
Pl25	1923	16.9	0.265	16.635	0.923	1.160E+09	0.380	350.040	564.176	214.136
Pl25	1923	0.778	0.127	0.651	0.058	1.240E+09	0.324	61.461	90.883	29.422
Pl25	1923	2.06	0.121	1.939	1.007	3.693E+09	0.417	133.563	229.133	95.570
Pl25	1923	5.20	0.130	5.070	0.929	9.656E+09	0.401	355.764	593.611	237.847
Pl25	1923	12.4	0.129	12.271	0.843	2.337E+10	0.440	768.792	1372.980	604.189
Pl25	1924	6.91	0.263	6.647	0.749	4.635E+08	0.405	123.020	206.584	83.564
Pl25	1924	16.8	0.265	16.535	0.911	1.153E+09	0.380	521.845	841.685	319.840
Pl25	1924	0.799	0.127	0.672	0.091	1.280E+09	0.431	50.485	88.761	38.276
Pl25	1924	2.17	0.121	2.049	1.029	3.903E+09	0.477	128.140	244.904	116.765
Pl25	1924	5.59	0.130	5.460	0.947	1.040E+10	0.447	354.693	641.914	287.221
Pl25	1924	13.8	0.129	13.671	0.875	2.604E+10	0.418	895.811	1538.839	643.027

Appendix B16. Turner and FIRe fluorescence measurements of *P. lutheri* during balanced and duplicate scaled-up growth at HT-LL. * indicates anamolous F_m and F_v.

Species	Tube#	T[Turner]	Bl[Turner]	Corr F[Turner]	mu	F_cum	Fv/Fm	F0	Fm	Fv
Pl25	202	13.0	0.275	12.725	0.442	8.908E+01	0.317	280.428	410.830	130.401
Pl25	202	15.8	0.287	15.513	0.165	1.086E+02	0.454	321.201	588.052	266.851
Pl25	202	18.9	0.266	18.634	0.198	1.304E+02	0.517	406.699	842.639	435.940

Pl25	202	24.5	0.260	24.240	0.254	1.697E+02	0.412	545.287	927.825	382.537
Pl25	202	32.2	0.277	31.923	0.268	2.235E+02	0.389	755.822	1236.081	480.259
Pl25	202	39.9	0.262	39.638	0.264	2.775E+02	0.458	922.296	1700.858	778.562
Pl25	202	14.9	0.269	14.631	0.390	4.097E+02	0.374	364.689	582.362	217.673
Pl25	202	18.5	0.272	18.228	0.221	5.104E+02	0.405	405.865	681.695	275.829
Pl25	202	23.1	0.258	22.842	0.240	6.396E+02	0.508	585.557	1189.781	604.225
Pl25	202	29.1	0.265	28.835	0.210	8.074E+02	0.388	742.490	1212.468	469.978
Pl25	202	6.83	0.254	6.576	0.412	1.289E+03	0.497	203.704	405.007	201.303
Pl25	202	8.33	0.268	8.062	0.212	1.580E+03	0.458	185.570	342.579	157.009
Pl25	202	10.4	0.265	10.135	0.268	1.986E+03	0.410	251.239	425.982	174.743
Pl25	202	14.0	0.265	13.735	0.257	2.692E+03	0.395	311.875	515.451	203.576
Pl25	202	17.6	0.263	17.337	0.289	3.398E+03	0.467	329.333	618.149	288.816
Pl25	202	22.6	0.265	22.335	0.253	4.378E+03	0.420	294.441	507.684	213.242
Pl25	202	9.59	0.267	9.323	0.445	7.309E+03	0.441	221.234	396.041	174.807
Pl25	202	12.4	0.270	12.130	0.243	9.510E+03	0.415	200.445	342.467	142.022
Pl25	202	15.8	0.258	15.542	0.240	1.218E+04	0.403	286.592	479.899	193.307
Pl25	202	18.6	0.261	18.339	0.227	1.438E+04	0.487	382.399	746.045	363.647
Pl25	202	24.2	0.264	23.936	0.264	1.877E+04	0.405	560.712	942.229	381.517
Pl25	202	31.8	0.274	31.526	0.274	2.472E+04	0.360	606.764	947.896	341.132
Pl25	202	13.0	0.269	12.731	0.373	3.992E+04	0.421	283.078	489.154	206.077
Pl25	202	16.2	0.256	15.944	0.210	5.000E+04	0.412	297.229	505.240	208.011
Pl25	202	20.6	0.253	20.347	0.288	6.381E+04	0.414	341.360	582.890	241.531
Pl25	202	27.9	0.264	27.636	0.277	8.667E+04	0.397	567.791	941.161	373.369
Pl25	202	34.3	0.255	34.045	0.213	1.068E+05	0.481	894.804	1723.148	828.344
Pl25	2022	0.338	0.132	0.206	-0.506	6.460E+04	0.424	16.510	28.678	12.169
Pl25	2022	0.377	0.130	0.247	0.253	1.645E+05	0.533	22.348	47.848	25.500
Pl25	2022	0.542	0.126	0.416	0.468	2.771E+05	1.000	30.687	2584661.582*	2584630.895*
Pl25	2022	0.590	0.126	0.464	0.106	3.090E+05	0.484	36.715	71.176	34.461
Pl25	2022	0.780	0.128	0.652	0.329	4.342E+05	0.477	43.400	82.983	39.583
Pl25	2022	0.943	0.130	0.813	0.202	5.415E+05	0.459	64.569	119.247	54.678
Pl25	2022	1.17	0.116	1.054	0.268	7.020E+05	0.491	73.469	144.326	70.857
Pl25	2022	1.45	0.119	1.331	0.308	8.865E+05	0.438	102.742	182.746	80.004
Pl25	2022	1.86	0.128	1.732	0.259	1.154E+06	0.418	127.163	218.356	91.193
Pl25	2022	2.55	0.132	2.418	0.276	1.610E+06	0.452	170.782	311.751	140.969
Pl25	2022	3.43	0.121	3.309	0.286	2.204E+06	0.409	246.709	417.229	170.519
Pl25	2022	4.19	0.135	4.055	0.230	2.701E+06	0.407	300.792	507.411	206.619
Pl25	2022	4.80	0.129	4.671	0.124	3.111E+06	0.448	300.472	544.319	243.846
Pl25	2022	6.42	0.127	6.293	0.309	4.191E+06	0.548	399.557	884.690	485.133
Pl25	2022	7.62	0.129	7.491	0.248	4.989E+06	0.458	475.971	878.861	402.890
Pl25	2022	10.3	0.134	10.166	0.233	6.771E+06	0.412	693.951	1180.205	486.254
Pl25	2022	12.3	0.132	12.168	0.188	8.104E+06	0.403	852.472	1426.797	574.326
Pl25	2023	0.359	0.132	0.227	-0.408	7.119E+04	0.578	9.629	22.838	13.208
Pl25	2023	0.395	0.130	0.265	0.215	8.310E+04	0.612	14.599	37.649	23.050
Pl25	2023	0.519	0.126	0.393	0.354	1.232E+05	0.677	16.916	52.398	35.482
Pl25	2023	0.659	0.126	0.533	0.295	1.671E+05	0.530	31.727	67.456	35.729
Pl25	2023	0.834	0.128	0.706	0.272	2.214E+05	0.540	44.827	97.514	52.687
Pl25	2023	1.04	0.130	0.910	0.232	2.854E+05	0.585	59.023	142.066	83.043
Pl25	2023	1.24	0.116	1.124	0.218	3.525E+05	0.368	96.326	152.467	56.141
Pl25	2023	1.55	0.119	1.431	0.319	4.488E+05	0.473	99.412	188.624	89.212
Pl25	2023	1.96	0.128	1.832	0.243	5.745E+05	0.470	119.120	224.755	105.635
Pl25	2023	2.79	0.132	2.658	0.308	8.335E+05	0.465	171.644	321.010	149.366
Pl25	2023	3.53	0.121	3.409	0.227	1.069E+06	0.389	259.253	424.074	164.821
Pl25	2023	4.48	0.135	4.345	0.274	1.363E+06	0.404	303.447	509.409	205.962
Pl25	2023	5.27	0.129	5.141	0.148	1.612E+06	0.422	338.966	586.036	247.070
Pl25	2023	6.81	0.127	6.683	0.272	2.096E+06	0.410	469.075	795.451	326.376
Pl25	2023	8.12	0.129	7.991	0.255	2.506E+06	0.393	566.093	933.012	366.918

Pl25	2023	10.0	0.134	9.866	0.161	3.094E+06	0.427	662.718	1156.125	493.408
Pl25	2023	12.7	0.132	12.568	0.253	3.941E+06	0.394	875.043	1445.117	570.074

Appendix B17. Turner and FIRe fluorescence measurements of *T. pseudonana* during balanced and triplicate scaled-up growth at LT-ML.

Species	Tube#	T[Turner]	Bl[Turner]	Corr F[Turner]	mu	F cum	Fv/Fm	F0	Fm	Fv
Tp35	132	13.6	0.264	13.336	1.617	2.114E+21	0.544	251.548	551.374	299.826
Tp35	132	26.8	0.245	26.555	0.800	4.209E+21	0.488	593.056	1158.052	564.996
Tp35	132	13.9	0.250	13.650	1.289	1.514E+22	0.559	282.151	639.752	357.601
Tp35	132	40.3	0.266	40.034	1.072	4.442E+22	0.562	853.926	1948.742	1094.817
Tp35	132	9.36	0.238	9.122	1.285	1.619E+23	0.588	174.775	424.193	249.419
Tp35	132	34.6	0.272	34.328	1.227	6.094E+23	0.538	824.096	1782.659	958.563
Tp35	132	11.4	0.266	11.134	1.242	2.174E+24	0.528	235.259	498.522	263.264
Tp35	132	39.4	0.267	39.133	1.110	7.642E+24	0.542	869.099	1898.220	1029.122
Tp35	1322	9.21	0.143	9.067	1.180	2.656E+25	0.611	166.244	427.705	261.461
Tp35	1322	25.4	0.139	25.261	1.537	7.399E+25	0.516	557.444	1150.751	593.307
Tp35	1322	1.09	0.150	0.940	0.177	8.879E+25	0.582	52.110	124.738	72.628
Tp35	1322	4.50	0.140	4.360	1.175	4.119E+26	0.568	270.537	626.419	355.882
Tp35	1322	9.86	0.144	9.716	1.104	9.178E+26	0.624	577.993	1537.770	959.777
Tp35	1323	9.08	0.143	8.937	1.166	2.618E+25	0.642	139.927	390.393	250.465
Tp35	1323	23.7	0.139	23.561	1.454	6.901E+25	0.517	518.349	1073.581	555.232
Tp35	1323	0.962	0.150	0.812	0.195	8.439E+25	0.574	47.166	110.646	63.480
Tp35	1323	4.24	0.140	4.100	1.240	4.261E+26	0.477	294.312	562.793	268.481
Tp35	1323	9.42	0.144	9.276	1.125	9.641E+26	0.557	572.542	1291.978	719.436
Tp35	1324	8.11	0.143	7.967	1.058	2.334E+25	0.593	147.307	361.612	214.305
Tp35	1324	19.6	0.139	19.461	1.340	5.700E+25	0.503	456.676	919.650	462.974
Tp35	1324	0.869	0.150	0.719	0.170	6.792E+25	0.445	54.714	98.516	43.802
Tp35	1324	3.77	0.140	3.630	1.240	3.429E+26	0.561	210.137	478.477	268.340
Tp35	1324	8.55	0.144	8.406	1.157	7.941E+26	0.548	527.552	1166.645	639.093

Appendix B18. Turner and FIRe fluorescence measurements of *T. pseudonana* during balanced and triplicate scaled-up growth at LT-LL.

Species	Tube#	T[Turner]	Bl[Turner]	Corr F[Turner]	mu	F cum	Fv/Fm	F0	Fm	Fv
Tp35	142	53.7	0.267	53.433	0.545	2.275E+09	0.525	1083.935	2281.327	1197.392
Tp35	142	8.48	0.266	8.214	0.731	3.847E+09	0.536	183.877	396.551	212.674
Tp35	142	13.1	0.279	12.821	0.448	6.005E+09	0.580	222.567	529.961	307.393
Tp35	142	22.3	0.267	22.033	0.530	1.032E+10	0.566	377.232	869.084	491.852
Tp35	142	34.5	0.268	34.232	0.441	1.603E+10	0.544	734.457	1612.167	877.710
Tp35	142	10.4	0.264	10.136	0.581	2.849E+10	0.610	191.780	491.591	299.811
Tp35	142	17.7	0.261	17.439	0.482	4.901E+10	0.640	303.290	843.134	539.844
Tp35	142	28.1	0.264	27.836	0.463	7.823E+10	0.532	587.486	1254.707	667.221
Tp35	142	38.6	0.245	38.355	0.372	1.078E+11	0.504	1120.897	2261.352	1140.455
Tp35	142	12.8	0.250	12.550	0.679	2.116E+11	0.525	302.093	636.221	334.128
Tp35	142	21.3	0.266	21.034	0.515	3.547E+11	0.541	460.274	1002.193	541.919
Tp35	142	35.1	0.238	34.862	0.502	5.879E+11	0.552	801.088	1789.492	988.405
Tp35	142	11.4	0.272	11.128	0.602	1.126E+12	0.637	211.483	582.370	370.886

Tp35	142	20.2	0.266	19.934	0.569	2.017E+12	0.539	402.907	873.243	470.336
Tp35	142	34.9	0.267	34.633	0.488	3.504E+12	0.542	869.099	1898.220	1029.122
Tp35	1422	10.6	0.143	10.457	0.390	5.290E+12	0.559	214.958	486.975	272.018
Tp35	1422	15.3	0.139	15.161	0.557	7.670E+12	0.522	338.798	709.256	370.458
Tp35	1422	26.4	0.263	26.137	0.528	1.322E+13	0.510	614.503	1254.343	639.840
Tp35	1422	48.7	0.245	48.455	0.473	2.451E+13	0.531	1100.420	2345.350	1244.930
Tp35	1422	11.6	0.261	11.339	0.680	4.015E+13	0.358	271.165	422.308	151.142
Tp35	1422	18.9	0.274	18.626	0.491	6.596E+13	0.587	355.330	860.887	505.557
Tp35	1422	33.2	0.262	32.938	0.530	1.166E+14	0.534	702.487	1508.071	805.584
Tp35	1422	0.863	0.135	0.728	-0.322	8.070E+13	0.618	44.021	115.314	71.293
Tp35	1422	1.26	0.145	1.115	0.602	1.236E+14	0.496	82.138	163.055	80.917
Tp35	1422	2.07	0.140	1.930	0.530	2.139E+14	0.571	122.305	284.845	162.540
Tp35	1422	3.47	0.140	3.330	0.544	3.691E+14	0.555	205.407	461.555	256.147
Tp35	1422	5.49	0.136	5.354	0.475	5.935E+14	0.511	364.351	745.648	381.297
Tp35	1422	9.53	0.131	9.399	0.485	1.042E+15	0.589	540.319	1315.581	775.262
Tp35	1423	10.9	0.143	10.757	0.417	5.442E+12	0.563	203.223	464.811	261.588
Tp35	1423	16.0	0.139	15.861	0.582	8.024E+12	0.498	354.476	706.779	352.303
Tp35	1423	26.5	0.263	26.237	0.488	1.327E+13	0.512	605.779	1242.246	636.467
Tp35	1423	48.1	0.245	47.855	0.460	2.421E+13	0.537	1006.703	2175.599	1168.896
Tp35	1423	10.7	0.261	10.439	0.583	3.697E+13	0.645	122.604	345.557	222.953
Tp35	1423	17.4	0.274	17.126	0.490	6.065E+13	0.512	385.283	789.253	403.970
Tp35	1423	31.5	0.262	31.238	0.558	1.106E+14	0.520	705.718	1470.259	764.541
Tp35	1423	0.859	0.135	0.724	-0.331	7.581E+13	0.585	43.692	105.155	61.463
Tp35	1423	1.27	0.145	1.125	0.622	1.178E+14	0.587	62.930	152.232	89.302
Tp35	1423	2.21	0.140	2.070	0.589	2.168E+14	0.565	131.456	302.374	170.918
Tp35	1423	3.77	0.140	3.630	0.560	3.801E+14	0.522	238.537	498.801	260.264
Tp35	1423	6.08	0.136	5.944	0.493	6.224E+14	0.511	415.533	849.083	433.550
Tp35	1423	10.7	0.131	10.569	0.496	1.107E+15	0.536	662.740	1429.598	766.859
Tp35	1424	10.7	0.143	10.557	0.399	5.341E+12	0.573	194.884	456.889	262.005
Tp35	1424	15.9	0.139	15.761	0.601	7.973E+12	0.513	328.551	674.088	345.537
Tp35	1424	25.7	0.263	25.437	0.464	1.287E+13	0.526	574.944	1212.080	637.136
Tp35	1424	45.9	0.245	45.655	0.448	2.310E+13	0.537	981.342	2120.630	1139.288
Tp35	1424	10.8	0.261	10.539	0.661	3.732E+13	0.609	220.371	563.099	342.727
Tp35	1424	17.5	0.274	17.226	0.486	6.100E+13	0.535	362.940	781.035	418.095
Tp35	1424	30.3	0.262	30.038	0.517	1.064E+14	0.550	639.679	1420.907	781.229
Tp35	1424	0.787	0.135	0.652	-0.388	6.827E+13	0.476	50.422	96.296	45.874
Tp35	1424	1.24	0.145	1.095	0.732	1.147E+14	0.504	71.594	144.332	72.738
Tp35	1424	1.96	0.140	1.820	0.491	1.906E+14	0.504	121.878	245.817	123.938
Tp35	1424	3.05	0.140	2.910	0.468	3.047E+14	0.555	181.032	406.864	225.832
Tp35	1424	5.26	0.136	5.124	0.566	5.366E+14	0.533	329.595	705.064	375.469
Tp35	1424	9.04	0.131	8.909	0.477	9.329E+14	0.497	607.012	1205.886	598.874

Appendix B19. Turner and FIRe fluorescence measurements of *T. pseudonana* during balanced and triplicate scaled-up growth at MT-HL.

Species	Tube#	T[Turner]	Bl[Turner]	Corr F[Turner]	mu	F cum	Fv/Fm	F0	Fm	Fv
Tp35	152	17.3	0.269	17.031	1.598	2.651E+09	0.429	390.674	683.994	293.320
Tp35	152	19.8	0.272	19.528	1.554	2.128E+10	0.483	407.819	789.025	381.206
Tp35	152	44.9	0.278	44.622	1.184	4.863E+10	0.473	915.741	1737.571	821.830
Tp35	152	13.4	0.258	13.142	1.606	2.291E+11	0.488	273.616	534.650	261.034
Tp35	152	8.98	0.277	8.703	1.624	1.062E+12	0.598	148.376	369.194	220.818

Tp35	152	29.7	0.259	29.441	1.182	3.593E+12	0.495	563.437	1114.903	551.466
Tp35	1522	18.8	0.265	18.535	1.302	1.357E+13	0.458	400.047	738.364	338.317
Tp35	1522	1.58	0.131	1.449	0.807	3.227E+13	0.573	86.698	202.969	116.271
Tp35	1522	18.1	0.124	17.976	1.675	4.003E+14	0.549	1186.515	2631.584	1445.069
Tp35	1523	18.5	0.265	18.235	1.286	1.335E+13	0.548	329.263	727.786	398.523
Tp35	1523	1.63	0.131	1.499	0.854	3.338E+13	0.461	110.203	204.458	94.256
Tp35	1523	18.0	0.124	17.876	1.649	3.981E+14	0.492	1120.020	2202.602	1082.582
Tp35	1524	16.5	0.265	16.235	1.172	1.189E+13	0.486	313.515	609.460	295.945
Tp35	1524	1.63	0.131	1.499	0.936	3.246E+13	0.500	108.186	216.518	108.332
Tp35	1524	16.4	0.124	16.276	1.586	3.525E+14	0.514	1007.500	2073.886	1066.387

Appendix B20. Turner and FIRe fluorescence measurements of *T. pseudonana* during balanced and triplicate scaled-up growth at MT-ML.

Species	Tube#	T[Turner]	Bl[Turner]	Corr F[Turner]	mu	F_cum	Fv/Fm	F0	Fm	Fv
Tp35	162	16.5	0.265	16.235	1.477	7.784E+11	0.538	332.452	719.447	386.995
Tp35	162	14.2	0.262	13.938	1.671	4.678E+12	0.462	362.756	673.942	311.186
Tp35	162	9.15	0.268	8.882	1.490	2.087E+13	0.538	192.896	417.639	224.743
Tp35	162	31.3	0.253	31.047	1.260	7.294E+13	0.488	690.463	1348.768	658.305
Tp35	162	12.1	0.277	11.823	1.705	3.056E+14	0.489	158.995	311.359	152.365
Tp35	162	47.2	0.264	46.936	1.355	1.213E+15	0.494	982.163	1939.462	957.299
Tp35	1622	15.2	0.264	14.936	1.466	5.790E+15	0.508	362.416	737.097	374.680
Tp35	1622	0.816	0.136	0.680	0.371	8.502E+15	0.532	43.256	92.343	49.087
Tp35	1622	3.25	0.127	3.123	1.562	3.904E+16	0.519	194.033	403.661	209.628
Tp35	1622	11.7	0.131	11.569	1.103	1.446E+17	0.593	806.565	1983.562	1176.997
Tp35	1623	14.5	0.264	14.236	1.421	5.519E+15	0.559	297.681	675.284	377.603
Tp35	1623	0.810	0.136	0.674	0.409	8.426E+15	0.463	44.248	82.342	38.094
Tp35	1623	2.79	0.127	2.663	1.408	3.329E+16	0.530	165.347	351.543	186.196
Tp35	1623	10.2	0.131	10.069	1.120	1.259E+17	0.522	685.843	1434.896	749.052
Tp35	1624	15.1	0.264	14.836	1.460	5.751E+15	0.480	376.489	724.471	347.983
Tp35	1624	0.832	0.136	0.696	0.400	8.702E+15	0.500	43.971	87.907	43.936
Tp35	1624	2.59	0.127	2.463	1.295	3.079E+16	0.505	160.950	324.937	163.987
Tp35	1624	9.04	0.131	8.909	1.083	1.114E+17	0.501	612.172	1226.257	614.085

Appendix B21. Turner and FIRe fluorescence measurements of *T. pseudonana* during balanced and triplicate scaled-up growth at MT-LL.

Species	Tube#	T[Turner]	Bl[Turner]	Corr F[Turner]	mu	F_cum	Fv/Fm	F0	Fm	Fv
Tp35	172	13.2	0.257	12.943	0.293	2.799E+03	0.591	272.471	665.940	393.470
Tp35	172	18.3	0.269	18.031	0.359	3.899E+03	0.517	386.621	800.439	413.817
Tp35	172	26.6	0.257	26.343	0.403	5.697E+03	0.556	583.978	1314.815	730.837
Tp35	172	45.4	0.261	45.139	0.411	9.762E+03	0.547	1026.150	2266.667	1240.516
Tp35	172	11.1	0.258	10.842	0.713	1.641E+04	0.564	229.104	524.984	295.880
Tp35	172	19.1	0.271	18.829	0.570	2.850E+04	0.544	474.512	1039.662	565.149

Tp35	172	32.9	0.269	32.631	0.552	4.940E+04	0.540	776.545	1689.953	913.408
Tp35	172	11.9	0.272	11.628	0.682	1.232E+05	0.548	254.410	562.501	308.091
Tp35	172	18.2	0.278	17.922	0.620	1.899E+05	0.529	376.956	800.779	423.822
Tp35	172	29.0	0.258	28.742	0.489	3.046E+05	0.511	627.547	1282.196	654.649
Tp35	172	8.68	0.277	8.403	0.758	6.233E+05	0.584	164.680	395.503	230.823
Tp35	172	14.7	0.259	14.441	0.525	1.071E+06	0.529	335.298	711.606	376.308
Tp35	172	25.5	0.265	25.235	0.547	1.872E+06	0.547	539.535	1191.228	651.692
Tp35	172	44.5	0.262	44.238	0.523	3.281E+06	0.536	1220.321	2630.588	1410.267
Tp35	1722	18.0	0.268	17.732	0.406	4.932E+06	0.520	348.880	726.831	377.951
Tp35	1722	31.4	0.253	31.147	0.567	8.664E+06	0.480	768.635	1478.069	709.434
Tp35	1722	0.859	0.132	0.727	-0.536	5.524E+06	0.470	61.268	115.580	54.311
Tp35	1722	1.59	0.129	1.461	0.686	1.110E+07	0.523	103.214	216.488	113.274
Tp35	1722	2.89	0.132	2.758	0.596	2.096E+07	0.557	181.852	410.419	228.567
Tp35	1722	4.90	0.136	4.764	0.528	3.620E+07	0.519	303.990	631.571	327.581
Tp35	1722	8.32	0.127	8.193	0.556	6.225E+07	0.554	620.788	1390.591	769.803
Tp35	1722	13.7	0.131	13.569	0.425	1.031E+08	0.572	1030.219	2409.738	1379.519
Tp35	1723	17.5	0.268	17.232	0.378	4.793E+06	0.471	224.229	423.679	199.451
Tp35	1723	31.4	0.253	31.147	0.596	8.664E+06	0.528	681.156	1443.705	762.549
Tp35	1723	0.821	0.132	0.689	-0.600	5.235E+06	0.497	56.701	112.715	56.014
Tp35	1723	1.52	0.129	1.391	0.691	1.057E+07	0.505	109.263	220.856	111.594
Tp35	1723	2.74	0.132	2.608	0.590	1.982E+07	0.467	200.647	376.414	175.768
Tp35	1723	4.61	0.136	4.474	0.522	3.399E+07	0.499	301.974	603.300	301.325
Tp35	1723	8.35	0.127	8.223	0.624	6.248E+07	0.512	550.087	1127.208	577.120
Tp35	1723	15.2	0.131	15.069	0.510	1.145E+08	0.512	1032.721	2116.646	1083.925
Tp35	1724	17.9	0.268	17.632	0.400	4.904E+06	0.559	367.963	835.046	467.084
Tp35	1724	31.5	0.253	31.247	0.576	8.692E+06	0.518	711.476	1475.535	764.059
Tp35	1724	0.846	0.132	0.714	-0.561	5.425E+06	0.497	56.701	112.715	56.014
Tp35	1724	1.59	0.129	1.461	0.704	1.110E+07	0.536	99.182	213.775	114.593
Tp35	1724	2.78	0.132	2.648	0.558	2.012E+07	0.480	202.411	389.412	187.000
Tp35	1724	4.96	0.136	4.824	0.580	3.665E+07	0.500	313.568	627.678	314.110
Tp35	1724	8.75	0.127	8.623	0.595	6.552E+07	0.527	580.817	1229.133	648.315
Tp35	1724	15.3	0.131	15.169	0.476	1.153E+08	0.493	1066.518	2103.272	1036.754

Appendix B22. Turner and FIRe fluorescence measurements of *T. pseudonana* during balanced and triplicate scaled-up growth at HT-ML.

Species	Tube#	T[Turner]	Bl[Turner]	Corr F[Turner]	mu	F_cum	Fv/Fm	F0	Fm	Fv
Tp35	192	21.7	0.266	21.434	1.252	1.500E+02	0.500	426.221	851.660	425.439
Tp35	192	11.8	0.260	11.540	1.282	5.655E+02	0.514	252.727	520.529	267.801
Tp35	192	40.4	0.277	40.123	1.212	1.966E+03	0.533	814.202	1744.845	930.643
Tp35	192	10.2	0.262	9.938	1.223	5.357E+03	0.443	252.643	453.938	201.295
Tp35	192	39.2	0.269	38.931	1.365	2.098E+04	0.499	884.120	1764.608	880.488
Tp35	192	13.8	0.272	13.528	1.346	8.021E+04	0.552	246.787	550.827	304.041
Tp35	192	43.1	0.258	42.842	1.225	2.540E+05	0.459	1061.254	1960.347	899.093
Tp35	1922	45.3	0.265	45.035	1.235	1.001E+06	0.474	1015.556	1930.667	915.110
Tp35	1922	4.09	0.131	3.959	0.794	2.467E+06	0.516	260.250	537.541	277.291
Tp35	1922	21.3	0.125	21.175	1.553	1.320E+07	0.565	1396.137	3208.037	1811.900
Tp35	1923	38.9	0.265	38.635	1.097	8.590E+05	0.462	913.337	1698.989	785.652

Tp35	1923	3.74	0.131	3.609	0.825	2.192E+06	0.502	242.035	486.201	244.166
Tp35	1923	19.4	0.125	19.275	1.551	1.171E+07	0.491	1199.930	2356.123	1156.194
Tp35	1924	35.6	0.265	35.335	1.016	7.856E+05	0.480	788.363	1516.534	728.171
Tp35	1924	3.17	0.131	3.039	0.752	1.846E+06	0.511	205.996	421.596	215.600
Tp35	1924	16.7	0.125	16.575	1.571	1.007E+07	0.489	1042.564	2040.479	997.915

Appendix B23. Turner and FIRe fluorescence measurements of *T. pseudonana* during balanced and triplicate scaled-up growth at HT-LL.

Species	Tube#	T[Turner]	Bl[Turner]	Corr F[Turner]	mu	F cum	Fv/Fm	F0	Fm	Fv
Tp35	202	12.9	0.269	12.631	0.462	5.052E+01	0.509	313.921	639.481	325.560
Tp35	202	20.3	0.272	20.028	0.463	8.011E+01	0.506	425.344	861.696	436.352
Tp35	202	30.7	0.258	30.442	0.445	1.218E+02	0.463	773.877	1441.299	667.422
Tp35	202	15.2	0.265	14.935	0.607	2.390E+02	0.556	358.909	807.531	448.622
Tp35	202	27.7	0.254	27.446	0.536	4.391E+02	0.509	657.981	1339.845	681.864
Tp35	202	12.8	0.268	12.532	0.626	8.020E+02	0.539	254.859	552.543	297.684
Tp35	202	19.4	0.265	19.135	0.495	1.225E+03	0.570	407.035	946.311	539.276
Tp35	202	10.6	0.265	10.335	0.651	2.646E+03	0.463	233.016	434.121	201.105
Tp35	202	16.1	0.263	15.837	0.530	4.054E+03	0.573	274.219	642.663	368.444
Tp35	202	27.1	0.265	26.835	0.527	6.870E+03	0.474	591.626	1125.171	533.545
Tp35	202	13.0	0.267	12.733	0.556	1.304E+04	0.514	299.085	615.975	316.891
Tp35	202	19.4	0.270	19.130	0.376	1.959E+04	0.435	325.365	575.792	250.427
Tp35	202	27.4	0.258	27.142	0.338	2.779E+04	0.466	465.338	870.776	405.439
Tp35	202	33.8	0.261	33.539	0.290	3.434E+04	0.455	764.359	1401.363	637.005
Tp35	202	11.7	0.264	11.436	0.307	4.684E+04	0.443	239.354	429.830	190.476
Tp35	202	14.1	0.274	13.826	0.188	5.663E+04	0.224	629.793	811.471	181.679
Tp35	202	16.7	0.269	16.431	0.134	6.730E+04	0.442	323.582	579.680	256.098
Tp35	2022	0.227	0.134	0.093	-0.530	3.809E+04	0.605	4.754	12.045	7.292
Tp35	2022	0.269	0.119	0.150	0.564	6.144E+04	0.378	13.282	21.363	8.080
Tp35	2022	0.408	0.124	0.284	0.578	1.163E+05	0.492	25.016	49.241	24.225
Tp35	2022	0.629	0.127	0.502	0.582	2.056E+05	0.573	31.351	73.469	42.118
Tp35	2022	0.972	0.132	0.840	0.518	3.441E+05	0.545	70.527	155.143	84.616
Tp35	2022	1.43	0.130	1.300	0.608	5.325E+05	0.505	90.686	183.338	92.651
Tp35	2022	2.31	0.126	2.184	0.465	8.946E+05	0.519	184.066	383.012	198.946
Tp35	2022	3.98	0.126	3.854	0.551	1.579E+06	0.536	264.406	570.204	305.798
Tp35	2022	6.68	0.128	6.552	0.513	2.684E+06	0.526	464.399	980.267	515.868
Tp35	2022	10.3	0.130	10.170	0.402	4.166E+06	0.505	677.669	1369.376	691.707
Tp35	2023	0.195	0.134	0.061	0.057	7.157E+04	0.622	3.759	9.951	6.191
Tp35	2023	0.232	0.119	0.113	0.728	1.326E+05	0.321	13.102	19.300	6.199
Tp35	2023	0.392	0.124	0.268	0.782	3.144E+05	0.544	17.668	38.741	21.074
Tp35	2023	0.619	0.127	0.492	0.620	5.773E+05	0.476	39.933	76.188	36.256
Tp35	2023	0.975	0.132	0.843	0.542	9.891E+05	0.538	57.336	123.993	66.657
Tp35	2023	1.31	0.130	1.180	0.468	1.384E+06	0.461	99.381	184.482	85.101
Tp35	2023	2.68	0.126	2.554	0.693	2.997E+06	0.514	184.049	378.555	194.507
Tp35	2023	3.57	0.126	3.444	0.290	4.041E+06	0.522	240.694	503.913	263.219
Tp35	2023	5.29	0.128	5.162	0.391	6.057E+06	0.497	394.187	783.340	389.153
Tp35	2023	8.78	0.130	8.650	0.472	1.015E+07	0.519	569.757	1183.406	613.650
Tp35	2024	0.219	0.134	0.085	0.002	6.744E+04	0.500	8.085	16.160	8.075
Tp35	2024	0.263	0.119	0.144	0.622	1.143E+05	0.998	16.770	6811.764	6794.994
Tp35	2024	0.494	0.124	0.370	0.855	2.936E+05	0.685	20.286	64.356	44.071
Tp35	2024	0.745	0.127	0.618	0.524	4.904E+05	0.621	36.319	95.731	59.412
Tp35	2024	1.31	0.132	1.178	0.650	9.347E+05	0.576	80.348	189.668	109.320
Tp35	2024	1.87	0.130	1.740	0.543	1.381E+06	0.564	119.263	273.240	153.977
Tp35	2024	3.48	0.126	3.354	0.589	2.661E+06	0.570	223.341	519.645	296.304

Tp35	2024	6.07	0.126	5.944	0.555	4.716E+06	0.550	493.389	1096.110	602.721
Tp35	2024	10.4	0.128	10.272	0.529	8.150E+06	0.529	823.832	1749.619	925.787
Tp35	2024	17.4	0.130	17.270	0.475	1.370E+07	0.537	1325.455	2864.458	1539.003

Appendix B24. Mean cell density of phytoplankton and bacteria in triplicate scaled-up *N. oculata* cultures.

Species treatment	Corr ave. [algae] (cell L^{-1})	Corr ave. [bacteria] (cell L^{-1})	Algae/bacteria ratio	Estimated ave. bacterial [C] (mg C L^{-1})
No25 1222 (LT-HL)	321697254.180	48688817.871	6.607	0.000974
No25 1223 (LT-HL)	335581775.958	26111605.520	12.852	0.000522
No25 1224 (LT-HL)	335396511.307	56868943.395	5.898	0.001137
No25 1322 (LT-ML)	260751137.273	49685794.018	5.248	0.000994
No25 1323 (LT-ML)	160586545.984	53189796.728	3.019	0.001064
No25 1324 (LT-ML)	180035752.426	45390222.886	3.966	0.000908
No25 1422 (LT-LL)	191650062.243	18963024.687	10.107	0.000379
No25 1423 (LT-LL)	171520242.649	9855111.240	17.404	0.000197
No25 1424 (LT-LL)	198886955.342	47899646.640	4.152	0.000958
No25 1522 (MT-HL)	720543137.833	38901892.968	18.522	0.000778
No25 1523 (MT-HL)	729272855.219	47287446.112	15.422	0.000946
No25 1524 (MT-HL)	631194634.309	37046905.936	17.038	0.000741
No25 1622 (MT-ML)	718423995.704	82582504.434	8.699	0.001652
No25 1623 (MT-ML)	658806556.949	85807181.227	7.678	0.001716
No25 1624 (MT-ML)	522880972.243	55979936.241	9.341	0.001120
No25 1722 (MT-LL)	480192897.141	57414670.527	8.364	0.001148
No25 1723 (MT-LL)	417464534.827	93168573.939	4.481	0.001863
No25 1724 (MT-LL)	399577266.922	103309447.905	3.868	0.002066
No25 1822 (HT-HL)	624885262.204	30440715.393	20.528	0.000609
No25 1823 (HT-HL)	1075583786.856	176329384.551	6.100	0.003527
No25 1824 (HT-HL)	771020905.186	83608017.629	9.222	0.001672

Appendix B25. Mean cell density of phytoplankton and bacteria in triplicate scaled-up *P. lutheri* cultures.

Species treatment	Corr ave. [algae] (cell L^{-1})	Corr ave. [bacteria] (cell L^{-1})	Algae/bacteria ratio	Estimated ave. bacterial [C] (mg C L^{-1})
Pl25 1222 (LT-HL)	81477965.197	82407435.430	0.989	0.001648
Pl25 1223 (LT-HL)	68631797.513	73686068.968	0.931	0.001474
Pl25 1224 (LT-HL)	52101679.524	51720932.331	1.007	0.001034
Pl25 1322 (LT-ML)	29338291.871	11823899.488	2.481	0.000236
Pl25 1323 (LT-ML)	42221576.590	38568931.228	1.095	0.000771
Pl25 1324 (LT-ML)	42653320.318	18857779.220	2.262	0.000377
Pl25 1422 (LT-LL)	28354785.938	5611190.344	5.053	0.000112
Pl25 1423 (LT-LL)	23269199.098	9601269.380	2.424	0.000192
Pl25 1424 (LT-LL)	24470170.816	6598926.433	3.708	0.000132
Pl25 1522 (MT-HL)	134741485.919	61146410.724	2.204	0.001223
Pl25 1523 (MT-HL)	152848666.843	72463111.721	2.109	0.001449
Pl25 1524 (MT-HL)	141151114.380	41722783.076	3.383	0.000834
Pl25 1622 (MT-ML)	69220615.586	49534375.592	1.397	0.000991
Pl25 1623 (MT-ML)	75776067.094	46046364.099	1.646	0.000921
Pl25 1624 (MT-ML)	91383088.895	82017405.794	1.114	0.001640

Pl25 1722 (MT-LL)	84135022.455	82060613.316	1.025	0.001641
Pl25 1723 (MT-LL)	106257265.295	111162984.000	0.956	0.002223
Pl25 1724 (MT-LL)	65434297.713	82418740.578	0.794	0.001648
Pl25 1822 (HT-HL)	116662419.293	78326382.911	1.489	0.001567
Pl25 1823 (HT-HL)	126642684.692	60721971.968	2.086	0.001214
Pl25 1824 (HT-HL)	126476694.558	53302869.572	2.373	0.001066
Pl25 1922 (HT-ML)	111466793.926	83328726.923	1.338	0.001667
Pl25 1923 (HT-ML)	94775222.145	94005850.309	1.008	0.001880
Pl25 1924 (HT-ML)	103163512.909	97108641.914	1.062	0.001942
Pl25 2022 (HT-LL)	53060111.048	35438168.526	1.497	0.000709
Pl25 2023 (HT-LL)	61510611.532	34393103.476	1.788	0.000688

Appendix B26. Mean cell density of phytoplankton and bacteria in triplicate scaled-up *T. pseudonana* cultures.

Species treatment	Corr ave. [algae] (cell L^{-1})	Corr ave. [bacteria] (cell L^{-1})	Algae/bacteria ratio	Estimated ave. bacterial [C] (mg C L^{-1})
Tp35 1322 (LT-ML)	149007466.568	14554191.367	10.238	0.000291
Tp35 1323 (LT-ML)	116131156.335	3156335.265	36.793	0.000063
Tp35 1324 (LT-ML)	119749925.145	6091309.593	19.659	0.000122
Tp35 1422 (LT-LL)	92634176.431	6638713.209	13.954	0.000133
Tp35 1423 (LT-LL)	92737910.232	2456413.164	37.753	0.000049
Tp35 1424 (LT-LL)	70728802.145	3919831.154	18.044	0.000078
Tp35 1522 (MT-HL)	716807889.064	217661840.076	3.293	0.004353
Tp35 1523 (MT-HL)	821459712.149	134609988.605	6.103	0.002692
Tp35 1524 (MT-HL)	565634730.723	48155759.336	11.746	0.000963
Tp35 1622 (MT-ML)	554462701.548	248717048.977	2.229	0.004974
Tp35 1623 (MT-ML)	521531890.604	265369049.563	1.965	0.005307
Tp35 1624 (MT-ML)	411030487.098	200514349.410	2.050	0.004010
Tp35 1722 (MT-LL)	169330157.087	80052541.730	2.115	0.001601
Tp35 1723 (MT-LL)	242258794.457	119591094.144	2.026	0.002392
Tp35 1724 (MT-LL)	231228778.330	97572564.560	2.370	0.001951
Tp35 1922 (HT-ML)	269220958.126	133612339.129	2.015	0.002672
Tp35 1923 (HT-ML)	272606988.223	86495438.499	3.152	0.001730
Tp35 1924 (HT-ML)	216901257.124	75417814.985	2.876	0.001508
Tp35 2022 (HT-LL)	115302361.399	4816553.721	23.939	0.000096
Tp35 2023 (HT-LL)	110034796.333	0.000	#DIV/0!	0.000000
Tp35 2024 (HT-LL)	206499124.510	16089965.398	12.834	0.000322

Appendix B27. Fatty acid profile of *N. oculata* including seawater (SW) blanks and duplicate injections.

Species Treatment	C12:0	C13:0	i-C14:0	C14:0	C14:1n-9	C14:1n-7	C14:1n-5	i-C15:0	ai-C15:0	C15:0	i-C16:0	C16:0	C16:1n-11	C16:1n-9	C16:1n-7	C16:1n-5	C17:1(a)	i-C17:0	C16:2n-6
No25 1222	0.17	0.12	0.24	4.3	0.01		0.05	0	0	0.31	0.03	31.11		0.68	32.16	0.31	0.05	0.02	0.3
No25 1223	0.21	0.12	0.42	4.38	0.01	0	0.04	0	0	0.33	0.02	31.58		0.66	32.46	0.28	0.05	0.01	0.28
No25 1224	0.16	0.13	0.05	4.26	0.01	0	0.05	0.01	0.01	0.31	0.03	30.77	0	0.67	32.68	0.29	0.03	0.01	0.32
SW	0.15	0.12	13.97	0.9		0.16		0.03	0.21	0.21	0.04	14.91	0.03	0.25	5.55	0.2	0.05	0.09	0.1
No25 1322	0.16	0.2	0.36	4.49	0.01	0	0.06	0.01	0.01	0.35	0.04	29.16	0.01	1.15	30.47	0.29	0.05	0.01	0.35
No25 1323	0.29	0.21	1.86	4.88	0.01	0	0.05	0.01	0.01	0.33	0.03	27.35	0.01	1.22	30.69	0.29	0.03	0.01	0.38
No25 1324	0.28	0.23	1.83	4.98	0.01	0	0.05	0.01	0.01	0.33	0.05	26.24	0.01	1.27	30.05	0.3	0.03	0.01	0.4
SW	0.03	0.11	0.94	0.96		0.14		0.28	0.17	0.27	0.07	13.55	0	0.27	6.28	0.23	0.02	0.11	0.08
No25 1422	0.24	0.46	0.47	4.12	0.02		0.05	0.03	0.03	0.33	0.09	19.34	0.01	3.11	22.17	0.15	0.04	0.02	0.54
No25 1423	0.51	0.45	4.54	4.39	0.02		0.05	0.03	0.03	0.35	0.07	18.28	0.01	2.92	21.31	0.14	0.03	0.01	0.46
No25 1423 dup	0.51	0.45	4.58	4.4	0.02		0.05	0.03	0.03	0.35	0.06	18.13	0.01	2.92	21.37	0.14	0.04	0.02	0.44
No25 1424	0.22	0.59	1.56	4.62	0.01		0.06	0.03	0.03	0.25	0.09	16.89	0	3.53	21.61	0.14	0.01	0.01	0.63
SW	0.07	0.05	4.28	0.62	0.06	0.2	0.2	0.04	0.16	0.44	0.07	19.38	0	0.13	1.44	0.02	0.01	0.15	0.08
No25 1522	0.22	0.17	0.03	4.03		0	0.03	0.3	0.01	0.32	0.01	31.55	0	1.28	30.3	0.34	0.04	0.01	0.46
No25 1523	0.25	0.15	0.04	4.08	0.01	0	0.03	0.26	0	0.33	0.01	33.12	0	1.08	30.32	0.37	0.05	0	0.4
No25 1524	0.25	0.16	0.06	4.08	0.01		0.03	0.25	0	0.34	0.01	32.39	0	1.13	30.23	0.35	0.03	0.01	0.42
SW	0.15	0.08	0.25	0.9	0.04	0.05		0.09	0.15	0.22	0.03	20.28	0.01	0.38	2.44	0.02	0.01	0.1	0.11
No25 1622	0.25	0.29	0.01	4.9	0.01	0	0.06	0.03	0.01	0.3	0.02	22.94	0	2.44	28.42	0.28	0.03		0.57
No25 1622 dup	0.26	0.3	0.02	4.91	0.01	0	0.06	0.01	0.01	0.3	0.02	22.98	0	2.45	28.46	0.29	0.04		0.57
No25 1623	0.2	0.35	0.02	4.94	0.01	0	0.06	0.01	0.02	0.3	0.03	22.96	0	2.51	27.32	0.28	0.04	0	0.55
No25 1624	0.37	0.33	0.02	5.35	0.01	0.01	0.06	0.02	0.02	0.32	0.03	22.9	0.01	2.53	25.92	0.27	0.03	0.01	0.51
SW	0.05	0.2	0.3	0.6		0.08	0.66	0.2	0.17	1.01	0.22	13.71	1.48		1.36	0.09	0.01	0.03	0.41
No25 1722	0.26	0.6	0.09	5.25	0.01		0.07	0.04	0.07	0.25	0.06	16	0.01	4.81	21.29	0.19	0.05		0.49
No25 1723	0.27	0.59	0.03	5.1	0		0.08	0.02	0.06	0.27	0.09	16.29	0	4.58	21.54	0.17	0.04		0.43
No25 1724	0.24	0.52	0.02	4.6	0		0.07	0.02	0.04	0.23	0.05	15.89	0.01	4.91	21.69	0.19	0.05		0.44
SW	0.14	0.1	0.31	0.61			0.1	0.2	0.43	0.42	0.16	12.11	0.53	0.08	0.13		0.07	0.07	0.2
No25 1822	0.34	0.13	0	5.18	0.01	0	0.05	0.01	0.01	0.33	0.01	33.68	0	1.12	28.78	0.24	0.04	0	0.41
No25 1823	0.21	0.18	0.04	4.48			0.04	0	0.01	0.32	0.01	32.52	0	1.39	28.76	0.23	0.04	0	0.47
No25 1824	0.33	0.16	0.13	5	0.01	0	0.05	0.03	0.01	0.35	0.01	32.62	0	1.32	28.65	0.25	0.06		0.44
SW	0.12	0.16	2.01	0.82				0.54	0.4	0.16	0.21	9.98	0.11	0.22	2.6	0.08	0	0.07	0

Appendix B27 (cont'd).

Species Treatment	ai-C17:0	C17:1(b)	C16:2n-4	C17:0	Phytane	C16:3n-4	C17:1	C16:4n-3	C16:4n-1	C18:0	C18:1n-13	C18:1n-11	C18:1n-9	C18:1n-7	C18:1n-5	C18:2d5,11	C18:2n-7
No25 1222	0.09	0.02	0.1	0.13	0.28	0.04	0.08	0.02	0.05	1.33		0.05	3	0.44	0.06	0.04	0.06
No25 1223	0.09	0.03	0.1	0.11	0.29	0.04	0.1	0.02	0.03	1.05	0.01	0.04	3.49	0.51	0.03	0.03	0.05
No25 1224	0.1	0.02	0.11	0.12	0.27	0.03	0.07	0.01	0.05	0.99	0	0.02	2.9	0.46	0.03	0.01	0.06
SW	0.05	0.04	0	0.27	0.03	0.32	0.65		0.16	11.74	0.22	0.34	1.23	3.3	0.05	0.15	0.05
No25 1322	0.11	0.02	0.15	0.19	0.33	0.05	0.09	0.02	0.05	1.13		0.04	2.54	0.39	0.03	0.03	0.06
No25 1323	0.11	0.02	0.15	0.14	0.29	0.05	0.09	0.02	0.05	1.07		0.04	2.29	0.35	0.03	0.03	0.06
No25 1324	0.11	0.02	0.18	0.14	0.33	0.06	0.11	0.02	0.06	1.39	0.02	0.05	2.12	0.37	0.03	0.03	0.07
SW	0.07	0.09		0.33	0.05	0.3	0.83		0.21	9.33	0.19	0.25	1.06	4.03	0.05	0.18	
No25 1422	0.15	0.04	0.42	0.13	0.37	0.05	0.12	0.02	0.12	3.43	0.02	0.07	2.67	0.37	0.04	0.06	0.17
No25 1423	0.15	0.03	0.39	0.12	0.38	0.04	0.13	0.02	0.12	3.27	0.02	0.07	2.63	0.4	0.04	0.07	0.16
No25 1423 dup	0.14	0.03	0.38	0.1	0.35	0.03	0.12	0.02	0.12	3.28	0.03	0.08	2.57	0.39	0.04	0.07	0.17
No25 1424	0.15	0.03	0.49	0.13	0.24	0.05	0.2	0.03	0.15	2.27	0.02	0.06	1.93	0.33	0.03	0.07	0.14
SW	0.01			0.3		0.21	1.52	0.11	0.23	21.25	0.35	0.46	2.06	2.56	0.58	0.16	
No25 1522	0.1	0.02	0.16	0.26	0.24	0.04	0.09	0.02	0.04	0.99		0.02	1.8	0.48	0.02	0.01	0.06
No25 1523	0.09	0.02	0.13	0.21	0.27	0.04	0.09	0.02	0.05	1.01		0.02	1.88	0.49	0.03	0.01	0.05
No25 1524	0.09	0.02	0.15	0.28	0.25	0.04	0.09	0.02	0.05	1.14		0.02	1.78	0.49	0.02	0.01	0.06
SW				0.24		0.24	0.09		0.18	19.42		0.34	2.26	0.37	1.08	0.05	
No25 1622	0.13	0.03	0.26	0.19	0.29	0.05	0.13	0.02	0.07	1	0.01	0.02	1.83	0.3	0.03	0.02	0.09
No25 1622 dup	0.13	0.03	0.26	0.18	0.29	0.04	0.11	0.01	0.07	1	0.01	0.02	1.83	0.29	0.03	0.01	0.09
No25 1623	0.13	0.03	0.26	0.19	0.28	0.04	0.11	0.01	0.09	1.15	0.01	0.02	1.77	0.28	0.02	0.01	0.09
No25 1624	0.13	0.03	0.28	0.19	0.3	0.04	0.12	0.02	0.19	1.71	0.01	0.03	1.79	0.28	0.02	0.01	0.1
SW	0.09	0.04	0.34	0.28		0.12	0.19	0.13		13.67	0.17	0.21	0.77	0.69	1.32	0.74	0.03
No25 1722	0.18	0.04	0.54	0.12	0.23	0.04	0.3		1.26	0.96		0.05	2.11	0.33	0.03	0.08	0.11
No25 1723	0.14	0.04	0.48	0.17	0.27	0.03	0.28		0.86	1.12	0.01	0.02	2.09	0.39	0.03	0.05	0.12
No25 1724	0.15	0.03	0.51	0.1	0.2	0.01	0.28	0.01	0.07	1.05	0.01	0.02	2.21	0.34	0.03	0.06	0.12
SW	0.25			0.22		0.49	0.83		0.06	9.23	0.05	0.04			0.81	0.05	
No25 1822	0.1	0.02	0.17	0.17	0.19	0.03	0.09	0.01	0.03	0.97		0.02	2.23	0.42	0.03	0.04	0.06
No25 1823	0.1	0.02	0.19	0.15	0.26	0.03	0.06	0.01	0.05	0.92		0	2.22	0.44	0.03	0.04	0.07
No25 1824	0.1	0.02	0.19	0.21	0.18	0.01	0.07	0.01	0.06	0.99		0.05	2.4	0.44	0.03	0.05	0.06
SW	0.23		0.12	0.26		1.55	0.77	0.05	0.29	7.36	0.37	0.16	0.78	1.83	0.05	0.17	

Appendix B27 (cont'd).

Species Treatment	C18:2n-6	C18:2n-4	C18:3n-6	C18:3n-4	C18:3n-3	C18:3n-1	C18:4n-3	C18:4n-1	C20:0	C20:1n-11	C20:1n-9	C20:1n-7	C20:2n-6	C20:3n-6	C20:4n-6	C20:3n-3	C20:4n-3
No25 1222	0.68	0.68	0.15	0.04	0.05	0.14	0.02	0.02	0.12	0.21	0.05	0.05	0.15	0.43	2.43	0	0.14
No25 1223	0.75	0.79	0.17	0.04	0.05	0.12	0.02	0.01	0.11	0.19	0.03	0.05	0.12	0.42	2.33	0.02	0.16
No25 1224	0.71	0.72	0.14	0.04	0.05	0.13	0.02	0.01	0.11	0.19	0.04	0.07	0.11	0.41	2.56	0.03	0.17
SW	0.3	0.37	0.02		0.32		0.13	0.44	0.12		0.02	0.55	0.02	0.16	0.28	0.16	0.11
No25 1322	0.77	0.83	0.12	0.07	0.05	0.19	0.02	0.02	0.12	0.22	0.04	0.06	0.12	0.36	2.88	0.02	0.18
No25 1323	0.76	0.69	0.12	0.05	0.06	0.2	0.01	0.01	0.11	0.22	0.04	0.05	0.13	0.37	2.86	0.03	0.15
No25 1324	0.78	0.75	0.12	0.06	0.06	0.24	0.01	0.02	0.1	0.2	0.04	0.07	0.12	0.39	2.94	0.02	0.12
SW	0.18	0.39	0.03		0.28	0.04	0.19	0.27	0.12	0.05	0	1.37	0.02	0.09	0.39	0.28	0.15
No25 1422	1.39	0.61	0.09	0.06	0.11	0.48	0.02	0.11	0.11	0.31	0.08	0.12	0.17	0.49	4.33	0.02	0.17
No25 1423	1.3	0.64	0.14	0.08	0.13	0.43	0.03	0.08	0.11	0.34	0.07	0.14	0.15	0.47	4.11	0.03	0.18
No25 1423 dup	1.31	0.52	0.19	0.07	0.13	0.43	0.02	0.08	0.12	0.37	0.07	0.14	0.14	0.47	4.08	0.02	0.18
No25 1424	1.41	0.74	0.07	0.07	0.15	0.5	0.02	0.13	0.06	0.27	0.07	0.24	0.11	0.35	4.52	0.02	0.16
SW	0.25	0.17	0.03	0.01	0.63	0.03	0.15	0.68	0.22	0.28	0.06	1.16	0.03	0.04	0.07	0.03	0.07
No25 1522	0.89	0.83	0.08	0.05	0.05	0.17	0.02	0.02	0.12	0.23	0.03	0.11	0.05	0.15	3.11	0.02	0.12
No25 1523	0.79	0.78	0.09	0.05	0.05	0.16	0.02	0.01	0.12	0.26	0.03	0.09	0.06	0.17	2.85	0	0.12
No25 1524	0.81	0.77	0.09	0.05	0.06	0.17	0.02	0.02	0.13	0.24	0.03	0.1	0	0.14	2.86	0.01	0.11
SW	0.32	0.32	0.02		0.07	0.02	0.3	0.65	1.86		0.15	2.01	0.02	0.2	0.45	0.69	0.28
No25 1622	1.31	0.84	0.11	0.04	0.07	0.26	0.03	0.04	0.1	0.28	0.04	0.12	0.1	0.3	4.03	0.03	0.11
No25 1622 dup	1.32	0.84	0.1	0.05	0.07	0.26	0.02	0.04	0.1	0.28	0.04	0.13	0.11	0.31	4.02	0.03	0.1
No25 1623	1.31	0.83	0.09	0.05	0.08	0.26	0.02	0.04	0.1	0.26	0.04	0.09	0.12	0.3	4.25	0.04	0.16
No25 1624	1.27	0.85	0.09	0.06	0.09	0.28	0.02	0.04	0.11	0.31	0.04	0.16	0.11	0.32	4.15	0.03	0.14
SW	0.26	0.42	0.07	0.18	0.82		0.02	0.16	0.27		0	2.13	0.14	0.06	0.12	4.65	0.19
No25 1722	2	0.78	0.1	0.06	0.14	0.3	0.02	0.12	0.06	0.39	0.09	0.12	0.1	0.36	4.98	0.33	0.11
No25 1723	1.9	0.68	0.12	0.06	0.11	0.28	0.02	0.1	0.08	0.41	0.08	0.14	0.14	0.37	5.09	0.04	0.14
No25 1724	2.09	0.68	0.08	0.06	0.14	0.3	0.02	0.13	0.06	0.4	0.1	0.22	0.15	0.35	5.14	0.11	0.12
SW		0.44	0.03	0.15	0.7		0.34	0.13	0.14		0.02	1.42	0.06	0.04	0.06	1.58	0.19
No25 1822	1.35	0.64	0.11	0.04	0.04	0.16	0.02	0.01	0.14	0.27	0.03	0.08	0.02	0.18	3.17	0.03	0.1
No25 1823	1.28	0.65	0.17	0.05	0.03	0.19	0.02	0.01	0.14	0.3	0.03	0.08	0.06	0.22	3.46	0.01	0.11
No25 1824	1.39	0.62	0.11	0.04		0.17	0.02	0.01	0.14	0.29	0.03	0.19	0.04	0.17	3.28	0.02	0.09
SW	0.25	1.69	0.02		1.11		0.41	0.26	0.29	0.51	0.1	4.94	0.03	0.04	0.15	0	0.11

Appendix B27 (cont'd).

Species Treatment	C20:5n-3	C22:0	C22:1n-11	C22:1n-9	C22:1n-7	C22:2n-6	C21:5n-3	C23:0	C22:4n-6	C22:5n-6	C20:2n-9	C22:4n-3	C22:5n-3	C24:0	C22:6n-3	C24:1n-9
No25 1222	17.3	0.06	0.17	0.11	0.01	0.03	0.2	0.94	0.02		0.02	0.06	0.02	0.02	0.04	0.03
No25 1223	16.09	0.09	0.17	0.1	0.02	0.03	0.17	0.86	0.02		0.02	0.07	0.04	0.03	0.05	0.02
No25 1224	17.64	0.08	0.17	0.13	0.01	0.03	0.18	0.95	0.02		0.02	0.08	0.05	0.03	0.07	0.03
SW	2.95	0.07	0.05	0	0.27			35.62				0.47	1.72		0.28	
No25 1322	19.22	0.12	0.2	0.16	0.03	0.03	0.16	1.35	0.04		0.02	0.08	0.02	0.03	0.03	0.03
No25 1323	19.22	0.09	0.19	0.15	0.02	0.03	0.17	1.4	0.02		0.02	0.09	0.04	0.06	0.16	0.03
No25 1324	20.34	0.08	0.16	0.09	0	0.03	0.18	1.6	0.06		0.02	0.09	0.02	0.02	0.05	0.02
SW	2.82	0.11	0.09	0	0.31			50.04					0.97		1.36	
No25 1422	27.37	0.13	0.36	0.17	0.01	0.03	0.17	3.32	0.05		0.02	0.1	0.01	0.03	0.06	0.03
No25 1423	25.22	0.1	0.39	0.27	0.03	0.04	0.18	3.37	0.03		0.02	0.1	0.02	0.04	0.07	0.04
No25 1423 dup	25.57	0.05	0.37	0.19	0.01	0.03	0.18	3.47	0.04		0.02	0.11	0.01	0.04	0.1	0.03
No25 1424	29.75	0.11	0.33	0.32	0.06	0.04	0.12	3.47	0.02		0.01	0.09	0.01	0.03	0.09	0.03
SW	0.42	0.35	0.06	0	0.15			36.47		0.18				0.12	1.15	
No25 1522	19.06	0.06	0.14	0.08	0.01	0.02	0.07	0.86	0.04	0.01	0.01	0.04	0.02	0.02	0.04	0.02
No25 1523	17.93	0.02	0.12	0.07	0.01	0.03	0.08	0.92	0.04		0.01	0.04	0.04	0.03	0.06	0.03
No25 1524	18.42	0.02	0.1	0.08	0.02	0.02	0.06	1.11	0.04		0.01	0.05	0.04	0.04	0.08	0.04
SW	2.62	0.11	0.04	0.01	0.09			35.76				0.92	2.37		1.15	
No25 1622	24.5	0.07	0.23	0.13	0.03	0.03	0.12	1.73	0.08		0.01	0.06	0.02	0.02	0.06	0.04
No25 1622 dup	24.53	0.02	0.19	0.1	0.03	0.02	0.11	1.73	0.06		0.01	0.05	0.04	0.04	0.1	0.04
No25 1623	25.27	0.08	0.22	0.18	0.03	0.02	0.12	1.65	0.05		0.01	0.05	0.03	0.05	0.08	0.04
No25 1624	24.99	0.03	0.21	0.1	0.03	0.03	0.11	2.25	0.03		0.01	0.05	0.02	0.05	0.05	0.02
SW	1.99	0.35	0.34	0.02	0.75	0.17		44.11	1.56			0.52	0.87		0.42	
No25 1722	29.03	0.22	0.36	0.14	0.02	0.03	0.12	3.88	0.1		0.01	0.04	0.01	0.02	0.03	0.02
No25 1723	29.57	0.05	0.34	0.39	0.03	0.03	0.13	3.57	0.09		0.02	0.05	0.02	0.07	0.13	0.04
No25 1724	30.8	0.02	0.3	0.16	0.04	0.04	0.13	4.04	0.04		0.01	0.03	0.03	0.02	0.03	0.01
SW	0.34	0.09	0.11	0.01	0.33			63.4	0.16						2.57	
No25 1822	17.35	0.03	0.09	0.06	0.02	0.03	0.09	0.82	0.02	0.02		0.06	0.04	0.02	0.02	0.02
No25 1823	18.51	0.02	0.12	0.09	0.02	0.03	0.08	0.68	0.04	0.02	0.02	0.05	0.05	0.05	0.05	0.05
No25 1824	17.56	0.04	0.1	0.05	0.02	0.02	0.06	0.84	0.06	0.02		0.09	0.07	0.05	0.08	0.03
SW	1.56	0.16	0.16		0.39			49.09				1.45	3.79		0.83	1.18

Appendix B28. Fatty acid profile of *P. lutheri* including seawater (SW) blanks and duplicate injections.

Species Treatment	C12:0	C13:0	i-C14:0	C14:0	C14:1n-9	C14:1n-7	C14:1n-5	i-C15:0	ai-C15:0	C15:0	i-C16:0	C16:0	C16:1n-11	C16:1n-9	C16:1n-7	C16:1n-5	C17:1(a)	i-C17:0	C16:2n-6
Pl25 1222	0.06	0.17	0.17	12.6	0	0.03	0.15	0.02	0.02	0.13	0.06	19.11	0	0.76	25.11	0.33	0.02	0.3	0.18
Pl25 1223	0.02	0.15	0.03	11.2	0	0.02	0.12	0.02	0.01	0.12	0.05	20.07		0.85	24.76	0.33	0.02	0.29	0.16
Pl25 1224	0.03	0.16	0.1	11.34	0	0.02	0.12	0.03	0.03	0.13	0.04	17.97	0	1.08	24.22	0.32	0.02	0.29	0.17
SW	0.03		1.41	0.64		0.21	0.01	0.13	0.1	0.17	0.06	14.29	0.12		5.04	0.12	0		0.09
Pl25 1322	0.02	0.25	0.08	9.14	0.01	0.05	0.1	0.03	0.02	0.13	0.08	17.92		1.49	21.44	0.26	0.01	0.27	0.38
Pl25 1323		0.24	0.34	10.63	0.01	0.03	0.12	0.05	0.04	0.15	0.05	16.69		1.57	21.17	0.26	0.01	0.27	0.36
Pl25 1324	0.05	0.23	0.1	9.49	0	0.02	0.1	0.04	0.03	0.16	0.05	17.61		1.7	21.07	0.25	0.02	0.27	0.33
Pl25 1324 dup	0.05	0.23	0.11	9.49	0	0.02	0.09	0.04	0.03	0.16	0.05	17.57		1.7	21.04	0.26	0.02	0.27	0.34
SW			2.51	0.48		0.08	0.01	0.14	0.15	0.15	0.01	18.8	0.12		1.76	0	0		0.08
Pl25 1422	0.07	0.53	0.41	8.97	0.01	0.03	0.14	0.04	0.04	0.23	0.12	13.43	0	3.38	15.98	0.17	0.02	0.33	1.25
Pl25 1423	0.04	0.44	0.04	6.64	0.02	0.02	0.1	0.03	0.04	0.23	0.11	12.68	0	4.42	15.24	0.16	0.01	0.36	1.3
Pl25 1424		0.44	0.03	6.78	0.01	0.02	0.09	0.03	0.03	0.21	0.12	12.53	0	3.78	14.93	0.16	0.02	0.3	1.13
SW	0.04	0.1	0.4	0.67		0.19	0.07	0.25	0.24	0.26	0.09	13.81	0	0.13	2.53	0	0		0.16
Pl25 1522	0.06	0.16	0.05	13.47	0	0.02	0.1	0.01	0.01	0.16	0.02	18.71		1.55	24.98	0.34	0.03	0.32	0.33
Pl25 1523	0.08	0.16	0.05	14.37	0	0.03	0.1	0	0.02	0.17	0.01	18.52	0	1.59	23.75	0.34	0.01	0.37	0.46
Pl25 1523 dup	0.08	0.16	0.05	14.34	0.01	0.04	0.1	0.01	0.02	0.17	0.01	18.49	0	1.57	23.7	0.33	0	0.35	0.45
Pl25 1524	0.1	0.15	0.05	14.06	0	0.02	0.11	0.01	0.02	0.16	0.01	18.11	0	1.42	24.58	0.33	0.01	0.32	0.35
SW		0.09	1.76	0.83		0.29	0	0.14	0.25	0.16	0.01	11.07	0.02	0.27	6.55	0.06	0	0.02	
Pl25 1622	0.03	0.4	0.01	10.67	0.01	0.04	0.08	0.03	0.02	0.19	0.05	16.12	0	3.01	18.4	0.24	0.01	0.39	0.69
Pl25 1623	0.04	0.32	0.23	11.99	0.01	0.06	0.08	0.03	0.03	0.22	0.02	17.09	0	3.03	17.37	0.25	0.02	0.44	0.93
Pl25 1624	0.04	0.38	0.02	12.33	0.01	0.06	0.08		0.03	0.23	0.04	18.72	0.01	3.08	17.65	0.25	0.02	0.46	1
SW	0.22	0.33	0.89	1.31	0.16	0.3	0.29	0.52	0.23	0.55	0.14	9.95	0	0.22	0.82	0.12	0.06	0.22	0.09
Pl25 1722	0.05	0.6	0.06	11.35	0	0.03	0.21	0.03	0.03	0.31	0.03	11.9		5.42	15.89	0.21	0.02	0.4	1.2
Pl25 1722 dup	0.05	0.59	0.08	11.33	0	0.03	0.21	0.03	0.03	0.3	0.03	11.82		5.38	15.8	0.21	0	0.41	1.2
Pl25 1723	0.04	0.47	0.05	10.71	0	0.03	0.2	0.03	0.06	0.3	0.04	11.44		4.99	15.31	0.19		0.42	1.25
Pl25 1724	0.09	0.69	0.19	11.09	0.01	0.03	0.22	0.04	0.06	0.32	0.07	11.37		5.59	15.12	0.16	0.01	0.38	1.24
SW		0.14	2.6	0.76	0.05	0.11	0.01	0.32	0.31	0.21	0.19	12.67	0	0.59	1.97	0.01		0.01	0.05
Pl25 1822	0.06	0.22	0.02	12.32		0.01	0.06	0.01	0.02	0.21	0.09	23.9	0	0.66	27	0.23	0.01	0.2	0.35
Pl25 1823	0.07	0.22	0.01	12.17	0	0.01	0.04	0.02	0.01	0.24	0.11	24.06	0	0.59	24.66	0.24	0.03	0.22	0.37
Pl25 1824	0.07	0.21	0.01	12.8		0.02	0.06	0.02	0.02	0.24	0.09	22.7	0	0.7	25.99	0.25	0.02	0.24	0.39
SW	0.21	0	0.26	0.75		0	0.01	0.46	0.19	0.3	0.17	16.14	0.09	0.27	2.94	0.01	0		0.13
Pl25 1922	0.56	0.47	0.02	12		0.02	0.05	0.03	0.03	0.29	0.19	20.76	0	1.55	18.68	0.21	0.02	0.35	0.65
Pl25 1923	0.05	0.45	0.02	12.22		0.02	0.06	0.05	0.03	0.29	0.22	20.66	0	1.17	19.75	0.22	0.02	0.34	0.66
Pl25 1924	0.05	0.48	0.02	11.87		0.02	0.05	0.04	0.03	0.28	0.19	20.1	0	1.54	19.24	0.23	0.02	0.34	0.56
SW		0.01	0.36	0.83			0.07	0.4	0.48	0.22	0.2	7.71	0.09	0.55	0.82	0.01			0.1
Pl25 2022	0.07	0.74	0.02	12.31		0.04	0.15	0.04	0.03	0.44	0.23	16.81	0	3.07	20.61	0.23	0.02	0.44	1.56
Pl25 2023	0.07	0.7	0.03	12.12		0.03	0.12	0.04	0.04	0.45	0.22	17.47	0	2.75	21.08	0.23	0.01	0.41	1.41
Pl25 2023 dup	0.07	0.69	0.02	12.14	0	0.03	0.12	0.04	0.04	0.45	0.22	17.46	0	2.75	21.1	0.24	0.01	0.41	1.41
SW	0.16	0.01	0.31	0.72			0.06	0.35	0.41	0.19	0.17	6.64	0.08	0.47	0.7	0.01			0.09

Appendix B28 (cont'd).

Species Treatment	ai-C17:0	C17:1(b)	C16:2n-4	C17:0	Phytane	C16:3n-4	C17:1	C16:4n-3	C16:4n-1	C18:0	C18:1n-13	C18:1n-11	C18:1n-9	C18:1n-7	C18:1n-5	C18:2d5,11	C18:2n-7
Pl25 1222	0.08	0.01	0.75	0.02		0.38	0.04		0.14	2.5	0.01	0.01	0.67	0.74	0.02	0.01	0.24
Pl25 1223	0.07	0.01	0.7	0.03		0.33	0.04		0.12	3.07	0.01	0.08	0.96	0.77	0.02	0.01	0.25
Pl25 1224	0.08	0.01	0.67	0.02		0.36	0.04		0.2	1.01	0.02	0.05	0.79	0.75	0.02	0.03	0.25
SW	0.15	0.06	0.03	0.2		0.03	0.91		0.4	12.92	0.37	0.15	0.89	2.58	0.09	0.15	0
Pl25 1322	0.06	0.01	0.57	0.04		0.42	0.07		0.18	4.52	0.02	0.04	0.72	0.8	0.03	0.01	0.26
Pl25 1323	0.07	0.01	0.59	0.04		0.44	0.11		0.34	2.66		0.02	0.71	0.76	0.02	0.02	0.26
Pl25 1324	0.06	0.01	0.49	0.06		0.35	0.08		0.36	2.9	0.04	0.07	0.91	0.78	0.03	0.02	0.24
Pl25 1324 dup	0.06	0.02	0.49	0.07		0.36	0.08		0.34	2.89	0.04	0.07	0.91	0.78	0.02	0.02	0.25
SW	0.05	0.07		0.19		1.23	0.41		0.35	21.18	0.14	0.03	0.59	1.48	0.05	0.13	
Pl25 1422	0.08		0.75	0.03		1.36	0.06		0.56	0.9	0	0.01	0.25	0.78	0.02	0.02	0.24
Pl25 1423	0.07	0	0.85	0.03		1.41	0.07		0.55	0.83	0	0.02	0.29	0.84	0.02	0.02	0.24
Pl25 1424	0.08		0.72	0.03		1.4	0.07		0.54	0.97	0.02	0.02	0.22	0.78	0.02	0.02	0.23
SW	0.22	0.01		0.23		0.02	0.79		0.92	11.76	0.16	0.06	0.86	2.52	0.08	0.27	
Pl25 1522	0.08	0	0.59	0.02		0.35	0.04		0.2	0.52	0	0.02	0.82	0.91	0.02	0.01	0.33
Pl25 1523	0.11	0.01	0.53	0.03		0.4	0.05		0.08	0.55	0.01	0.01	0.8	0.95	0.02	0.01	0.37
Pl25 1523 dup	0.09	0	0.52	0.03		0.39	0.05		0.08	0.55	0.01	0.01	0.8	1.01	0.02	0.01	0.37
Pl25 1524	0.09	0.01	0.59	0.02		0.39	0.04		0.08	0.54	0.01	0.01	0.77	0.89	0.02	0.01	0.33
SW	0.18	0.03	0.04	0.15		2.06	0.84		0.23	6.46	0.09	0.04	1.54	2.82	0.07	0.2	
Pl25 1622	0.14	0.01	0.56	0.04		0.63	0.06		0.27	1.18	0.01	0.01	0.53	0.87	0.02	0.01	0.38
Pl25 1623	0.14	0.01	0.5	0.03		0.61	0.04		0.2	0.94	0	0.01	0.47	0.9	0.03	0.01	0.38
Pl25 1624	0.13	0.01	0.47	0.06		0.61	0.05		0.27	0.85	0	0.01	0.51	0.94	0.04	0.01	0.37
SW	0.32	0.11	0.12	0.31		0.02	0.93		0.96	8.73	0.08	0.03	0.71	2.04	0.27	0.42	
Pl25 1722	0.13	0.01	1.38	0.04		1.69	0.05		0.41	0.57	0	0.01	0.2	1.23	0.02	0.02	0.27
Pl25 1722 dup	0.13		1.35	0.04		1.56	0.03		0.44	0.57	0	0.01	0.2	1.23	0.02	0.02	0.26
Pl25 1723	0.15	0.01	1.39	0.03		1.74	0.07		0.48	0.56	0	0.01	0.25	1.14	0.02	0.03	0.25
Pl25 1724	0.12	0.01	1.37	0.04		1.58	0.07		0.5	0.77	0	0.01	0.31	1.32	0.03	0.01	0.26
SW	0.15	0.02		0.33		2.08	1.1		0.3	10.7	0.13	0.02	0.81	2.03		0.14	
Pl25 1822	0.05	0	0.38	0.03		0.15	0.04		0.1	0.83	0.01	0.01	1.34	1.24	0.02	0.01	0.39
Pl25 1823	0.04	0	0.23	0.03		0.08	0.05		0.12	0.81	0.02	0.18	2.15	1.08	0.02	0.02	0.31
Pl25 1824	0.06	0	0.36	0.04		0.15	0.05		0.1	0.74	0.02	0.01	1.31	1.15	0.02	0.01	
SW	0.1	0.03	0.02	0.03		0	1.21		0.13	12.33	0.48	0.17	0.92	2.41	0.06		
Pl25 1922	0.12	0.01	0.31	0.04		0.22	0.05		0.2	0.94	0.02	0.1	1.19	1.13	0.04	0.02	0.38
Pl25 1923	0.13	0	0.33	0.04		0.27	0.07		0.23	1.08	0.03	0.02	0.85	1.21	0.04	0.01	0.41
Pl25 1924	0.14	0	0.33	0.03		0.23	0.06		0.21	1.01	0.03	0.06	1.06	1.14	0.04	0.01	0.38

SW	0.19	0.06	0.1	0		0.02	0.55		0.19	6.36	0.46		0.87	2.17	0.08		
Pl25 2022	0.13	0.01	0.77	0.03		0.8	0.06		0.34	0.6	0.03	0.01	0.41	2.3	0.06		0.38
Pl25 2023	0.13	0.01	0.68	0.03		0.59	0.06		0.32	0.67	0.03	0.04	0.62	2.35	0.06	0.06	0.4
Pl25 2023 dup	0.14	0.01	0.67	0.03		0.59	0.07		0.32	0.67	0.03	0.04	0.62	2.34	0.06	0.06	0.4
SW	0.17	0.05	0.09	0		0.02	0.47		0.16	5.48	0.4		0.75	1.87	0.07		

Appendix B28 (cont'd).

Species Treatment	C18:2n-6	C18:2n-4	C18:3n-6	C18:3n-4	C18:3n-3	C18:3n-1	C18:4n-3	C18:4n-1	C20:0	C20:1n-11	C20:1n-9	C20:1n-7	C20:2n-6	C20:3n-6	C20:4n-6	C20:3n-3	C20:4n-3
Pl25 1222	2.64	0.06	0.2	0.06	0.38	0.06	5.01	0.03	0.07	0	0.01	0.1	0.15	0.06	0.24	0.06	0.04
Pl25 1223	2.75	0.06	0.19	0.06	0.38	0.06	4.84	0.03	0.1	0.03	0.02	0.1	0.15	0.06	0.24	0.05	0.04
Pl25 1224	2.64	0.06	0.21	0.06	0.41	0.07	5.7	0.03	0.07	0.02	0.02	0.12	0.15	0.05	0.27	0.07	0.04
SW	0.2	0	0.69		0.79	0.02	0.2	0.27	0.19	0.72		1.77	0.82	0.12	0.13	0.15	0.11
Pl25 1322	1.8	0.07	0.21	0.09	0.52	0.11	6.49	0.07	0.1	0.02	0.01	0.19	0.13	0.05	0.23	0.06	0.04
Pl25 1323	1.62	0.05	0.24		0.51	0.14	6.46	0.09	0.11	0.06	0.04	0.24	0.16	0.07	0.29	0.13	0.09
Pl25 1324	1.93	0.05	0.18	0.05	0.5	0.09	6.68	0.06	0.11	0.03	0.02	0.12	0.14	0.05	0.27	0.07	0.04
Pl25 1324 dup	1.92	0.05	0.2	0.05	0.5	0.1	6.64	0.05	0.09	0.02	0.01	0.14	0.13	0.05	0.26	0.06	0.03
SW	0.09		1.42	0.32	0.72		0.16	0.57	0.2	0.16		1.67	1.49	0.03	0	0.01	0.08
Pl25 1422	0.38	0.22	0.37	0.15	0.84	0.18	9.01	0.06	0.03	0.08	0.01	0.34	0.19	0.02	0.35	0.32	0.08
Pl25 1423	0.43	0.29	0.13	0.14	0.98	0.18	9.38	0.05	0.03	0.06	0.02	0.21	0.26	0.02	0.45	0.4	0.09
Pl25 1424	0.39	0.25	0.13	0.15	0.88	0.17	10.2	0.06	0.03	0.03	0.02	0.19	0.21	0.03	0.43	0.33	0.08
SW	0.16	0	0.18		0.98		0.09	0.25	0.21	0.13		2.13	0.3	0.05	0.02	0.12	0.21
Pl25 1522	2.11	0.06	0.07	0.06	0.4	0.06	5.46	0.03	0.06	0.02	0.01	0.1	0.14	0.06	0.26	0.06	0.04
Pl25 1523	1.42	0.07	0.04	0.08	0.34	0.07	4.76	0.03	0.07	0.02	0.02	0.1	0.13	0.07	0.26	0.06	0.05
Pl25 1523 dup	1.42	0.07	0.03	0.07	0.34	0.07	4.79	0.03	0.07	0.03	0.02	0.11	0.13	0.07	0.26	0.07	0.05
Pl25 1524	2.08	0.06	0.07	0.06	0.37	0.06	5.54	0.02	0.05	0.03	0.01	0.12	0.14	0.06	0.25	0.06	0.05
SW	0.12	0	1.02		0.1	0.03	0.11	0.18	0.16	1.32	0.23	3.4	2.61	0.03	0.04	0	0.11
Pl25 1622	0.89	0.08	0.19	0.09	0.77	0.09	9.1	0.04	0.05	0.01	0.01	0.24	0.1	0.04	0.25	0.07	0.04
Pl25 1623	0.54	0.28	0.14	0.1	0.56	0.1	6.72	0.04	0.07	0.01	0.01	0.27	0.11	0.05	0.26	0.07	0.05
Pl25 1624	0.49	0.11	0.14	0.1	0.48	0.09	5.77	0.04	0.09		0.01	0.1	0.11	0.06	0.26	0.08	0.05
SW	0.33	0.01	0.77	0.17	1.26		0.16	0.32	0.27	0.34	0.15	4.82	0.11	0.01	0.27	0.29	0.55
Pl25 1722	0.29	0.59	0.12	0.19	1.15	0.24	7.54	0.06	0.03	0.04	0.01	0.15	0.27	0.03	0.54	0.31	0.06
Pl25 1722 dup	0.29	0.56	0.12	0.21	1.16	0.25	7.54	0.08	0.03	0.05	0.02	0.16	0.28	0.03	0.53	0.31	0.06
Pl25 1723	0.31	0.52	0.11	0.19	1.17	0.23	7.92	0.05	0.02	0.01	0.04	0.25	0.29	0.03	0.59	0.35	0.07
Pl25 1724	0.3	0.56		0.17	1.1	0.25	7.22	0.06	0.04	0.05	0.02	0.46	0.31	0.03	0.63	0.33	0.07
SW	0.18	0.01	2.32	0.39	1.38		0.15	0.31	0.25	0.94	0.09	4.62	2.37	0.04	0.03	0.01	0.16
Pl25 1822	2.71	0.05	0.33	0.04	0.53	0.05	3.93	0.02	0.06	0	0.02	0.03	0.21	0.11	0.5	0.06	0.06

Pl25 1823	3	0.03	0.34	0.02	0.57	0.04	4.12	0.02	0.05	0.02	0.04	0.02	0.25	0.11	0.5	0.07	0.07
Pl25 1824	2.46	0.04	0.29	0.04	0.52	0.05	4.27	0.02	0.06	0.01	0.03	0.03	0.2	0.1	0.51	0.06	0.06
SW		0	0.17	0	0.95	0.07	0.26	0.41	0.16	0.02		0.37	0.2	0.13	0.22	0.05	
Pl25 1922	1.02	0.08	0.41	0.05	0.82	0.07	6.06	0.03	0.07	0.01	0.03	0.03	0.21	0.08	0.59	0.09	0.07
Pl25 1923	1.08	0.08	0.44	0.05	0.84	0.06	5.95	0.02	0.06	0	0.02	0.04	0.21	0.1	0.58	0.08	0.08
Pl25 1924	1.19	0.07	0.54	0.05	0.9	0.05	6.72	0.02	0.05	0.01	0.02	0.04	0.21	0.07	0.62	0.09	0.08
SW			0.25	0.01	0.93				0.15	0.02		0.23	0.33	0	0.09	0.12	0.01
Pl25 2022	0.39	0.53	0.17	0.14	0.76	0.23	3.42	0.05	0.03	0	0.04	0.05	0.47	0.06	0.87	0.26	0.07
Pl25 2023	0.37	0.44	0.18	0.12	0.73	0.19	3.75	0.04	0.06	0	0.05	0.09	0.44	0.1	0.78	0.25	0.08
Pl25 2023 dup	0.37	0.43	0.17	0.12	0.73	0.19	3.75	0.04	0.06	0.01	0.05	0.09	0.43	0.09	0.79	0.26	0.08
SW			0.22	0.01	0.8				0.13	0.02		0.19	0.28	0	0.08	0.1	0.01

Appendix B28 (cont'd).

Species Treatment	C20:5n-3	C22:0	C22:1n-11	C22:1n-9	C22:1n-7	C22:2n-6	C21:5n-3	C23:0	C22:4n-6	C22:5n-6	C20:2n-9	C22:4n-3	C22:5n-3	C24:0	C22:6n-3	C24:1n-9
Pl25 1222	14.66	0.06	0.03	0.04	0.01	0.04	0.01	1.63	0.18	1.15		0.03	0.57	0.01	7.56	0.02
Pl25 1223	14.55	0.05	0.01	0.02	0	0.04	0.01	1.51	0.19	1.19		0.04	0.97		7.54	0.01
Pl25 1224	16.42	0.05	0.02	0.03	0	0.04	0.02	2.05	0.19	1.24		0.04	0.98	0.07	8.3	0.18
SW	0.84	0.1	0.06		0.33	0.68		42.82	0				6	0	0.24	1.42
Pl25 1322	17.41	0.05	0.02	0.08	0.04	0.03	0.01	3.37	0.11	1.19		0.01	0.31	0.01	7.73	0.02
Pl25 1323	17.25	0.1	0.06	0.15	0.04	0.14	0.06	3.02	0.17	1.4		0.1	0.74	0.13	8.14	0.14
Pl25 1324	17.73	0.07	0.03	0.04	0.01	0.03	0.01	3.13	0.11	1.41		0.03	0.55	0.1	8.31	0.15
Pl25 1324 dup	17.63	0.06	0.03	0.07	0.01	0.01	0.01	3.12	0.12	1.43		0.11	0.64	0.11	8.33	0.16
SW	0.5	0.13		0.27	0.82	0.56		31.68	0			1.2	4.87	0.29	1.08	1.47
Pl25 1422	23.64	0.06	0.05	0.17	0.07	0.02		5.08	0	1.48		0.03	0	0.01	6.57	0.02
Pl25 1423	25.4	0.09	0.06	0.14	0.03	0.07		4.97	0.39	1.53		0.01	0.23	0.01	6.8	0.02
Pl25 1424	25.92	0.1	0.05	0.14	0.03	0.04		5.2	0	1.74		0.02	0.15		7.26	0.03
SW	0.53	0.17	0.01		0.04			54	0.01				1.94	0	1.14	0.46
Pl25 1522	15.7	0.05	0.03	0.02	0	0.02	0.01	1.76	0.08	1.01		0.04	0.27	0	7.5	0.01
Pl25 1523	15.99	0.09	0.01	0.02	0	0.04	0	1.66	0.14	1.22		0.04	0.46	0.02	8.56	0.01
Pl25 1523 dup	16.02	0.1	0.03		0.13	0.05	0.01	1.67	0.13	1.23		0.04	0.39	0.01	8.54	0.01
Pl25 1524	16.05	0.06	0.04	0.06	0	0.05	0.01	1.49	0.1	1.05		0.05	0.34	0	7.82	0.01
SW	0.28	0.11	0.01		0.25			44.68	0.25			0.61	3.54	0.36	1.34	2.88
Pl25 1622	22.1	0.03	0.03	0.03	0.01	0.02		1.81	0.04	1.07		0.02	0.06	0.01	7.62	0.01
Pl25 1623	22.22	0.08	0.02	0.02	0	0.04	0.01	1.55	0.03	1.3		0.02	0.14	0	8.73	0.01
Pl25 1624	21.62	0.11	0.03	0.09	0.02	0.02		1.49	0.02	1.21		0.03	0.14	0.03	8.45	0.01
SW	0.47	0.1	0.03	0.18	0.11	0.72		45.5	1.12			1.07	6.3	0.05	0.65	2.46
Pl25 1722	25.07	0	0.04	0.17	0.05	0.03		2.42	0	1.14		0.01	0.03	0	5.61	0.01
Pl25 1722 dup	25.23	0.03	0.06	0.09	0.02	0.04		2.47	0	1.14		0.01	0.18	0.01	5.69	0.01
Pl25 1723	25.61	0.04	0.05	0.08	0.02	0.06	0.01	2.41	0.02	1.35		0.01	0.11	0.01	5.98	0.41
Pl25 1724	25.13	0.04	0.05	0.1	0.02	0.04	0	3.01	0	1.14		0.01	0.05	0	5.75	0.01
SW	0.4	0.11	0		0.03			45.42	0.74	0.15			2.03	0	0.02	

Pl25 1822	12.76	0.07	0.01	0.02	0.01	0.03	0	1.21	0.1	1.2		0.02	0.33	0.01	5.5	0.01
Pl25 1823	13.58	0.07	0.02	0.04	0.01	0.03	0.01	1.14	0.1	1.32		0.05	0.49	0.01	5.64	0
Pl25 1824	13.71	0.08	0.03	0.04	0.01	0.03	0.01	1.17	0.08	1.39		0.01	0.47	0	6.03	0.01
SW	0.2	0	1.57		0.16	2.19		48.96	0	0.01		2.67		0.01	0.49	0.92
Pl25 1922	18.9	0.08	0.06	0.04	0.01	0.04		2.08	0.03	1.57		0.01	0.1	0.02	6.69	0.01
Pl25 1923	18.29	0.07	0.03	0.04	0.01	0.02	0	2.14	0.04	1.64		0.05	0.27		6.71	0.01
Pl25 1924	18.7	0.04	0.04	0.03	0.01	0.03	0.01	2.14	0.03	1.61		0.01	0.21	0	6.59	0.01
SW	0.04	0		3.97	0.17	4.84		56.67	3.73	0		5.35		0.02	0.16	
Pl25 2022	20.04	0.04	0.07	0.05	0	0.02		1.95	0.05	1.22		0.02	0.06	0.01	6.17	0.01
Pl25 2023	19.35	0.07	0.03	0.04	0.01	0.03		1.92	0.06	1.23		0.02	0.17	0	6.17	0.02
Pl25 2023 dup	19.31	0.07	0.06	0.06	0.01	0.04		1.94	0.05	1.2		0.02	0.18	0	6.16	0.01
SW	0.03	0		3.42	0.15	4.17		48.78	3.21	0		4.6	13.76	0.02	0.13	

Appendix B29. Fatty acid profile of *T. pseudonana* including seawater (SW) blanks and duplicate injections.

Species Treatment	C12:0	C13:0	i-C14:0	C14:0	C14:1n-9	C14:1n-7	C14:1n-5	i-C15:0	ai-C15:0	C15:0	i-C16:0	C16:0	C16:1n-11	C16:1n-9	C16:1n-7	C16:1n-5	C17:1(a)	i-C17:0	C16:2n-6
Tp35 1322	0.04	0.37	0.03	6.38	0	0.02	0.02	0.02	0.03	1.02	0.04	19.01	0.01	2.78	17.64	0.18	0.02	0.02	1.34
Tp35 1323	0.03	0.31	0.03	6.8	0.01	0.03	0.03	0.03	0.05	1.02	0.01	17.9	0.01	2.69	17.17	0.21	0.03	0.01	1.34
Tp35 1324	0.06	0.3	0.15	6.22	0.01	0.02	0.02	0.03	0.03	1.03	0.03	19.13	0.01	2.77	17.4	0.17	0.01	0.01	1.21
SW	0.08	0.16	0.44	2.09		0.08	0.03	0.17	0.14	0.26	0.05	18.85	0.03	0.7	12.86		0		0.13
Tp35 1422	0.01	0.51	0.02	7.78	0	0.04	0.07	0.05	0.04	0.73	0.06	13.1	0.02	4.03	19.07	0.22	0.02	0.01	3.77
Tp35 1422 dup	0	0.52	0.03	7.9	0	0.04	0.07	0.05	0.04	0.74	0.05	13.21	0.02	4.04	19.2	0.2	0.01	0	3.76
Tp35 1423	0	0.48	0.02	7.71	0.01	0.03	0.06	0.05	0.04	0.71	0.03	13.42	0.01	4.1	19.43	0.21	0.01		3.33
Tp35 1424	0.01	0.52	0.4	7.92	0.02	0.04	0.06	0.05	0.04	0.79	0.04	11.51	0.02	4.56	20.79	0.2	0	0.01	3.3
SW		0.07	0.13	2.16		0.16	0.01	0.19	0.11	0.25	0	25.14	0.02	0.52	18.16	0.07	0.01	0	0.05
Tp35 1522		0.22	0.04	10.29	0.01	0.03	0.05		0.02	0.77	0.01	25.44	0.02	1.82	20.02	0.23	0.02	0.01	1.16
Tp35 1523	0.08	0.23	0.04	10.79	0.01	0.03	0.05		0.02	0.76	0	26.78	0.02	1.75	20.17	0.23	0.02	0.01	1.18
Tp35 1524		0.25	0.13	10.05	0.01	0.03	0.05		0.02	0.78	0.02	25.53	0.02	1.76	20.22	0.24	0.03	0.01	1.15
SW	0.3	0.27	2.8	1.69	0.19	0.38	0.46	0.54	0.18	0.71	0.1	14.65	0.05	0.3	1.81			0.38	0.31
Tp35 1622	0.28	0.37	0.16	9.08	0	0.03	0.04	0.03	0.05	0.74	0.02	21.82	0.03	2.42	18.04	0.21	0.01		1.34
Tp35 1623	0.1	0.35	0.06	9.37	0.01	0.03	0.04	0.03	0.03	0.77	0.02	21.6	0.02	2.81	18.97	0.23			1.46
Tp35 1624	0.08	0.29	0.07	9.42	0	0.03	0.04	0.02	0.02	0.76	0.01	23.18	0.03	2.51	19.49	0.22	0.02		1.45
Tp35 1624 dup	0.08	0.29	0.08	9.38	0	0.03	0.04	0.02	0.02	0.76	0.02	23.15	0.02	2.5	19.47	0.22	0.02		1.44
SW		0.24	2.55	0.93	0.1	0.07	0.01	0.2	0.27	0.35	1.37	12.9	0.12	0.35	1.84			0	
Tp35 1722	0.05	0.69	0.24	10.44	0	0.02	0.11	0.02	0.02	0.67	0.06	10.28	0.02	5.03	25.18	0.18	0.01		2.21
Tp35 1723	0.08	0.65	0.13	10.14	0	0.02	0.1	0.02	0.03	0.71	0.05	10.75	0.02	4.86	23.86	0.19	0.01		2.37
Tp35 1724	0.04	0.62	0.03	10.82	0	0.02	0.11	0.02	0.02	0.7	0.05	10.66	0.02	4.99	24.93	0.2	0.01		2.25
SW		0.39	0.57	1.06		0.39	0.01	0.22	0.24	0.33	0.05	13.25	0.11	0.41	7.26	0.14	0.05	0.03	
Tp35 1922	0.03	0.6	0.01	10.54	0	0.02	0.03	0.02	0.03	0.67	0.17	16.76	0.02	2.68	15.46	0.18	0.01	0	1.29

Tp35 1923	0.04	0.61	0.01	10.47	0	0.02	0.03	0.02	0.03	0.7	0.2	16.76	0.02	2.36	15.83	0.16	0.02	0	1.19
Tp35 1924	0.03	0.64	0.05	10.13	0	0.02	0.03	0.02	0.03	0.66	0.2	16.36	0.02	2.61	15.4	0.18	0.01		1.3
SW	0.15		0.37	0.88	0.01	0.01	0.03	0.58	0.44	0.2	0.05	16.23	0.19	0.8	1.52			0.09	0.08
Tp35 2022	0.03	0.81	0.02	10.12	0.01	0.01	0.04	0.05	0.05	0.64	0.25	12.61	0.03	3.56	25.03	0.19		0	1.75
Tp35 2023	0.04	0.77	0.02	8.94	0	0.02	0.04	0.04	0.04	0.7	0.21	14.91	0.02	3.65	22.7	0.16	0.02	0	1.42
Tp35 2024	0.05	0.84	0.03	11.08	0	0.01	0.06	0.03	0.03	0.66	0.2	11.99	0.02	3.81	23.72	0.2		0	1.83
Tp35 2024 dup	0.05	0.82	0.02	11.07	0	0.02	0.06	0.03	0.03	0.66	0.2	11.99	0.03	3.82	23.7	0.19	0.02	0	1.82
SW	0.08		0.37	0.61	0.03	0	0.02	0.28	0.55	0.22	0.07	20.46	0	0.67	1.13			0.06	0.03

Appendix B29 (cont'd).

Species Treatment	ai-C17:0	C17:1(b)	C16:2n-4	C17:0	Phytane	C16:3n-4	C17:1	C16:4n-3	C16:4n-1	C18:0	C18:1n-13	C18:1n-11	C18:1n-9	C18:1n-7	C18:1n-5	C18:2d5,11	C18:2n-7
Tp35 1322	0.17	0.01	2.41	0.05	0.02	12.34	0.07	0.05	2.14	0.72	0.07	0.02	0.28	0.51	0.05	0.03	0.01
Tp35 1323	0.18	0.01	2.44	0.06	0.03	13.27	0.07	0.05	2.29	0.93	0.05	0.02	0.3	0.47	0.05	0.03	0
Tp35 1324	0.17	0.01	2.33	0.06	0.02	11.82	0.08	0.04	2.25	0.94	0.05	0.01	0.33	0.51	0.04	0.04	0
SW	0.04	0.03	0.59	0.16	0	1.06	0.49		0.66	9.41	0.08	0.02	3.04	1.57	0.09	0.47	
Tp35 1422	0.13		2.25	0.06	0.04	9.54	0.1	0.03	1.07	5.04	0.24	0.11	0.83	0.34	0.07	0.03	0.02
Tp35 1422 dup	0.11	0	2.26	0.06	0.03	9.62	0.1	0.03	1.08	5.05	0.24	0.12	0.84	0.34	0.07	0.03	0.02
Tp35 1423	0.14	0.01	2.11	0.06	0.03	8.97	0.08	0.03	0.87	5.74	0.22	0.16	1.23	0.3	0.06	0.03	0.02
Tp35 1424	0.13	0.01	1.92	0.09	0.04	9.41	0.09	0.03	0.83	2.93	0.34	0.08	0.51	0.33	0.08	0.03	0.02
SW	0.02	0.07	0.31	0.17	0	0.42	0.38	0.09	0.35	12.75	0.11	0.03	3.07	2.17	0.06	0.32	0.01
Tp35 1522	0.13	0	2	0.02	0.02	9.96	0.03	0.03	1.59	0.48	0.04	0.02	0.13	0.32	0.06	0.02	0.01
Tp35 1523	0.12	0	1.98	0.02	0.02	9.74	0.02	0.03	1.32	0.61	0.03	0.02	0.15	0.3	0.06	0.02	0
Tp35 1524	0.13	0	1.95	0.03	0.02	9.74	0.05	0.03	1.65	0.4	0.04	0.01	0.15	0.35	0.06	0.02	0
SW	0.09	0.04	0.13	0.34		0.44	0.64	0.1	0.56	11.94	0.28	0.29	1.08	1.91	0.21	0.24	
Tp35 1622	0.18	0	1.81	0.04	0.01	9.74	0.08	0.03	0.62	1.42	0.04	0.15	2.44	0.48	0.07	0.09	0
Tp35 1623	0.17	0.01	2.04	0.02	0.02	10.38	0.07	0.03	0.61	0.71	0.07	0.02	0.2	0.4	0.05	0.02	0
Tp35 1624	0.16	0.02	1.9	0.04	0.04	10.24	0.09	0.03	0.59	1.3	0.04	0.02	0.2	0.37	0.05	0.02	0
Tp35 1624 dup	0.15	0.01	1.86	0.02	0.02	10.16	0.08	0.02	0.59	1.31	0.04	0.02	0.2	0.37	0.05	0.02	0
SW	0.2	0.04	0.08	0.27	0.02		0.29	0.03	1.26	12.48	0.13	0.48	2.84	2.12	0.22	0.26	0.06
Tp35 1722	0.17	0	3.27	0.03	0.02	5.6	0.1	0.02	0.49	0.65	0.01	0.01	0.31	0.26	0.05	0.03	0.01
Tp35 1723	0.16	0	3.24	0.04	0.02	6.58	0.1	0.02	0.49	1.57	0.03	0.03	0.48	0.31	0.06	0.03	0.02
Tp35 1724	0.17	0.01	3.47	0.03	0.02	5.66	0.08	0.02	0.4	1.43	0.01	0.01	0.33	0.24	0.04	0.02	0.01
SW	0.21	0.05	0.13	0.21	0.01	0.53	0.7	0.05	1.91	9	0.21	0.35	2.64	3.9	0.12	0.13	
Tp35 1922	0.23	0.01	3.17	0.02	0.02	11.38	0.04	0.02	0.46	0.72	0.05	0.03	0.38	0.48	0.05	0.03	0.01
Tp35 1923	0.22	0	3.37	0.04	0.02	10.91	0.05	0.02	0.44	0.77	0.05	0.02	0.35	0.46	0.05	0.02	0.01
Tp35 1924	0.23	0.01	3.13	0.03	0.02	11.2	0.06	0	0.44	0.88	0.04		0.31	0.49	0.05	0.02	0.01

SW	0.25	0.01	0	0.17		0.19	0.89		0.1	14.81	0.22	0.09	0.68	1.74	0.12	0.08		
Tp35 2022	0.2	0.01	3.58	0.02	0.01	4.65	0.1		0.47	0.89	0.02	0.01	0.39	0.24	0.08	0.04	0.01	
Tp35 2023	0.17	0	3.48	0.03	0.02	4.53	0.08		0.4	1.79	0.17	0.07	1.05	0.4	0.1	0.04	0.01	
Tp35 2024	0.21	0.01	3.82	0.02	0.01	5.43	0.07	0	0.44	0.65	0.01		0.4	0.24	0.06	0.03	0	
Tp35 2024 dup	0.21	0.01	3.88	0.02	0.01	5.43	0.07		0.44	0.65	0.01		0.41	0.27	0.11	0.04		
SW	0.13	0.02	0.01	0.15		0.26	0.39	0.07	0.11	21.22	0.26	0.08	0.49	1.38		0		

Appendix B29 (cont'd). * indicates anomalously high amounts of fatty acid 18:4n-3, which was removed and renormalized.

Species Treatment	C18:2n-6	C18:2n-4	C18:3n-6	C18:3n-4	C18:3n-3	C18:3n-1	C18:4n-3	C18:4n-1	C20:0	C20:1n-11	C20:1n-9	C20:1n-7	C20:2n-6	C20:3n-6	C20:4n-6	C20:3n-3	C20:4n-3
Tp35 1322	0.15	0	0.27	0.03	0.07	0.16	10.6*	0.02	0.02	0.01	0.03	0.11	0.01	0.01	0.07	0.01	0.12
Tp35 1323	0.18	0	0.32	0.02	0.07	0.15	11.04*	0.03	0.03	0.03	0.04	0.18	0.01	0.01	0.08	0.01	0.14
Tp35 1324	0.18		0.23	0.03	0.08	0.15	10.66*	0.03	0.03	0.02	0.05	0.21		0.01	0.08	0.01	0.17
SW	0.21	0	0.7		0.54	0.05	0.4	0.29	0.16	0.61		1.3	0.09	0.03	0.06		0.11
Tp35 1422	0.2	0	0.27	0.02	0.12	0.17	6.03*	0.02	0.11	0.06	0.05	0.17	0	0.01	0.08	0.02	0.1
Tp35 1422 dup	0.2	0	0.29	0.03	0.12	0.17	6.02*	0.02	0.11	0.05	0.05	0.18	0.01	0.01	0.08	0.02	0.07
Tp35 1423	0.3	0	0.36	0.02	0.1	0.15	6.6*	0.01	0.12	0.04	0.05	0.19	0.01	0.02	0.1	0.03	0.2
Tp35 1424	0.25	0.52	0.02	0.03	0.12	0.19	6.31*	0.03	0.11	0.05	0.06	0.41	0.01	0.04	0.13	0.02	0.07
SW	0.25	0	0.22		0.46	0	0.4	0.36	0.34	1.01	0.06	0.64	0.04	0.05	0.09	0.08	0.09
Tp35 1522	0.22	0	0.27	0.02	0.07	0.11	13.43*		0.02	0.03	0.01	0.09	0	0	0.03	0	0.04
Tp35 1523	0.24	0	0.25	0.02	0.07	0.1	13.04*	0.01	0.02	0.01	0.01	0.1	0	0	0.02	0	0.04
Tp35 1524	0.26	0.1	0.24	0.01	0.08	0.12	13.29*	0.01	0.01	0.01	0.01	0.14	0	0	0.03	0	0.05
SW	0.33	0.02	2.34	0.17	0.94	0.07	0.76	0.65	0.23	0.99		4.36		0.14	0.2	0.26	0.52
Tp35 1622	1.16	0.12	0.36	0.01	0.16	0.11	11.8*	0.02	0.05	0.02	0.09	0.25	0	0.01	0.08	0.05	0.09
Tp35 1623	0.24	0	0.32	0.02	0.11	0.1	12.71*	0.02	0.04	0.04	0.03	0.21	0	0.01	0.07	0.01	0.06
Tp35 1624	0.25	0.01	0.29	0.02	0.11	0.12	12.29*	0.02	0.03	0.03	0.02	0.23	0	0.01	0.06	0.02	0.06
Tp35 1624 dup	0.25	0	0.32	0.02	0.11	0.12	12.38*	0.01	0.03	0.03	0.02	0.23	0	0.01	0.06	0.03	0.06
SW	0.87	0.12	2.15		0.31	0.08	0.16	0.13	0.3	0.39	0.14	6.42	0.07	0.03	0.07	0.7	0
Tp35 1722	0.48	0.19	0.59	0.01	0.13	0.11	7.94*	0.01	0.02	0.04	0.06	0.35	0	0.03	0.26	0.01	0.11
Tp35 1723	0.55		0.56	0.01	0.14	0.1	8.59*	0	0.06	0.04	0.07	0.22	0	0.02	0.2	0.01	0.09
Tp35 1724	0.47	0.03	0.55	0.01	0.12	0.1	9.14*	0.01	0.04	0.08	0.07	0.16	0	0.02	0.22	0.01	0.08
SW	0.58	0	0.52	0.13	0.24	0.05	0.12	0.2	0.15	0.11		1.71	0.09			0.49	0
Tp35 1922	0.39	0	0.54	0.01	0.11	0.12	15.61*	0.02	0.03	0.01	0.03	0.02	0.01	0.02	0.14	0	0.09
Tp35 1923	0.42	0	0.54	0.01	0.12	0.11	14.94*	0.02	0.05	0	0.04	0.01	0	0.03	0.15	0	0.11
Tp35 1924	0.43	0	0.64	0.02	0.14	0.13	15.15*	0.02	0.03	0	0.03	0.05	0.01	0.01	0.17	0	0.1
SW			0.22		1.29	0.01	0.17	0.49	0.31	0.02		0.41	0.2			0.01	0.09
Tp35 2022	0.5	0.02	0.59	0.01	0.18	0.11	7.71	0.01	0.02	0	0.05	0.02	0.02	0.04	0.28	0.02	0.13

Tp35 2023	0.55	0.02	0.52	0.01	0.25	0.1	7.29	0.02	0.06	0.02	0.04	0.07	0.01	0.03	0.15	0	0.19
Tp35 2024	0.56	0	0.63	0.01	0.15	0.12	8.88	0.01	0.02	0.01	0.05	0.03	0.02	0.03	0.34	0.01	0.14
Tp35 2024 dup	0.56	0	0.62	0.01	0.16	0.12	8.88	0.01	0.02	0.01	0.05	0.03	0.01	0.03	0.33	0	0.13
SW		0	0.31	0.1	0.79	0	0.06	0.48	0.32	0.12		5.22	0.31			0.01	0.01

Appendix B29 (cont'd).

Species Treatment	C20:5n-3	C22:0	C22:1n-11	C22:1n-9	C22:1n-7	C22:2n-6	C21:5n-3	C23:0	C22:4n-6	C22:5n-6	C20:2n-9	C22:4n-3	C22:5n-3	C24:0	C22:6n-3	C24:1n-9
Tp35 1322	14.22	0.01	0.02	0.04	0	0.01	0	2.4				0.02	0.09	0.03	3.5	
Tp35 1323	13.92	0.01	0.01	0.01	0	0.01	0	2.49				0.03	0.08	0.01	3.11	
Tp35 1324	14.28	0.01	0.01	0.04	0.01	0.02	0	2.76				0.01	0.1	0.03	3.5	
SW	4.96	0.09		0.05	0		0	36.05						0.22	0.25	
Tp35 1422	16.35	0.05	0.03	0.04	0	0.01	0	3.67				0.02	0.01	0.04	2.83	
Tp35 1422 dup	16.14	0.04	0.03	0.04	0	0.01	0	3.59				0.02	0.01	0.03	2.76	
Tp35 1423	16.01	0.06	0.04	0.05	0.01	0.01	0	3.06				0.02	0.02	0.03	2.71	
Tp35 1424	17.09	0.12	0.03	0.04	0	0.02	0	4.15				0.02	0.02	0.07	2.91	
SW	3.32	0.07	0	0.01	0		0	24.66						0.2	0.23	
Tp35 1522	8.04	0.01	0.01	0.04	0.01	0.01	0	0.91				0.01	0.08	0.03	1.49	
Tp35 1523	6.97	0.02	0.01	0.02	0.01	0.03	0.01	0.96				0.01	0.06	0.04	1.28	
Tp35 1524	7.98	0.01	0.01	0.02	0.01	0.01	0	1				0.01	0.08	0.04	1.53	
SW	0.4	0.13			0.69	0.8	0.15	42.35							0.1	
Tp35 1622	9.63	0.06	0.02	0.1	0.01	0.03	0.02	2.18			0.01	0.02	0.04	0.02	1.61	
Tp35 1623	11.06	0.02	0.01	0.04	0.01	0.03	0	2.32				0.01	0.01	0.02	1.79	
Tp35 1624	9.82	0.01	0.01	0.03	0	0.01	0	2.15				0.01	0.01	0.02	1.61	
Tp35 1624 dup	9.91	0.01	0.01	0.02	0	0.02	0	2.21			0	0.01	0.01	0.02	1.63	
SW	0.25	0.14			0.17	0.33	0.01	44.97							0.09	
Tp35 1722	18.59	0.01	0.02	0.04	0	0.01	0	2.68				0.02	0.01	0.03	1.94	
Tp35 1723	17.85	0.01	0.02	0.03	0.01	0.03	0	2.08				0.02	0.02	0.03	2.02	
Tp35 1724	17.43	0.01	0.01	0.03	0.01	0.02	0	2.05				0.02	0.01	0.02	1.8	
SW	0.36	0.11			0.2	0.35	0.01	49.81							0.11	
Tp35 1922	13.9	0.06	0.06	0.09	0.01	0.02	0.01	1.33				0.01	0.01	0.08	1.66	
Tp35 1923	14.52	0.08	0.02	0.12	0	0.03	0.01	1.52				0.01	0.01	0.11	1.74	
Tp35 1924	14.61	0.05	0.02	0.13	0.01	0.02	0.01	1.81					0.01	0.09	1.7	
SW	0.18	0.28	0.04	6.33	0.17		0	48.8								
Tp35 2022	19.36	0.06	0.03	0.09	0	0.03	0	2.74					0.01	0.09	1.99	
Tp35 2023	18.87	0.05	0.02	0.11	0.01	0.03	0	3.12					0.02	0.1	2.27	
Tp35 2024	19.21	0.04	0.05	0.09	0.01	0.05	0	1.62				0.01	0.02	0.07	1.82	
Tp35 2024 dup	19.23	0.03	0.03	0.08	0.01	0.04	0	1.59			0.01	0.01	0.02	0.07	1.84	
SW	0.25	0.23	0		0.12		0	42.52								

Appendix B30. Mean growth rates (μ), concentrations of EPA, ARA, carbon, and Chl-a, and production rates of EPA, ARA, and Chl-a in *N. oculata.*

Species treatment	Ave. μ (day^{-1})	Ave. [EPA] (ug EPA L^{-1})	Ave. [ARA] (ug ARA L^{-1})	Ave. [Chl-a] (ug Chl-a L^{-1})	[C] (mg L^{-1}) rep 1	[C] (mg L^{-1}) rep 2	[C] (mg L^{-1}) rep 3	Ave. [C] (mg L^{-1})	Corr [C] (mg L^{-1})
No25 1222	0.742	275.616	38.733	104.164	3.280	3.760	3.200	3.413	3.199
No25 1223	0.735	280.192	40.596	108.202	3.640	3.900	3.320	3.620	3.406
No25 1224	0.737	278.079	40.377	114.977	3.580	3.760	3.380	3.573	3.359
No25 1322	0.700	213.108	31.956	113.472	2.220	2.820	2.360	2.467	2.252
No25 1323	0.704	205.481	30.599	123.464	2.600	3.120	2.640	2.787	2.572
No25 1324	0.703	190.240	27.519	129.897	3.240	2.840	3.120	3.067	2.852
No25 1422	0.341	123.212	19.519	73.914	1.620	1.540	1.700	1.620	1.406
No25 1423	0.338	110.947	17.922	63.237	1.380	1.540	1.560	1.493	1.280
No25 1424	0.342	128.155	19.495	82.811	1.700	1.620	1.560	1.627	1.412
No25 1522	0.904	331.994	54.200	96.772	4.120	4.420	4.800	4.447	4.233
No25 1523	0.901	291.889	46.424	77.883	3.820	4.260	4.200	4.093	3.879
No25 1524	0.896	248.471	38.605	74.941	4.660	4.280	3.940	4.293	4.079
No25 1622	0.835	212.110	34.855	100.331	3.300	3.560	3.420	3.427	3.212
No25 1623	0.840	229.280	38.593	102.384	3.640	3.540	3.500	3.560	3.345
No25 1624	0.838	166.152	27.623	74.188	2.980	2.720	2.480	2.727	2.512
No25 1722	0.349	111.782	19.209	129.760	1.800	2.280	1.920	2.000	1.786
No25 1723	0.346	123.796	21.343	123.874	2.020	2.320	1.900	2.080	1.865
No25 1724	0.343	113.909	19.040	111.829	1.640	1.720	1.760	1.707	1.491
No25 1822	0.954	316.930	57.944	95.404	4.660	4.220	4.300	4.393	4.179
No25 1823	0.983	407.861	76.280	158.231	5.140	6.120	5.620	5.627	5.410
No25 1824	0.952	313.124	58.528	115.525	4.160	5.220	4.900	4.760	4.545

Appendix B30 (cont'd).

Species treatment	[EPA] (ug EPA mg C^{-1})	[ARA] (ug ARA mg C^{-1})	[Chl-a] (ug Chl-a mg C^{-1})	EPA/Chl ratio (ug mg C^{-1})	ARA/Chl-a ratio (ug mg C^{-1})	EPA production (ug EPA mg C^{-1} day^{-1})	ARA production (ug ARA mg C^{-1} day^{-1})	Chl-a production (ug Chl-a mg C^{-1} day^{-1})
No25 1222	86.156	12.108	32.561	2.646	0.372	63.914	8.982	24.155
No25 1223	82.261	11.918	31.767	2.590	0.375	60.446	8.758	23.342
No25 1224	82.790	12.021	34.231	2.419	0.351	60.985	8.855	25.215
No25 1322	94.616	14.188	50.379	1.878	0.282	66.273	9.938	35.288
No25 1323	79.883	11.896	47.998	1.664	0.248	56.227	8.373	33.784
No25 1324	66.694	9.647	45.539	1.465	0.212	46.891	6.783	32.017
No25 1422	87.615	13.880	52.560	1.667	0.264	29.857	4.730	17.911
No25 1423	86.690	14.003	49.412	1.754	0.283	29.316	4.735	16.709
No25 1424	90.737	13.803	58.632	1.548	0.235	31.055	4.724	20.067
No25 1522	78.438	12.806	22.864	3.431	0.560	70.903	11.575	20.667
No25 1523	75.248	11.968	20.078	3.748	0.596	67.811	10.785	18.094
No25 1524	60.911	9.464	18.371	3.316	0.515	54.594	8.482	16.466
No25 1622	66.043	10.853	31.239	2.114	0.347	55.124	9.058	26.074

No25 1623	68.545	11.538	30.609	2.239	0.377	57.583	9.692	25.714
No25 1624	66.138	10.995	29.531	2.240	0.372	55.421	9.214	24.746
No25 1722	62.605	10.758	72.674	0.861	0.148	21.829	3.751	25.340
No25 1723	66.386	11.445	66.428	0.999	0.172	22.985	3.963	23.000
No25 1724	76.384	12.768	74.989	1.019	0.170	26.225	4.384	25.747
No25 1822	75.832	13.864	22.827	3.322	0.607	72.343	13.226	21.777
No25 1823	75.393	14.100	29.249	2.578	0.482	74.130	13.864	28.759
No25 1824	68.894	12.877	25.418	2.710	0.507	65.571	12.256	24.192

Appendix B31. Mean growth rates (μ), concentrations of EPA, DHA, carbon, and Chl-a, and production rates of EPA, DHA, and Chl-a in *P. lutheri.*

Species treatment	Ave. μ (day^{-1})	Ave. [EPA] (ug EPA L^{-1})	Ave. [DHA] (ug DHA L^{-1})	Ave. [Chl-a] (ug Chl-a L^{-1})	[C] (mg L^{-1}) rep 1	[C] (mg L^{-1}) rep 2	[C] (mg L^{-1}) rep 3	Ave. [C] (mg L^{-1})	Corr [C] (mg L^{-1})
Pl25 1222	0.741	134.460	69.369	71.176	4.200	3.700	4.620	4.173	3.958
Pl25 1223	0.742	144.089	74.699	72.956	4.320	5.160	4.600	4.693	4.479
Pl25 1224	0.740	119.699	60.530	69.808	3.700	4.140	3.980	3.940	3.726
Pl25 1322	0.739	77.045	34.205	71.998	2.420	2.140	2.400	2.320	2.106
Pl25 1323	0.736	85.231	40.229	69.397	2.280	2.280	2.500	2.353	2.139
Pl25 1324	0.738	84.416	39.734	68.439	2.080	2.180	2.620	2.293	2.080
Pl25 1422	0.368	69.356	19.198	88.834	1.640	1.500	1.320	1.487	1.273
Pl25 1423	0.366	76.212	20.321	103.206	1.840	2.020	1.460	1.773	1.560
Pl25 1424	0.365	74.322	20.740	85.138	1.500	1.520	1.460	1.493	1.280
Pl25 1522	1.107	133.359	63.719	67.481	4.540	4.260	4.580	4.460	4.245
Pl25 1523	1.110	143.743	76.826	74.598	4.640	4.520	4.580	4.580	4.365
Pl25 1524	1.111	161.130	78.523	76.104	5.880	5.080	5.200	5.387	5.172
Pl25 1622	0.972	182.702	62.947	119.220	3.620	2.920	3.900	3.480	3.266
Pl25 1623	0.983	214.585	84.282	128.939	3.920	4.220	3.480	3.873	3.659
Pl25 1624	0.989	217.203	84.865	127.981	3.960	4.160	4.620	4.247	4.032
Pl25 1722	0.334	153.858	34.462	151.113	N/A	2.580	2.560	2.570	2.355
Pl25 1723	0.334	158.951	37.018	155.082	2.340	2.340	2.300	2.327	2.111
Pl25 1724	0.331	124.785	28.453	127.570	2.000	2.160	1.920	2.027	1.812
Pl25 1822	0.999	157.734	67.980	73.640	3.860	3.380	3.960	3.733	3.518
Pl25 1823	1.004	178.237	74.009	84.864	3.960	3.920	4.200	4.027	3.812
Pl25 1824	1.000	175.322	77.106	74.872	3.880	3.460	3.880	3.740	3.526
Pl25 1922	1.004	135.851	48.043	95.404	2.700	2.860	3.000	2.853	2.638
Pl25 1923	0.997	127.753	46.831	86.917	2.420	2.460	2.720	2.533	2.318
Pl25 1924	1.000	130.627	45.990	98.552	2.900	2.760	2.860	2.840	2.625
Pl25 2022	0.267	153.706	47.260	157.409	3.020	2.900	2.560	2.827	2.613
Pl25 2023	0.266	149.790	47.714	152.482	2.920	2.840	3.060	2.940	2.726

Appendix B31 (cont'd).

Species treatment	[EPA] (ug EPA mg C^{-1})	[DHA] (ug DHA mg C^{-1})	[Chl-a] (ug Chl-a mg C^{-1})	EPA/Chl ratio (ug mg C^{-1})	DHA/Chl-a ratio (ug mg C^{-1})	EPA production (ug EPA mg C^{-1} day^{-1})	DHA production (ug DHA mg C^{-1} day^{-1})	Chl-a production (ug Chl-a mg C^{-1} day^{-1})
Pl25 1222	33.969	17.525	17.981	1.889	0.975	25.173	12.987	13.325
Pl25 1223	32.173	16.679	16.290	1.975	1.024	23.873	12.376	12.087
Pl25 1224	32.128	16.247	18.737	1.715	0.867	23.772	12.021	13.864
Pl25 1322	36.576	16.238	34.180	1.070	0.475	27.045	12.007	25.273
Pl25 1323	39.842	18.805	32.440	1.228	0.580	29.342	13.849	23.890
Pl25 1324	40.592	19.106	32.909	1.233	0.581	29.949	14.097	24.281
Pl25 1422	54.473	15.078	69.771	0.781	0.216	20.062	5.553	25.696
Pl25 1423	48.860	13.028	66.166	0.738	0.197	17.897	4.772	24.236
Pl25 1424	58.070	16.205	66.521	0.873	0.244	21.197	5.915	24.282
Pl25 1522	31.412	15.009	15.895	1.976	0.944	34.764	16.610	17.591
Pl25 1523	32.929	17.600	17.089	1.927	1.030	36.563	19.542	18.975
Pl25 1524	31.151	15.181	14.713	2.117	1.032	34.618	16.870	16.351
Pl25 1622	55.946	19.275	36.507	1.532	0.528	54.396	18.741	35.496
Pl25 1623	58.644	23.034	35.238	1.664	0.654	57.668	22.650	34.651
Pl25 1624	53.874	21.050	31.744	1.697	0.663	53.258	20.809	31.381
Pl25 1722	65.332	14.633	64.166	1.018	0.228	21.827	4.889	21.438
Pl25 1723	75.293	17.535	73.460	1.025	0.239	25.169	5.862	24.557
Pl25 1724	68.878	15.705	70.415	0.978	0.223	22.785	5.195	23.294
Pl25 1822	44.831	19.321	20.930	2.142	0.923	44.772	19.296	20.902
Pl25 1823	46.755	19.414	22.262	2.100	0.872	46.950	19.495	22.355
Pl25 1824	49.728	21.870	21.237	2.342	1.030	49.722	21.868	21.234
Pl25 1922	51.491	18.210	36.161	1.424	0.504	51.716	18.289	36.318
Pl25 1923	55.111	20.202	37.495	1.470	0.539	54.946	20.142	37.383
Pl25 1924	49.768	17.522	37.548	1.325	0.467	49.786	17.528	37.561
Pl25 2022	58.832	18.089	33.268	1.768	0.544	15.706	4.829	8.882
Pl25 2023	54.949	17.503	36.153	1.520	0.484	14.618	4.656	9.617

Appendix B32. Mean measurements of growth rates (μ), concentrations of EPA, carbon, and Chl-a, and production rates of EPA and Chl-a in *T. pseudonana,* including carbon concentrations of f/2 culture media.

Species treatment	Ave. μ (day^{-1})	Ave. [EPA] (ug EPA L^{-1})	Ave. [Chl-a] (ug Chl-a L^{-1})	[C] (mg L^{-1}) rep 1	[C] (mg L^{-1}) rep 2	[C] (mg L^{-1}) rep 3	Ave. [C] (mg L^{-1})	Corr [C] (mg L^{-1})
Tp35 1322	1.189	88.427	131.403	3.040	2.880	2.900	2.940	2.726
Tp35 1323	1.188	83.408	122.916	2.940	2.380	2.680	2.667	2.453
Tp35 1324	1.184	77.161	104.711	2.760	2.500	2.500	2.587	2.373
Tp35 1422	0.559	66.684	135.783	1.660	1.660	1.540	1.620	1.407
Tp35 1423	0.560	78.033	154.398	1.840	1.700	1.820	1.787	1.573
Tp35 1424	0.559	61.324	131.403	1.540	1.600	1.640	1.593	1.380
Tp35 1522	1.450	132.080	121.274	6.160	7.420	6.280	6.620	6.402
Tp35 1523	1.448	108.459	110.323	6.060	5.340	6.320	5.907	5.691
Tp35 1524	1.437	119.252	111.966	6.320	6.140	5.840	6.100	5.886

Tp35 1622	1.393	65.814	87.054	3.540	3.720	3.300	3.520	3.302
Tp35 1623	1.384	71.061	71.587	2.820	2.540	2.340	2.567	2.348
Tp35 1624	1.378	67.439	64.196	2.720	2.460	2.460	2.547	2.329
Tp35 1722	0.534	103.601	145.090	2.200	2.140	2.040	2.127	1.912
Tp35 1723	0.541	128.278	146.870	2.520	2.380	2.340	2.413	2.198
Tp35 1724	0.540	127.089	150.976	2.620	2.240	2.240	2.367	2.151
Tp35 1922	1.299	156.319	190.315	3.820	4.620	4.360	4.267	4.051
Tp35 1923	1.284	142.842	177.771	3.620	3.960	4.240	3.940	3.725
Tp35 1924	1.277	120.630	165.228	3.080	3.600	3.420	3.367	3.152
Tp35 2022	0.460	105.538	127.844	1.680	1.660	1.440	1.593	1.380
Tp35 2023	0.467	90.274	107.723	1.660	1.540	1.380	1.527	1.313
Tp35 2024	0.480	179.195	214.104	2.620	2.840	2.380	2.613	2.400
f/2 Media				0.220	0.180	0.240	0.213	

Appendix B32 (cont'd).

Species treatment	[EPA] (ug EPA mgC^{-1})	[Chl-a] (ug Chl-a mgC^{-1})	EPA/Chl ratio (ug mgC^{-1})	EPA production (ug EPA mgC^{-1} day^{-1})	Chl-a production (ug Chl-a mgC^{-1} day^{-1})
Tp35 1322	32.434	48.197	0.673	38.553	57.290
Tp35 1323	33.999	50.103	0.679	40.405	59.544
Tp35 1324	32.513	44.122	0.737	38.501	52.248
Tp35 1422	47.410	96.537	0.491	26.498	53.955
Tp35 1423	49.599	98.137	0.505	27.773	54.951
Tp35 1424	44.440	95.225	0.467	24.859	53.266
Tp35 1522	20.630	18.942	1.089	29.914	27.466
Tp35 1523	19.059	19.387	0.983	27.588	28.063
Tp35 1524	20.261	19.023	1.065	29.119	27.340
Tp35 1622	19.933	26.367	0.756	27.770	36.732
Tp35 1623	30.264	30.488	0.993	41.872	42.182
Tp35 1624	28.952	27.560	1.051	39.887	37.968
Tp35 1722	54.192	75.895	0.714	28.927	40.512
Tp35 1723	58.372	66.832	0.873	31.562	36.136
Tp35 1724	59.073	70.176	0.842	31.884	37.876
Tp35 1922	38.591	46.984	0.821	50.139	61.042
Tp35 1923	38.347	47.725	0.804	49.229	61.266
Tp35 1924	38.273	52.423	0.730	48.874	66.943
Tp35 2022	76.482	92.647	0.826	35.161	42.593
Tp35 2023	68.736	82.022	0.838	32.103	38.309
Tp35 2024	74.675	89.222	0.837	35.822	42.800
f/2 Media					